AD_____

Award Number: DAMD17-01-1-0744

TITLE: Molecular Genetic Studies of Bone Mechanical Strain and of Pedigrees with Very High Bone Density

PRINCIPAL INVESTIGATOR: Subburaman Mohan, Ph.D.

CONTRACTING ORGANIZATION: Loma Linda Veterans Association for Research and Education
Loma Linda, CA 92357-1000

REPORT DATE: June 2005

TYPE OF REPORT: Annual

PREPARED FOR: U.S. Army Medical Research and Materiel Command
Fort Detrick, Maryland 21702-5012

REPORT DOCUMENTATION PAGE

Form Approved
OMB No. 074-0188

1. AGENCY USE ONLY (Leave blank)	2. REPORT DATE	3. REPORT TYPE AND DATES COVERED
	June 2005	Annual (15 May 2004 - 14 May 2005)

4. TITLE AND SUBTITLE
Molecular Genetic Studies of Bone Mechanical Strain and of Pedigrees with Very High Bone Density

5. FUNDING NUMBERS
DAMD17-01-1-0744

6. AUTHOR(S)
Subburaman Mohan, Ph.D.

7. PERFORMING ORGANIZATION NAME(S) AND ADDRESS(ES)
Loma Linda Veterans Association for Research and Education
Loma Linda, CA 92357-1000

E-Mail: Subburaman.mohan@med.va.gov

8. PERFORMING ORGANIZATION REPORT NUMBER

9. SPONSORING / MONITORING AGENCY NAME(S) AND ADDRESS(ES)
U.S. Army Medical Research and Materiel Command
Fort Detrick, Maryland 21702-5012

10. SPONSORING / MONITORING AGENCY REPORT NUMBER

11. SUPPLEMENTARY NOTES

12a. DISTRIBUTION / AVAILABILITY STATEMENT
Approved for Public Release; Distribution Unlimited

12b. DISTRIBUTION CODE

13. ABSTRACT (Maximum 200 Words)

The primary goal of the proposed work on bone mechanical strain focuses on identifying the genes and their functions involved in mediating the anabolic skeletal response to mechanical stress. Two hypotheses have been proposed:1) Quantitative trait loci analysis using the four point bending technique in two strains of mice exhibiting extreme differences in loading response will lead to identification of chromosomal locations of genes involved in variation in skeletal response to mechanical loading. 2) Application of microarray and tyrosine phosphorylation studies using bone cells derived from inbred strains of mice exhibiting extreme differences to loading response and physiologically relevant fluid flow shear strain will lead to identification of key signaling genes and their pathways that contribute to variation in bone cell response to mechanical strain. During the last funding period, we proposed several specific objectives for each of the above-mentioned hypothesis. We have successfully accomplished all of the specific objectives. Our work during this reporting period has resulted in one published manuscript, one manuscript in press, and seven abstracts. We believe that successful accomplishment of the proposed studies will provide a better understanding of the molecular mechanisms involved in identifying the genes and their function as related to mechanical stress.

14. SUBJECT TERMS
Mechanical strain, quantitative trait loci analysis, microarray analysis, osteoblasts, signaling pathways, bone formation

15. NUMBER OF PAGES
134

16. PRICE CODE

17. SECURITY CLASSIFICATION OF REPORT	18. SECURITY CLASSIFICATION OF THIS PAGE	19. SECURITY CLASSIFICATION OF ABSTRACT	20. LIMITATION OF ABSTRACT
Unclassified	Unclassified	Unclassified	Unlimited

Table of Contents

Molecular Genetic Studies of Bone Mechanical Strain - In Vivo Studies

Introduction:

It is well established that maintenance of bone mass and the development of skeletal architecture are dependent on mechanical stimulation. A number of studies have shown that mechanical loading promotes bone formation in the modeling skeleton and that removal of this stimulus results in a reduction in bone mass (1). In addition, recent studies have also shown that increases in bone mass were variable in different subjects given the same amount of mechanical stress, with some exhibiting a robust osteogenic response and others responding more modestly (2,3). We and others have found evidence that this variation in response to mechanical loading is, in large part, genetically determined. Accordingly, we have identified two inbred mouse strains that differ in peak bone density and exhibit considerable differences in their bone response to immobilization (4) and mechanical loading (5). In our studies, we found that the C57Bl/6J mouse strain showed a greater loss of bone and immobilization by sciatic neurectomy compared to the C3H/HeJ strain. Furthermore, Histomorphometeric studies by Umemura et al. and Kodama et al. (4,5) as well as four-point bending studies by Akhter et al. (6) have revealed that an identical amount of mechanical strain applied to both mouse models produces a greater increase in the bone formation [periosteal and endosteal formation] parameters in the C57B/6J mice compared to the C3H/HeJ mice.

A number of *in vitro* studies have employed mechanical stimulation using various models in human and mouse cells (7,8) and have found that several signaling pathways, including MAPK (9), FAK (10), and nitric oxide (11), mediate the effects of mechanical loading in bone. However, the genetic mechanisms that contribute to any variations in anabolic response to loading remain unclear. One approach often used to identify the genetic factors or genes that contribute to differences in phenotypic variation is the quantitative trait loci (QTL) technique. In the QTL approach, two inbred mouse strains exhibiting a phenotypic difference of interest are crossed and any genetic loci that co-segregate with the phenotype are identified. A successful QTL requires the following components: a) optimal inbred mouse strains; b) an optimized *in vivo* loading model; c) valid endpoints to measure the difference in bone anabolic response; and d) an optimal age that shows the greatest difference in the phenotype in response to mechanical loading. We have addressed these components in the proposed Technical Objectives, as given below.

Body:

Our goals for the last twelve months of the funding period for the revised Technical Objective-I, as well as our progress for each of the specific objectives in Technical Objective-I, are described below.

Technical Objectives

Revised Technical Objective 1: Molecular Genetic Studies of Bone Mechanical Strain

Our Specific Objectives during the remainder of this continuation proposal are:

1) To establish the optimal method for inducing mechanical strain on the tibia.
2) To determine the optimal method for quantitating the bone formation response to mechanical strain on the tibia *in vivo.*

3) To determine the number of days required of four-point bending induced mechanical strain on the tibia in order to elicit an optimal response for quantitative measurements.
4) To select the optimal mouse inbred strain pair (i.e. B6 and C3 or some other strain pair) to perform the QTL mapping study.
5) To determine the appropriate age of animals to apply the four-point bending in order to obtain valid quantitative measurements of the bone formation response.
6) To test four-point bending responses in CAST and HS stock mice. These two strains of mice exhibit more polymorphisms with the traditional inbred strains of mice than any other strains. Therefore, such strains of mice would be excellent mating partners in our genetic studies. Accordingly, the greater the genetic polymorphism between the two strains of mice used for QTL mapping studies, the greater the opportunity to fine-map the QTL down to an operational size.

Specific Objective 1: To establish the optimal method for inducing mechanical strain on the tibia.

We previously used jump training as a method to induce bone response in mice. Since the amount of response produced by jump training was not sufficient to quantitate, we choose our next alternative-loading model, four-point bending, for the following reasons: 1) Histomorphometeric studies using this model on rats and mice have shown greater increase in the periosteal bone formation; 2) In the four-point bending method, the amount of load, cycles and frequency applied on the tibia of the test mice are controlled by an external device and the loading area is specific; and 3) also the right tibia is used for loading and the left tibia is used as internal control, thus avoiding the need of extra mice for control groups. For these reasons, we chose this model as a method to induce bone formation in our study.

Recent studies on rats have shown that the magnitude of load applied by four-point bending is important in increasing the anabolic response of bone. Histomorphometric studies on mice have shown increased bone formation using a fixed load, cycle and frequency. All these observations led us to hypothesize that the magnitude of load applied by four-point bending is very important in determining the anabolic response within and between the strains of mice. To test this hypothesis, we evaluated the anabolic response of bone as a function of different loads, (6-9N) on 10-wk female B6 and C3H mice for 12 days using four-point bending device. The rationale for selecting these range of loads: 1) the four-point bending device is not sensitive below a load of 5N; 2) loads above 12 N result in fracture in some mice; and 3) higher loads produce greater mechanical strain on the bone that might be more than that possible from a physiological range. Based on these observations, we selected the above dose of loads for our study

The mouse right tibia was used for the loading test while the left tibia was used as an internal control. Prior to loading, and while the mice were anesthetized, we used the ankle of the tibia that sits on the lower secondary immobile point as a reference, which allowed us to position the loading region of the tibia similarly for each mouse. To anesthetize the mice we used halothane [95% Oxygen and 5% Halothane] for 2-3 minutes and performed mechanical loading while the mice were anesthetized. The mice were trained for 6 days/week with 1 day of rest for 2-weeks. Two days after the last loading, mice were sacrificed, tibias collected and changes in the bone parameters (loaded vs. unloaded) were measured using pQCT system from Stratec XCT Research. Scanning was performed using the manufacturer supplied software program which is

designed to analyze the data and generate the values for the change in bone parameters. The X-ray attenuation data are based on the software-defined threshold. We set up two thresholds for our analysis. A 180-730 mg/cm^3 threshold was used to measure total area, total mineral content, periosteal circumference, and endosteal circumference in the loaded vs. unloaded bones. A 730-730-mg/cm^3 threshold was used to measure cortical thickness, total volumetric density, and material bone mineral density. In order to minimize the measurement errors caused by positioning of the tibia for the pQCT, we used the tibia-fibular junction as the reference line. We selected four-slices that start at a distance of 3 mm proximal from tibia-fibular junction for pQCT measurement. This region corresponded to the loading zone. Each slice was made at a 1mm interval and the values presented in the results are as an average of these four slices. After successfully troubleshooting these difficulties in the four-point bending method, we evaluated bone response from loads of 6 to 9N for 12 days in 10-week old B6 and C3H. The results are as follow;

Total bone mineral content: Four-point bending caused an increase in total bone mineral content in both the B6 and C3H mouse strains. The magnitude of increase varied depending on the amount of load between the B6 and C3H (Table-1). At 9N, the percentage increase in total bone mineral content in response to four-point bending was significantly greater in the B6 (48%) mice than in the C3H (19%) mice (Fig.1).

Area: Total area increased in response to four-point bending in both the B6 and C3H strains of mice. A dramatic increase of 44% and 26% in total area was seen after 12 days of four-point bending in the B6 and C3H mice, respectively (Table-1). The B6 mice ($p<0.05$) showed a greater increase in total area than in the C3H mice at a 9N load in contrast to other loads (Table-1 & Fig.1).

Periosteal circumference: The periosteal circumference increased by 20% and 12% in the B6 and C3H mice, respectively, in response to four-point bending (Table-1). The B6 mice showed a greater increase in periosteal circumference than in the C3H ($p<0.05$) mice at 9N compared to other loads (Table-1 & Fig.1).

Total volumetric density: Four-point bending caused a dose-dependent increase in the total bone density seen in the B6 mice (regression analysis $p<0.01$), but not in the C3H mice (Table-1). The B6 mice showed 5% and 15% greater density at loads of 8 and 9N after 12 days of loading, while the C3H mice exhibited no change (Table-1, Fig.1&2).

Cortical density: Cortical density increased by 4% in the B6 mice, but not in the C3H mice, at a load of 9N after 12 days of four-point bending (Fig.1).

Cortical thickness: Four-point bending increased cortical thickness in both the B6 and C3H mouse strains after two-weeks of mechanical loading at a load of 9N. The magnitude of increase was much greater in the B6 mice (27%) compared to that seen in the C3H mice (7%) (Fig.1).

Endosteal circumference: Endosteal circumference in response to four-point bending increased by 23% and 18% in both the B6 and C3H mouse strains, respectively (Table-1). The C3H mice showed a greater increase in the endosteal circumference compared to the B6 mice at a load of 8N ($p<0.05$).

Table-1 Changes in the bone parameters in response to varying magnitude of loads applied by four-point bending in 10-week old female B6 and C3H inbred strains of mice *in vitro*.

	C57BL/6J							
	6N		7N		8N		9N	
Bone parameters	Un loaded	Loaded	Un loaded	Loaded	Un loaded	Loaded	Un loaded	Loaded
Total Area, mm^2	1.42±0.06	1.52±0.06[a]	1.40±0.07	1.60±0.10[b]	1.47±0.04	1.74±0.04[c]	1.50±0.10	2.13±0.10[d]
Total Mineral Content, mg/mm	0.89±0.03	0.96±0.06[a]	0.83±0.07	0.96±0.07[a]	0.89±0.03	1.08±0.02[c]	0.87±0.02	1.29±0.06[d]
Periosteal circumference, mm	4.21±0.09	4.36±0.09[a]	4.18±0.10	4.47±0.13[b]	4.30±0.06	4.67±0.05[c]	4.33±0.14	5.17±0.12[d]
Endosteal circumference, mm	3.12±0.12	3.21±0.05	3.15±0.04	3.35±0.12[b]	3.25±0.07	3.46±0.07[c]	3.29±0.16	4.02±0.13[d]
Total Density, mg/ccm	678±31.59	680±18.63	637±29.8	655±27.9	646±24.0	675±15.4[a]	626±41.5	721±29.2[c]
Cortical Density mg/ccm	1110.0±17	1114.8±15	1090±21	1095±18	1095±14	1110±6.63[a]	1078±40	1115±35[b]

Bone parameters	C3H/HeJ							
	6N		7N		8N		9N	
	Un loaded	Loaded	Un loaded	Loaded	Un loaded	Loaded	Un loaded	Loaded
Total Area, mm^2	1.15±0.04	1.2±0.07	1.16±0.03	1.30±0.10[b]	1.15±0.04	1.41±0.08[b]	1.13±0.08	1.42±0.05[d]
Total Mineral Content, mg/mm	1.03±0.03	1.07±0.03[a]	1.04±0.04	1.16±0.07[b]	1.04±0.05	1.24±0.05[b]	1.04±0.07	1.24±0.03[c]
Periosteal circumference, mm	3.79.06	3.88±0.11	3.81±0.05	4.04±0.16[b]	3.79±0.07	4.20±0.12[b]	3.76±0.1	4.22±0.08[d]
Endosteal circumference, mm	2.31±0.04	2.38±0.16	2.32±0.04	2.49±0.11[b]	2.30±0.07	2.62±0.15[b]	2.26±0.10	2.70±0.17[c]
Total Density, mg/ccm	1001±11.7	1017±25.7	1013±16.6	1019±24.8	1021±12.1	1029±11.9	1047±9.7	1042±19.7
Cortical Density mg/ccm	1267±8.7	1264±17	1272±14	1258±8.0	1267±13	1256±3.66	1269±36	1250±34

The values shown are mean ± standard deviation of loaded zone compared to unloaded bones from the same mice.
[a] *$p<0.05$,* [b] *$p<0.01$,* [c] *$p<0.001$,* [d] *$P<0.0001$ vs. corresponding unloaded bones* N=6 for each load in both strains

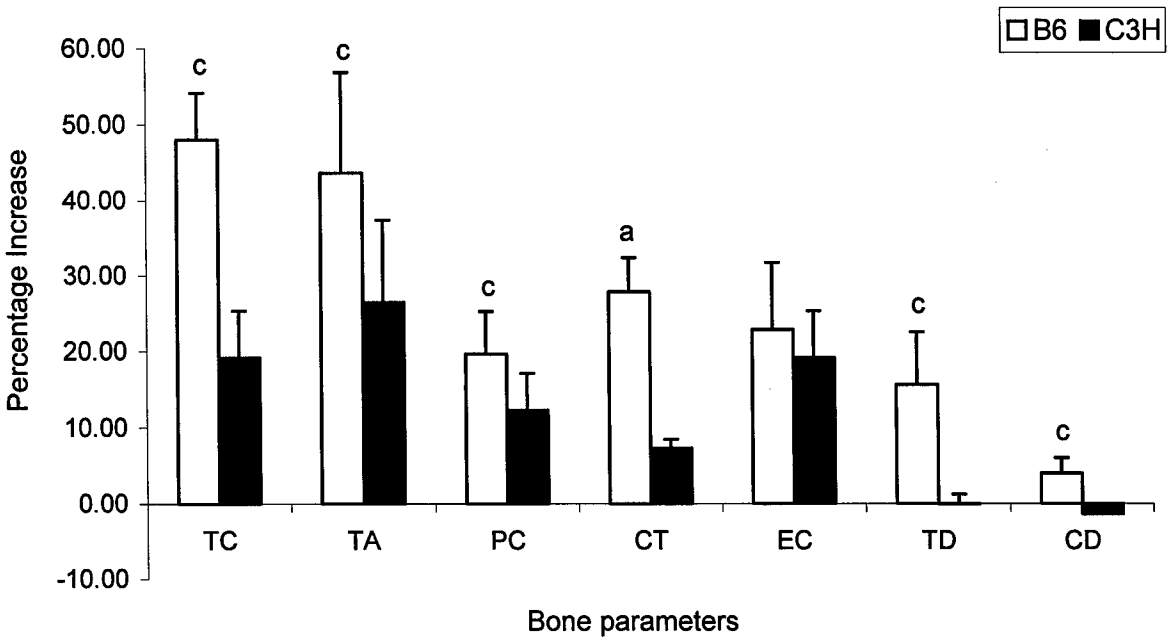

Figure 1: Changes in the bone geometrical parameters after 12 days of four-point bending at 9N load in 10-week old B6 and C3H inbred strains of mice *in vitro*. The data shows percentage change in Total content-TC, Total area-TA, Periosteal circumference-PC, Cortical thickness-CT, Endosteal circumference-EC, Total density-TD and Cortical density-CD. The values shown are as Mean ± standard deviation of loaded zone from compared to corresponding unloaded controlateral bones. The y-axis represents the percentage change and x-axis represents various bone phenotypes as measured by pQCT. N=6, [a] $p<0.05$, [c] $p<0.001$ between the strains In our dose response study we found four-point bending

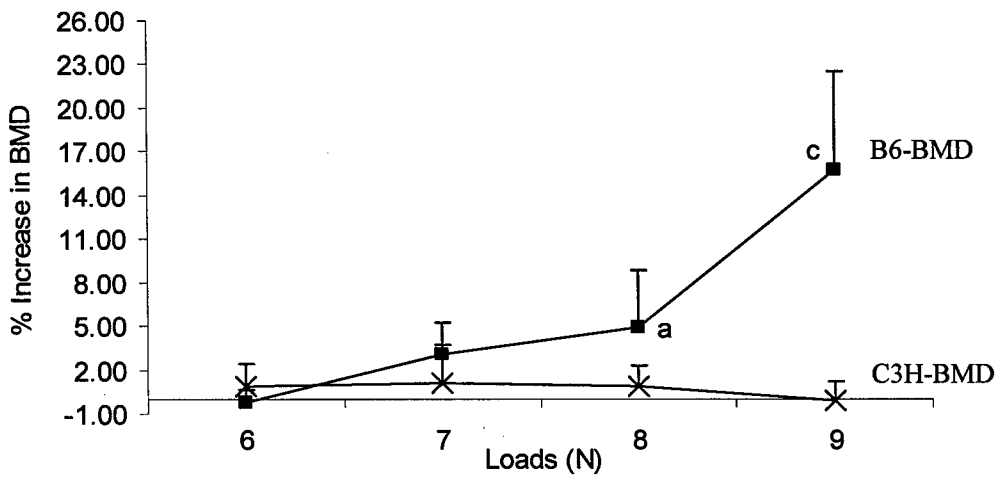

Figure 2: Changes in the bone mineral density (BMD) in response to varying magnitude of loads applied by four-point bending in 10-week old female B6 and C3H inbred strains of mice. The values shown are mean ± standard deviation of loaded bone compared to unloaded bones from the same mice. The y-axis represents the percentage increase and x-axis represents varying magnitude of load. *N=6* for each load in both strains, [a]*p<0.05*, [c]*p<0.001 vs. corresponding unloaded bones*

caused significant increases of 15% and 4.5% in total volumetric bone mineral density (vBMD) and cortical vBMD, respectively, in B6 mice with a 9N load. In contrast to the response observed in the B6 mice, none of the four loading regimens applied (i.e. 6, 7, 8, and 9N) produced any significant increase in total vBMD or cortical vBMD in the tibia of the C3H mice. The increased BMD response in B6 and not in C3H mice led us to hypothesize that the amount of mechanical strain produced by loads on the tibia of B6 mice was higher compared to the C3H mice due to a difference in bone geometrical properties. To test this hypothesis, we measured the amount of mechanical strain produced by loads in the loaded area of both B6 and C3H inbred strains of mice using the strain gauge technique. We used a single gauge to measure the strain on this loaded area since our 4mm vertically movable points touch this area, which is 3mm away from the tibia-fibular junction.

In brief, a P-3500 portable strain indicator and strain gauge of a specific range (EP-XX-015DJ-120, used to measure strains of up to 5000 με, according to the manufacturer instruction) were used to measure the amount of strain produced by different loads. Initially, the ends of the strain-gauge circuits were soldered to copper wire and glued on the medial side of the tibia, 2.09 mm away from the tibia-fibular junction, to provide a consistent position on the 4mm loading zone. These copper wires were connected to the indicator and the amounts of strain produced by the loads were recorded. The strain-gage data from four individual mice were averaged for each load. The results from our study as shown in Table-2 revealed an increase in mechanical strain with an increase in mechanical load in both the B6 and C3H mice. The C3H mice showed slightly higher mechanical strain compared to B6 mice in all the loads and the difference was statistically significant ($p<0.01$, ANOVA) (Table-2). Therefore the lack of significant change in total vBMD cannot be explained on by inadequate mechanical strain, since a load of 9N produced 3865 με in the tibia of the C3H mice, which is notably higher than the mechanical strain produced in the tibia of the B6 mice. Furthermore, a mechanical load of 9N caused a significant increase in both total area and periosteal circumference in the C3H mice, suggesting that the observed increase in vBMD response in the tibia of this strain is not caused by a lack of reduced mechanical strain.

In terms of the rapid increase in total vBMD in B6 mice in response to four-point bending, cortical thickness is increased by 27% in B6 mice. Consistent with this increase in cortical thickness, bone area increased significantly as well in the B6 response to mechanical loads of 9N. The increase in bone area and cortical thickness can be explained by the observed increase of nearly 20% in periosteal circumference, which results in a near by 50% increase in total area in the loaded tibia compared to unloaded tibia after 12 days of four-point bending. In contrast to the increases observed in the B6 mice, the magnitude of increase in periosteal circumference, total area, and cortical thickness were substantially less in the C3H mice as determined by histomorphometric analysis. Consistent with these data, Recker et al., (6) have found a greater increase in the periosteal bone formation response in B6 mice compared to C3H mice after four-point bending. Similarly, we found a significantly greater increase in the expression of bone formation marker genes in the loaded tibia of tested B6 mice compared to C3H mice (Table-6). Based on these data, we have concluded that a greater increase in periosteal bone response in the B6 mouse contributes, in part, to the observed increase in total vBMD.

Our findings demonstrate for the first time that mechanical loading results in a significant increase in material BMD, which also contributes to an increase in total vBMD. In this regard, we consider the increase in cortical density to represent changes in metacarpal bone mineral

density (mBMD), since the vascular canal volume, as determined by histological analysis, was too low in the loaded bones to account for the increase in cortical BMD. Therefore, we believe that a mechanical load of 9N caused a maximum mineralization and an increase in bone size in the tibia of the B6 mice. Consistent with this interpretation, we found that four-point bending caused an acute down regulation of expression of bone resorption marker genes at two and four days of four-point bending. Thus, the loading-induced decrease in remodeling could contribute to an increase in the rate of mineralization, and thereby contribute to the observed increase in mBMD and total vBMD in the tibia of the B6 mice.

As we mentioned earlier, in our pQCT analysis we used two thresholds to measure changes in bone parameters: 1) A threshold of 180-730 mg/cm3 for evaluation of loading induced changes in total area, total mineral content, periosteal and endosteal circumference, and 2) A threshold of 730-730 mg/cm3 for evaluating total vBMD and mBMD. These two thresholds were selected to include the newly formed bone, which may not have been fully mineralized. Thus, it is possible that the dramatic changes in mineral content and bone size after two weeks of loading may represent woven bone in addition to mature lamellar bone. Further studies are needed to evaluate the relative contribution of woven and lamellar bone to loading induced increase in bone size and total mineral content.

Table-2 Mechanical strain produced by varying magnitude of loads applied by four-point bending in the tibia of 10-week old B6 and C3H mice, as measured by strain gauge.

Load	με (Mean ± SD)	
	B6	C3H *
6N	2610 ± 219	2763 ± 64
7N	3020 ± 173	3188 ± 116
8N	3371 ± 143	3545 ± 157
9N	3682 ± 181	3865 ± 182

N=4 in each load

*p<0.01 is significantly higher compared to B6 by ANOVA)

Specific Objective 2: To determine the optimal method for quantitating the bone formation response to mechanical strain on the tibia in vivo.

To date, changes in bone parameters are largely measured by pQCT and histology. These two methods are well established but are time consuming and require long-term loading. In the present study we evaluated if changes in the mRNA of bone formation/resorption genes measured by real time PCR could be used as surrogates for pQCT measurement of bone loading response. To test this, we performed mechanical loading using the four-point bending device on 10-week female B6 mice for 12 days at a load of 9N. Two days after the last loading, in vivo pQCT was performed to measure changes in bone parameters (loaded vs. unloaded) (Fig.3). Later the same mice were sacrificed and the tibias were collected for gene expression study using real time PCR. The results from our study are shown in Table-3. In this study, we compared gene expression changes with changes in skeletal parameters measured by pQCT to determine the usefulness of gene expression data as a surrogate marker for the bone anabolic response to mechanical loading. We therefore hypothesized that expression levels of one or more genes in bone formation would reflect BMD changes, and therefore could be used as phenotypes for our QTL studies. Accordingly, in our correlation study we found that bone sialoprotein (BSP),

MMP-9, and TRAP showed the strongest correlation with bone parameters measured by pQCT, suggesting that expression phenotypes of these genes may be used as surrogates for pQCT measurement of bone's response to mechanical loading. It remains to be determined why the correlation between gene expression changes and cortical BMD was higher compared to the correlation between real time PCR data and total vBMD.

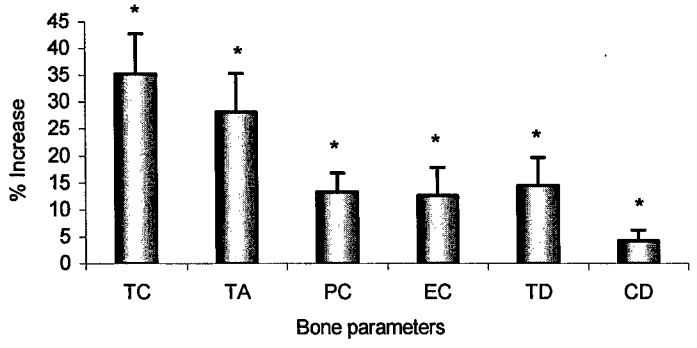

Figure 3. Changes in bone parameters in response to 12 days of four-point bending measured by in *vivo* pQCT in the tibia of 10-week old female B6 mice. The data shown here is the percentage that corresponds to the loading zone of tibia compared to unloaded tibia and are Mean ± standard deviation. P-values are calculated using t-test by comparing the loaded and unloaded bones. The y-axis represents percentage and x-axis represent bone parameters TC; Total content, TA; Total area, PC; periosteal circumference, EC; endosteal circumference; TD; total density and CD; cortical density. N=9, *$p<0.0001$ vs. corresponding unloaded bones

Table-3 Correlation between pQCT and Real time PCR data from tibia [same mouse tibia was used for pQCT and mRNA quantitation] measurement obtained from 12 days of four-point bending in 10-week old female B6 mice.

Bone markers	Total Density	Cortical Density
Type-I collagen	-0.08	0.05
Bone sialoprotein	0.60	0.68[a]
Alkaline phosphatase	0.25	0.22
Osteocalcin	0.28	0.36
Matrix-metalloproteinase 2 (MMP-9)	0.11	0.70[a]
Tartrate Resistant Acid Phosphatase (TRAP)	0.39	0.67[a]
Cycloxygenase 2 (COX-2)	0.47	0.57

For pQCT measurement N=9

For Real time PCR N=9
[a]$p<0.05$

Specific Objective 3: To determine the number of days required of four-point bending-induced mechanical strain on the tibia in order to elicit an optimal response for quantitative measurements.

The increase in bone mass in response to skeletal loading is an important adaptive response. It is likely that regulation of both osteoblast and osteoclast cell functions are involved in producing an optimal response to a given mechanical load. In order to evaluate the osteoblast and osteoclast cell response to mechanical input, we carried out a time course of mechanical loading using four-point bending device on 10-week female B6 mice. A 9N load at 2Hz for 36 cycles was applied on the right tibia by four-point bending and the left tibia was used as an internal control. Two days after the last loading, mice were sacrificed, 4mm-tibias were collected and RNA was extracted using a Qiagen Kit. The quality and quantity of RNA was evaluated using Bioanalyzer and Nano-Drop. Expression changes were measured using real time PCR in 12 genes that related to bone formation and resorption at 2, 4, 8, and 12 days of training. The data were normalized using β-actin and the exact fold changes of genes were calculated by applying mathematical formula ($2^{-\square\square CT}$) from Applied Biosystems. Primers for the bone markers genes were designed using Vector NTI and purchased from IDT-DNA.

As shown in Table-4 and Fig.4, 2 days of four-point bending performed on the B6 mice caused significant decreases in the expression of bone resorption genes, but had no significant effect on the expression levels of bone formation genes in loaded tibia compared to unloaded tibia of B6 mice. In addition, 4 days of loading induced expression of both type-I collagen and bone sialoprotein (BSP) by 2-fold and down regulated Matrix-metalloproteinase 2 (MMP-9), Tartrate Resistant Acid Phosphatase (TRAP), Sodium-potassium pump, and Cathespin K by 3-, 5- and 2-fold, respectively, in B6 mice. No change was found in the expression of osteocalcin and alkaline phosphatase (Table-4). Eight days of loading caused an increase in the expression of type-I collagen, bone sialoprotein, alkaline phosphatase, and osteocalcin by 3-fold, and down regulation of TRAP by 3-fold. No change in expression was found between loaded and unloaded bones for MMP-9 and Na-K pump genes after 8 days of loading (Table-4). Prolongation of loading of up to 12 days showed significant changes in expression for both bone formation (type-I collagen, bone sialoprotein, alkaline phosphotase and osteocalcin with 4.2-, 8-, 6-, and, 4-fold) and resorption marker genes (receptor activator of nuclear factor {kappa}B ligand (RANKL), MMP-9, TRAP with 5-, 12-, and 7.5-fold, respectively) (Table-4). It is interesting to note that mechanical loading caused an acute inhibition of bone resorption, as evidenced by down regulation of MMP-9 and TRAP. This finding is consistent with the previous *in vitro* study in which mechanical stress reduced the expression of RANKL, inhibiting both osteoclast formation and activation (12). However, 12 days of prolonged loading induced expression of bone resorption marker genes as shown in Table-4. This increased bone resorption that occurs at 12 days after loading may be the consequence of remodeling in response to increased bone formation. Accordingly, in our pQCT analysis we found endosteal circumference was increased after 12 days loading. Furthermore, the expression of RANKL, a key regulator of bone resorption, was increased by 5-fold after 12 days of loading, suggesting that any loading-induced increase in bone resorption at the endosteum may be mediated via an increase in the production of RANKL. These findings suggest that 12 days of loading involves both osteoblast and osteoclast cell functions.

Table-4 Fold change in the mRNA levels of bone formation and resorption genes in response to 2, 4, 8, and 12 days of four-point bending in 10-week old female B6 mice.

(a) Bone Formation genes

Duration of loading	Genes	$2^{-\Delta\Delta}Ct$	Fold Change	P-value
2-days	Type-I Collagen	-0.27 ± 0.43	1.21	0.45
	Bone sialoprotein	-0.05 ± 1.09	1.03	0.29
	Alkaline Phosphatase	-0.41 ± 0.37	1.3	0.66
	Osteocalcin	-1.20 ± 1.24	-2.3	0.08
4-days	Type-I Collagen	-1.02 ± 0.29	2.04	0.03
	Bone sialoprotein	-1.03 ± 0.37	2.04	0.006
	Alkaline Phosphatase	-0.53 ± 0.39	1.45	0.18
	Osteocalcin	-0.12 ± 1.02	1.0	0.73
8-days	Type-I Collagen	-1.93 ± 0.25	3.84	0.00001
	Bone sialoprotein	-1.89 ± 1.15	3.71	0.003
	Alkaline Phosphatase	-1.53 ± 0.73	2.88	0.001
	Osteocalcin	-1.45 ± 0.97	2.72	0.01
12-days	Type-I Collagen	-2.06 ± 0.25	4.18	0.000001
	Bone sialoprotein	-3.01 ± 0.19	7.82	0.00000002
	Alkaline Phosphatase	-2.55 ± 0.43	5.86	0.0000005
	Osteocalcin	-2.01 ± 0.34	4.03	0.0005

(b) Bone Resorption genes

Duration of loading	Genes	$2^{-\Delta\Delta}Ct$	Fold Change	P-value
2-days	TRAP	-1.88 ± 0.79	-3.70	0.005
	MMP-9	-1.61 ± 0.89	-3.06	0.002
4-days	TRAP	-1.68 ± 0.76	-3.20	0.004
	MMP-9	-1.98 ± 0.53	-3.95	0.002
	Na-K pump	-2.47 ± 0.39	-5.56	0.0008
	Cathepsin K	-0.93 ± 0.87	-1.90	0.07
8-days	MMP-9	-0.28 ± 0.47	1.21	0.2
	TRAP	-1.61 ± 1.0	-3.06	0.007
	Na-K pump	0.10 ± 1.12	0.92	0.12
	Cathepsin K	1.14 ± 0.84	0.45	0.34
12-days	TRAP	-3.61 ± 0.53	12.25	0.00000003
	MMP-9	-2.91 ± 0.35	7.54	0.000000008
	RANKL	-2.65 ± 0.37	5.17	0.00001
	Osteoprotegerin (OPG)	0.47 ± 0.33	1	0.81

N=5-7

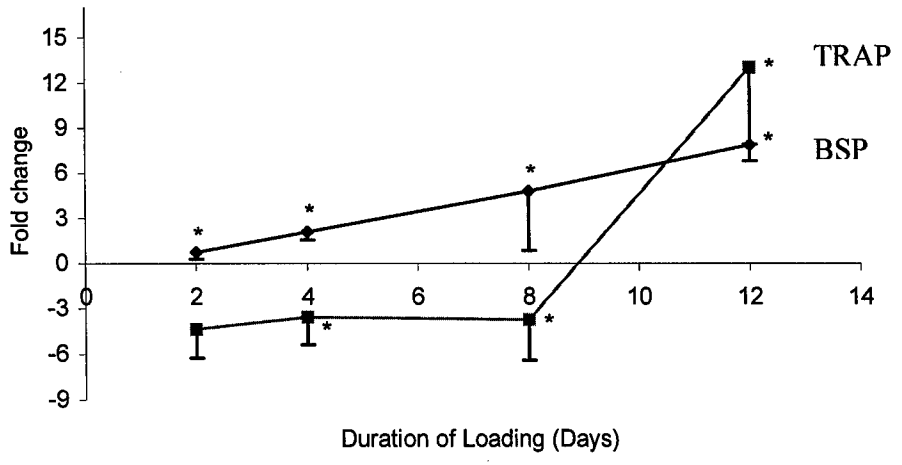

Figure 4: Changes in the expression of bone sialoprotein (BSP)and TRAP in response to a time course of mechanical loading. The x-axis corresponds to varying time points and the y-axis represents fold change measured by real time PCR. N=5-7, *p<0.01 vs corresponding unloaded bones

Specific Objective 4: To select the optimal mouse inbred strain pair (i.e. B6 and C3 or some other strain pair) to perform the QTL mapping study.

One of our main objectives in this study was to select two mouse strains that show extreme differences in their bone response to mechanical loading. To achieve this, we compared the bone anabolic response to four-point bending using pQCT in four different inbred mouse strains that differ in the genetic background, namely B6, DBA, Balb/c, and C3H mice. A 9N load was applied to the tibia of these inbred strains (expect Balb/c, in which 8N was used since 9N caused fractures) for 12 days and changes in the bone parameters were measured using pQCT in the loaded vs. unloaded bone. We used total vBMD and bone size as endpoints to compare the bone response between four inbred strains because they are major determinants of bone strength. The results from this study are shown in Table-5. A dramatic 15% and 10% increase in the total vBMD was observed in the B6 and DBA mice after 12 days of loading (Table-5). However, there was no significant change in the BMD of the Balb/c and C3H mice after the same duration of loading. Mechanical loading increased bone size, as measured by total area or periosteal circumference, in all four strains tested. However, the increase in bone size was greatest in the B6 mice. Based on these data, we chose the B6 as the good responder for further studies. Although neither the C3H or Balb/c mice showed any increase in BMD in response to four-point bending, we chose C3H as a poor responder for further studies for two main reasons. First, both the C3H and B6 mice exhibited similar body and bone size while Balb/c mice were smaller both in body size and bone size. Second, 9N load could not be applied to Balb/c as repeated application of 9N load led to fracture in some mice. In conclusion, our pQCT data demonstrate that the skeletal response to mechanical loading is variable among inbred strains of mice, as it has been reported in other studies using histology (13). Furthermore, these data suggest that the effects of mechanical loading on bone size and BMD are influenced by distinct genetic mechanisms.

Table-5. Changes in bone parameters [measured by pQCT] in response to 12 days of four-point bending at 9N load in 10-week old female Balb/c, B6, DBA/J, and C3H mice.

Bone parameters	Balb/c[#]	C3H	DBA/J	B6
Total Content	14.03 ± 4.7[a]	19.17 ± 6.14[a]	48.37 ± 2.85[ab]	47.83 ± 6.0[ac]
Total area	13.04 ± 1.89[a]	26.45 ± 10.85[a]	33.56 ± 6.00[a]	43.5 ± 13[a]
Periosteal circumference	6.22 ± 0.92[a]	12.3 ± 4.8[a]	18.50 ± 7.15[ab]	19.5 ± 5.6[ac]
Endosteal circumference	5.75 ± 2.33[a]	20.35 ± 9.9[a]	16.81 ± 12.85[a]	23.0 ± 8.8[a]
Total density	2.97 ± 1.8	-0.45 ± 1.75	10.82 ± 5.50[ab]	15.67 ± 6.7[ac]
Cortical density	0.80 ± 1.35	-1.45 ± 1.08	2.72 ± 2.12[a]	4.00 ± 2.0[ad]

The values represent % increase in the loaded bone compared to unloaded bone and are mean ± standard deviation of 6 animals for each strain. [#]8N was applied on Balb/c since some of the tibias fractured at 9N.
[a]p<0.05 vs. unloaded bones.
[b]p<0.05 between Balb/c and C3H.[c]p<0.05 between Balb/c and C3H.[d]p<0.05 between Balb/c, DBA/J, and C3H.

Using the above loading regimen, we compared gene expression changes between B6 (good responder) and C3H (poor responder) mice to test the hypothesis that the difference in the bone response between these strains in pQCT can be observed in the expression levels of bone formation and resorption genes. As anticipated, we found B6 and C3H mice showed increased expression of both bone formation and resorption marker genes after 12 days loading. However, the magnitude of increases in the expression phenotypes was found to be significantly greater in B6 compared to C3H mice (Table-6). This is consistent with our pQCT data that showed greater change in the bone parameters in B6 compared to C3H mice after 12 days of 9N load. Thus, we show the influence of genetics in determining the bone anabolic response to mechanical load using expression changes of genes as well as change in bone parameters. Our ongoing QTL studies will examine the genetic traits that contribute to variation in bone anabolic response using BMD and gene expression changes as end points.

Table-6 Fold change in the mRNA expression of bone formation and resorption markers genes in response to 12 days four-point bending in 10-week old female B6 and C3H mice.

Genes	B6*	C3H	p-value
	Mean ± SD	Mean ± SD	
Type-I collagen	4.23 ± 0.74	3.19 ± 0.77	0.02
Bone sialoprotein	7.88 ± 1.03	2.90 ± 0.54	0.0000
Alkaline phosphatase	6.08 ± 4.64	3.83 ± 1.12	0.01
Osteocalcin	4.13 ± 1.0	2.93 ± 0.77	0.02
TRAP	13.02 ± 5.06	7.66 ± 2.30	0.02
MMP-9	7.75 ± 2.02	4.20 ± 1.25	0.001
RANKL	5.38 ± 1.68	3.36 ± 1.41	0.04

N=7 in both B6 and C3H mice
*B6 is significant over C3H in the expression of bone markers genes.

Specific Objective 5: To determine the appropriate age of animals to apply the four-point bending in order to obtain valid quantitative measurements of the bone formation response.

Another goal in the study was to select an optimal age that shows a significant difference in the anabolic response of bone between the two strains. To perform this, we carried out four-point bending with a similar loading regimen in varying age groups [10-week, 16-week, and retired breeders] of the B6 and C3H mice to study the anabolic response of bone to a load of 9N as a function of age. The results from our experiment indicated that four-point bending caused significant changes in the bone parameters of both strains of mice in all three age groups tested (Fig.5). B6 mice showed greater changes than C3H mice in the total mineral content, total area, periosteal circumference, and total volumetric density and cortical density in all 3 age groups studied. Most surprising was mechanical strain-induced bone response showed no difference regardless of age in three age groups tested [10, 16, and 36 weeks] in either the B6 or the C3H mouse strains. This was determined using bonferroni Post Hoc test. In contrast to our report, other studies on mice, rats, turkeys, and humans have shown that bone response induced by mechanical stimuli declines with age. There are a number of potential explanations for the discrepancy between our data and previous studies, which include: 1) Age-related impairment in bone anabolic response may be seen in mice older than 36-weeks of age; 2) Aging may have a greater effect on bone's response to loading in some inbred strains of mice than in others; and 3) Bone's response to mechanical load may vary with age at lower loads but not at higher loads.

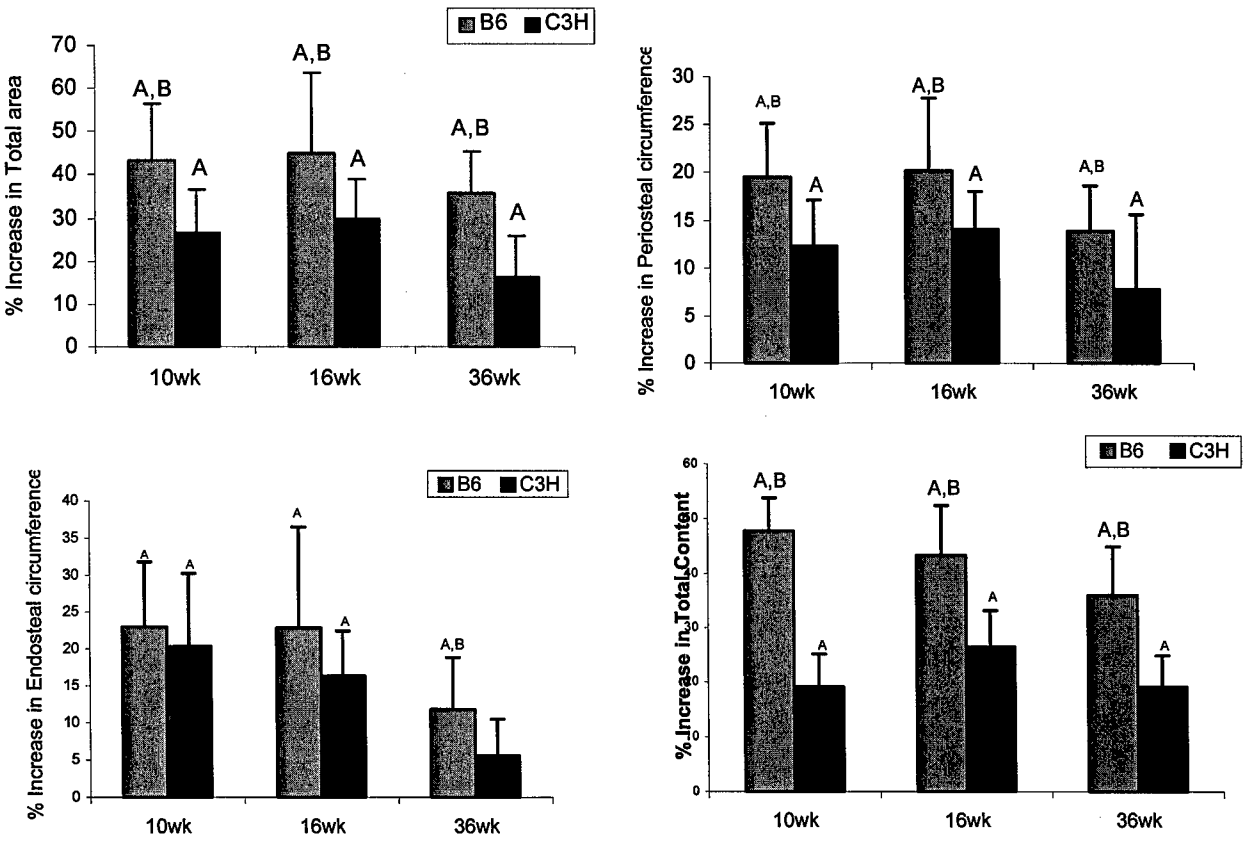

Figure 5. Changes in the bone parameters in response to 12 days four-point bending in different age groups of B6 and C3H mice. The y-axis represents percentage increase and x-axis represents varying ages. The blue color histogram corresponds to B6 mice and brown color represents C3H mice. A= $p<0.05$ vs unloaded control bones; B=$p<0.05$ v C3H mice

Specific Objective 6: To test four-point bending responses in CAST and HS stock mice.
These two strains of mice exhibit more polymorphisms with the traditional inbred strains of mice than any other strains. Therefore, such strains of mice would be excellent mating partners in our genetic studies. Accordingly, the greater the genetic polymorphism between the two strains of mice used for QTL mapping studies, the greater the opportunity to fine-map the QTL down to an operational size.

Our final goal in the study was to use CAST or HS stock mice to perform the QTL study if we do not get a larger difference in the anabolic response of bone between the inbred strains of mice. Since B6 and C3H mice showed large difference in the bone adaptation to mechanical loading, we have selected this two inbred strains as optimal mouse pair for our QTL study and therefore we did not proceed further with CAST and HS stock mice.

Key Research Accomplishments:

1. Jump training produced a significant difference in the osteogenic response between B6 and C3H mice, but the response was too small to measure in the individual F2 mice.
2. Four-point bending technique was established and validated.
3. Four-point bending increased material BMD and volumetric BMD significantly in B6 but not in C3H mice.
4. 9N load showed peak differences in the bone anabolic responses between B6 and C3H mice.
5. 12 days of loading induced caused 40% increase in bone area and 15% increase in vBMD in B6 mice.
6. Gene expression changes showed difference in the bone anabolic response to a given load between B6 and C3H mice.
7. PQCT and Real time PCR were used as endpoints in the measurement of bone phenotypes in response to mechanical loading.
8. Chronological age (10-wk to 36 wk) had no effect on bone response to mechanical loading.
9. B6 and C3H mice were selected as the optimal mouse pair for the QTL study out of four strains tested.

Reportable Outcomes:

1. Chandrasekhar K, Mohan S, Susanna O and Baylink DJ. Evidence that BMD response to mechanical loading (ML) in vivo is caused by acute up-regulation of both bone formation (BF) genes and down regulation of bone resorption (BR) genes. ASBMR 26th Annual Meeting, October 1-5, 2004, Washington State Convention & Trade Center, Seattle, WA, USA. 1 October 2004.
2. Chandrasekhar K, Baylink DJ, Wergedal J E and Mohan S. Inbred mouse strain development variations in the skeletal adaptive response to four-point bending evidence for involvement of different genetic mechanisms. ASBMR 26th Annual Meeting, October 1-5, 2004, Washington State Convention & Trade Center, Seattle, WA, USA. 1 October 2004.

3. Chandrasekhar K, Mohan S, Wergedal J E and Baylink DJ. Bone anabolic response to a mechanical load is a complex trait and involves bone size, material bone density (mBMD) and volumetric bone density (vBMD) phenotypes. ASBMR 26th Annual Meeting, October 1-5, 2004, Washington State Convention & Trade Center, Seattle, WA, USA, 1 October 2004.

Conclusions:

1. Out of four-strains tested, we found B6 is a good responder and C3H is poor responder for mechanical loading in terms of BMD response and expression levels of bone marker genes. We therefore selected these two inbred mouse strains to identify the genetic loci contributing for mechanical loading induced phenotypes.
2. On the selected inbred strains we applied varying magnitudes of load to select an appropriate load that shows greater increase and difference in the anabolic response of bone within and between the strains of mice. B6 mice showed dose dependent increase in BMD while C3H no change in all the loads. 9N load showed maximum changes and differences in the bone parameters of B6 mice compared to C3H mice compared to other loads.
3. We showed that the lack of BMD response in C3H is not caused due to lower mechanical strains because C3H mice produced higher mechanical strain than B6 mice measured by strain gage. Therefore the observed change in the vBMD of C3H mice is not caused by lack of mechanosensitivity because 9N load caused increase in other bone parameters in C3H mice.
4. When we correlated the *in vivo* changes in the bone parameters (measured by pQCT) with expression levels of bone markers genes measured by real time PCR, we found a significant correlation, which supports the view that expression levels of genes can be used as surrogates for bone anabolic response to mechanical loading. In our proposed QTL study we will be using expression levels of genes as phenotypes to identify the QTL for mechanical load phenotypes.
5. Bone response to mechanical loading tested on three age (10-, 16- & 36-week) groups showed similar changes suggesting that all three age groups do not have any effect on mechanical loading. We therefore proposed to use the 10-week age group to perform the QTL study because younger mice will progress our study much faster than using older mice.
6. Selecting an optimal time point: We found expression levels of bone marker genes increased throughout the loading. Further, at 12 days loading, B6 mice showed maximum changes and difference in the bone marker genes over C3H mice. We therefore selected 12 days as the time point to perform the loading in F2 population of our QTL study.

References:

1. Umemura Y, Baylink DJ, Wergedal JE, Mohan S, Srivastava AK. 2002 A time course of bone response to jump exercise in C57BL/6J mice. J Bone Miner Metab, 20(4):209-15.
2. Dalsky GP, Stocke KS, Ehsani AA, Slatopolsky E, Lee WC, Birge SJ. 1988 Weight Bering exercise training and lumbar bone mineral content in postmenopausal women. Ann Intern Med, 108:824-828.
3. Snow-Harter C, Bouxsein ML, Lewis Bt, Carter DR, Marcus R. 1992 Effects of resistance and endurance exercise on bone mineral status of young women: a randomized exercise intervention trail. J Bone Miner Res, 7:761-769.

4. Kodama Y, Dimai HP, Wergedal J, Sheng M, Malpe R, Kutilek S, Beamer W, Donahue LR, Rosen C, Baylink DJ et al . 1999Cortical tibial bone volume in two strains of mice: effects of sciatic neurectomy and genetic regulation of bone response to mechanical loading. Bone, 25(2):183-90.
5. Kodama Y, Umemura Y, Nagasawa S, Beamer WG, Donahue LR, Rosen CR, Baylink DJ, Farley JR. 2000 Exercise and mechanical loading increase periosteal bone formation and whole bone strength in C57BL/6J mice but not in C3H/Hej mice. Calcif Tissue Int.Apr;66(4):298-306
6. Akhter MP, Cullen DM, Pedersen EA, Kimmel DB, Recker RR. 1998 Bone response to in vivo mechanical loading in two breeds of mice. Calcif Tissue Int, 63(5):442-9.
7. Boutahar N, Guignandon A, Vico L, Lafage-Proust MH. 2004 Mechanical strain on osteoblasts activates autophosphorylation of focal adhesion kinase and proline-rich tyrosine kinase 2 tyrosine sites involved in ERK activation. J Biol Chem, 279(29):30588-99.
8. Kapur S, Baylink DJ, Lau KH. 2003 Fluid flow shear stress stimulates human osteoblast proliferation and differentiation through multiple interacting and competing signal transduction pathways. Bone, 32(3):241-51.
9. Peverali FA, Basdra EK, Papavassiliou AG. 2001 Stretch-mediated activation of selective MAPK subtypes and potentiation of AP-1 binding in human osteoblastic cells. Mol Med, 7(1):68-78.
10. Boutahar N, Guignandon A, Vico L, Lafage-Proust MH. 2004 Mechanical strain on osteoblasts activates autophosphorylation of focal adhesion kinase and proline-rich tyrosine kinase 2 tyrosine sites involved in ERK activation. J Biol Chem. Jul 16;279(29):30588-99
11. Kunnel JG, Igarashi K, Gilbert JL, Stern PH. 2004 Bone anabolic responses to mechanical load in vitro involve COX-2 and constitutive NOS. Connect Tissue Res, 45(1):40-9.
12. Rubin J, Murphy TC, Fan X, Goldschmidt M, Taylor WR. 2002 Activation of extracellular signal-regulated kinase is involved in mechanical strain inhibition of RANKL expression in bone stromal cells. J Bone Miner Res, 17(8):1452-60.
13. Robling AG and Turner CH. 2002 Mechanotransduction in bone: genetic effects on mechanosensitivity in mice. Bone, Nov31 (5):562-9.

Molecular Genetic Studies of Bone Mechanical Strain – In Vitro Studies

Introduction:

Mechanical loading is essential for skeletal development and the maintenance of skeletal architectural integrity (1). Mechanical loading produces strains in the mineralized matrix of bone that are thought to generate interstitial fluid flow through the lacunar/canalicular spaces (2). This fluid flow exerts a shear stress at surfaces of osteoblasts and osteocytes lining these spaces and the shear stress then generates biochemical signals that transducer to the nucleus of bone cells to exert biological effects. Consequently, fluid flow shear stress is considered a surrogate in vitro model for mechanical loading. In these studies, we used the fluid shear stress model to investigate the mechanism(s) whereby the shear stress transduces biochemical signals from the membrane to the nucleus is commonly referred to as the mechanotransduction mechanism.

There is increasing evidence that cellular response to mechanical loading contains a genetic component. Accordingly, studies from our group and others have shown that, while C57BL/6J (B6) inbred strain of mice responded to mechanical loading with an increase in bone formation, C3H/HeJ strain of mice showed no bone formation response to the same loading (3,

4). A major goal of this portion of the studies was to use the fluid shear stress cell culture model to identify the genetic component that is responsible for the differential response to mechanical loading in these mice strains. This shear stress cell culture model was also used to identify different pairs of inbred mice showing differential osteogenic response to mechanical loading.

Body:

In our previous report, we optimized the conditions to develop an *in vitro* system to apply defined mechanical strain to cultured osteoblasts and compared the phenotypic differences between osteoblasts derived from the C3H/HeJ (C3H) and the C57BL/6J (B6) inbred strains of mice in their osteogenic responses to fluid flow shear stress. Specifically, we found that osteoblasts isolated from B6 mice were highly responsive to shear stress in terms of cell proliferation and differentiation; whereas osteoblasts isolated from C3H mice were unresponsive to the same shear stress under the same experimental conditions. We also studied the effects of fluid flow shear stress-induced phosphorylation of MAPK/ERK1/2 and integrin expression in these cells and found that shear strain induced a significant increase in the integrin β1 expression as well as the phosphorylation levels of ERK1 and ERK2 in B6 bone cells, but not in C3H bone cells. These findings are consistent with the similar differential in the *in vivo* osteogenic response to mechanical loading in these two inbred strains of mice. Consequently, these findings indicate that our *in vitro* fluid shear stress model would be a good surrogate cell culture model for investigations into the genetic differences in the osteogenic responses to mechanical loading and for dissecting the signal transduction mechanisms regulating the osteogenic response to mechanical loading.

Our work during this reporting period was primarily to follow the leads found in our previous studies. Our ultimate goal in this project was to dissect the signal transduction mechanism(s) and the genes involved in the mechanical stimulation of bone formation in this fluid shear stress cell culture model for mechanical loading. The following is a brief description of our progress toward each of the aforementioned objectives during the reporting period.

Technical Objectives:

To continue *in vitro* studies to identify signaling proteins that show differential response to mechanical loading in osteoblasts. We will have the following specific objectives:

1) Determine dose- and time-dependent responses of osteoblasts isolated from various inbred strains of mice to fluid flow shear stress generated by Cytodyne flow chamber on cell proliferation and differentiation.
2) Compare the effects of fluid flow shear stress on key signaling proteins in osteoblasts of mouse strains that respond to mechanical stress and in osteoblasts that fail to respond to mechanical stress.
3) Perform DNA microarray studies in osteoblasts isolated from other pairs of inbred mice e.g., Balb/c and 129J, before and after fluid flow shear stress to identify gene expression in osteoblasts in response to mechanical stress.

Specific Objective 1: Determine responses of osteoblasts isolated from various inbred strains of mice (Balb/c and 129J) to fluid flow shear strain generated by Cytodyne flow chamber on cell proliferation and differentiation.

With respect to studies of time-and dose-response of osteoblasts to fluid shear stress in the stimulation of cell proliferation and differentiation, our past work has focused on determining the optimal experimental conditions for the osteogenic response to the fluid shear stress. Accordingly, only two magnitudes of shear stress (i.e. 20 dynes/cm^2 and 50 dynes /cm^2) were assessed. We found that: 1) bone cell proliferation (assessed by [^{3}H]thymidine incorporation) was significantly ($p<0.001$) increased in response to shear stress of 20 dynes/cm^2 as well as to a stress of 50 dynes /cm^2 in human osteosarcoma TE85 cells; and 2) there was no significant difference in the [^{3}H]thymidine incorporation induction between the two levels of shear stress. Since fluid flow shear stress greater than 50 dynes/cm^2 would probably be beyond the physiological levels of shear stress, almost all of our subsequent work has used the shear stress of 20 dynes/cm^2. To determine the optimal time to obtain measurable response in the cell proliferation, bone cells were subjected to shear stress of 20 dynes/cm^2 for a duration ranging from 30 minutes to 10 hours. There was a significant increase in [^{3}H]thymidine incorporation for up to 4 hours. After that time point, cell proliferation induced by fluid flow began to reduce with no significant induction seen at 10 hours. Moreover, we did not see a time-dependent increase in [^{3}H]thymidine. Based on these results, we decided to use shear stress of 20 dynes/cm^2 for 30 minutes as the optimal conditions to get a response in cell proliferation for further studies.

An additional goal of this specific technical objective was to characterize and compare the osteogenic response of osteoblasts of several pairs of inbred mouse strains that show differential response to shear stress. In this regard, we have previously shown that osteoblasts

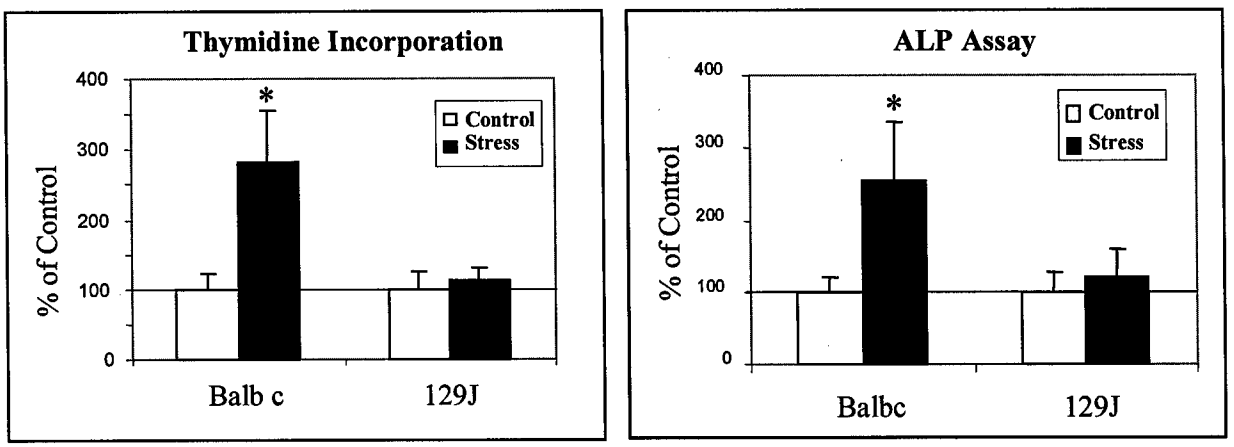

Figure 1: Effect of shear stress on cell proliferation and differentiation in osteoblasts isolated from Balb/c and 129J mice. Cells were subjected to steady fluid flow shear stress of 20 dynes/cm^2 for 30 min. [^{3}H]Thymidine incorporation (left panel) and ALP specific activity (right panel) was measured at 24 hours after the shear stress. Results are shown as mean ± SD (n=6 each) *$p<0.001$, two-tailed Student's t-test.

isolated from B6 mice were highly responsive to shear stress in terms of cell proliferation and differentiation, whereas osteoblasts isolated from C3H mice were unresponsive to the same shear strain. In this regard, our past preliminary work with this cell culture model identified that osteoblasts derived from another pair of inbred strains of mice (i.e., Balb/c and 129J) showed similar differential osteogenic responses to the fluid shear stress, in that Balb/c bone cells responded to the fluid shear stress with a highly significant increase in cell proliferation and differentiation while bone cells derived from 129J mice did not respond to the same shear stress with an increase in cell proliferation and differentiation. We reason that investigations into the differences between the C3H-B6 pair and the Balb/c-129J pair may yield important information

in the mechanotransduction mechanisms as well as the identity of genes that are involved in the regulation of osteogenic response to mechanical loading.

Accordingly, during the past reporting period, we wanted to confirm and further characterize the differential osteogenic responses of bone cells derived from these two mouse strains to a shear stress of 20 dynes/cm^2. Briefly, osteoblasts were isolated from six-week old Balb/c and 129J mice by sequential collagenase digestion and subjected to the fluid flow shear stress of 20 dynes/cm^2 for 30 minutes as described previously. The effect of the shear stress on [^{3}H]thymidine incorporation (an index of cell proliferation) and the specific activity of alkaline phosphatase (a marker of osteoblast differentiation) in these cells were then measured at 24-hr after the shear stress. Figure 1 clearly shows that Balb/c osteoblasts exhibited a highly significant ($P<0.001$) increase in [^{3}H]thymidine incorporation to the shear stress. In contrast, osteoblasts derived from the 129J mice did not show a mitogenic response to the same shear stress in the same experiment. Similarly, this fluid shear stress also significantly increased the specific activity of ALP in Balb/c osteoblasts, but not in 129J osteoblasts. These results are highly reproducible. In addition, these findings confirmed our preliminary findings of a differential response to shear stress of bone cells of these two mouse strains. These findings led us to conclude that Balb/c osteoblasts, like B6 osteoblasts, are responsive to mechanical stresses. However, osteoblasts derived from 129J mice, like those of C3H mice, failed to elicit an osteogenic response to the fluid shear stress. As a result, comparison of the responses in the signaling mechanisms and their corresponding genes in the C3H-B6 and 129J-Balb/c pairs of mice could be useful in determining the mechanotransduction mechanisms and the corresponding genes.

Specific Objective 2: Compare the effects of fluid flow shear strain on key signaling proteins in osteoblasts of mouse strains that respond to mechanical strain and in osteoblasts that fail to respond to mechanical strain.

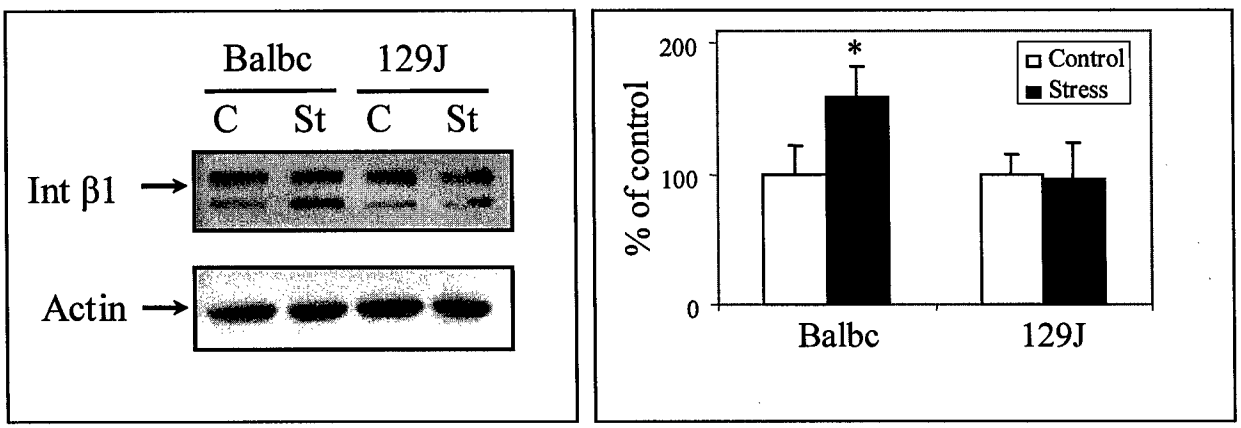

Figure 2. Effect of shear stress on integrin β1 in osteoblasts isolated from Balb/c and 129J mice. Isolated osteoblasts were subjected to a steady fluid flow of 20 dynes/cm^2 for 30 minutes. Cell lysates were immunoblotted with the anti-integrin β1 antibody and reblotted with the anti-actin antibody for normalization. The relative densities of the immunoreative band were determined by laser densitometry. Left panel shows a representative Western blot, and the right panel summarizes the results of the densitometric measurements (in % control) of the relative amounts of integrin β1 band normalized against actin. Results are shown as mean ± SD (n=6). *$p<0.01$.

In order to further clarify the signaling pathways which could be responsible for the differential responses to fluid shear stress-induced in cell proliferation and differentiation between Balb/c and 129J osteoblasts, we first focused on the response in Erk1/2 (MAPK) phosphorylation and integrin β1 expression to the fluid shear stress, since we has previously discovered that B6 osteoblasts, but not C3H osteoblasts, displayed a shear stress-induced MAPK phosphorylation and integrin β1 expression (our previous progress reports). Moreover, there is abundance of evidence that ERK1/2 and integrin activation is involved in the molecular mechanism of osteogenic response to fluid shear stress (5,6). Figure 2 shows that the 30-min steady shear stress of 20 dynes/cm^2 significantly increased the expression of integrin β1 (normalized against the house-keeping gene, actin) by >150% in Balb/c bone cells. In contrast, the same stress had no significant effect on the integrin β1 expression in the 129J bone cells.

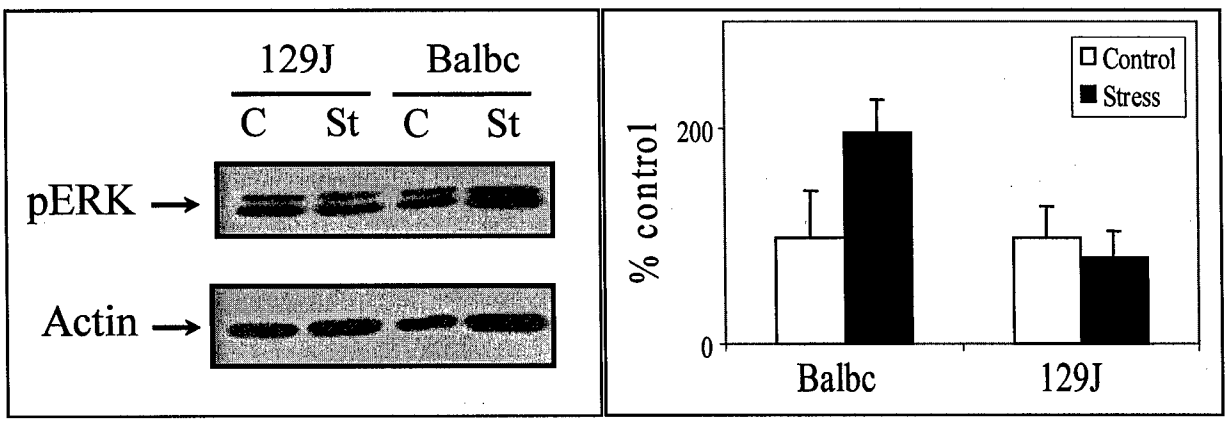

Figure 3. Effect of shear stress on phosphorylation levels of MAPK in osteoblasts isolated from 129J and Balb/c mice. Isolated osteoblasts were subjected to a steady fluid flow of 20 dynes/cm^2 for 30 minutes. Cell lysates were immunoblotted with the anti-phosphorylated ERK1/2 (pERK) antibody and reblotted with the anti-actin antibody for normalization. The relative densities of the immunoreative band were determined by laser densitometry. Left panel shows a representative Western blot, and the right panel summarizes the results of the densitometric measurements (in % control) of the relative amounts of pERK band normalized against actin. Results are shown as mean ± SD (n=6). *p<0.01.

Similarly, when the effect of fluid flow on Erk1/2 (MAPK) phosphorylation was evaluated, it was found that there was a significant increase in the phosphorylation levels of Erk1/2 in Balb/c bone cells in response to the fluid shear stress. Conversely, there was no significant effect on the Erk1/2 phosphorylation level in response to the fluid shear stress in 129J osteoblasts (Figure 3). These results are consistent with our previous results of C3H and B6 osteoblasts (our previous progress report) and suggest that the "defect" in the mechanotransduction pathway in 129J osteoblasts, just like that in C3H osteoblasts, is upstream to the MAPK and integrin activation. Our future studies will attempt to identify the "defect" and to determine whether or not the "defect" in 129J osteoblasts is similar to that in C3H osteoblasts.

Specific Objective 3: Perform DNA microarray studies in osteoblasts isolated from other pairs of inbred mice e.g., Balb/c and 129J, before and after fluid flow shear strain to identify gene expression in osteoblasts in response to mechanical strain.

Studies from our group or others have demonstrated that, while B6 inbred mice responded to *in vivo* mechanical loading with an increased bone formation, C3H mice showed no

such response (3). These findings strongly indicate that genetics play a major part in determining the bone response to mechanical loading. Moreover, our findings that isolated osteoblasts of C3H and B6 strain C3H-B6 and Balb/c-129J mouse pairs in our fluid shear stress cell culture model displayed differential osteogenic responses to the fluid shear stress indicate that the differential response to mechanical loading in B6 (or Balb/c) and C3H (or 129J) inbred strains of mice is intrinsic to their bone cells and strongly suggest that our osteoblast shear stress model can be used in studies to identify the genetic components that are responsible for the differential responses in osteoblasts of these two sets of mouse strains. Accordingly, we postulated that comparative studies of gene expression profiling in osteoblasts derived from the B6-C3H pair or Balb/c-129J pair of inbred mouse strains in response to shear stress could provide important information concerning the signal transduction pathways involved in mechanical stimulation of bone formation. Consequently, the objective of this technical objective was to perform genome-wide gene expression profiling with the microarray approach, first in isolated B6 and C3H osteoblasts 4 hr after the shear stress, to identify potential signaling pathways to account for the differential shear stress response in osteoblasts of these two inbred strains of mice.

Briefly, osteoblasts were isolated from these two strains of mice and subjected to shear stress of 20 dynes/cm^2 for 30 minutes as previously described. RNA was extracted 4 hours after the application of shear stress and in-house microarray was then performed. For the preparation of our in-house microarray chips, cDNA inserts of 5,500 cDNA clones of mouse, rat, human, and monkey genes or Expressed Sequence Tags (ESTs) (a large majority of these were mouse genes and ESTs) were isolated, purified, and evaluated with agarose gel electrophoresis. The microarrays were printed on the amino-silane-coated microscope slides (Corning, NY) using a GMS 417 Arrayer (Genetic MicroSystems). Six replicates of each individual clone were printed on each slide. DNA was fixed to the slides by baking at 80°C for two hours. The experimental approach and the strategy of the preliminary analyses of the microarray experiment are briefly as follows: Primary osteoblasts isolated from B6 or C3H inbred strain of mice were plated on glass slides and subjected to a 30-min steady shear stress as described above. Replicate plates of B6 or C3H osteoblasts were placed in flow chamber without the shear stress as static control. Four hours after the shear stress, total RNA was isolated from cells on each slide. Fluorescently labeled cDNA with Cy5 was synthesized from 1 μg total RNA of cells received the shear stress and fluorescently labeled cDNA with Cy3 was prepared from 1 μg total RNA of corresponding static control as described previously. The microarray hybridization was performed on our in-house microarray chips as described previously. The slide was immediately scanned using a ScanArray 4000 scanner (GSI Lumonics, San Jose, CA). The fluorescent images were acquired using ScanArray software (version 2.1) (GSI Lumonics) and data were analyzed using GeneSpring Image Analysis program (Silicon Genetics, San Jose, CA). Each array spot was individually inspected to eliminate bad samples using the GeneSpring Image Analysis program. Each sample had four replicates. Differences in gene expression between each stress sample and corresponding static control was analyzed using Lowess Normalization. Differences with $p<0.05$ were considered significant. Only known mouse genes (and not ESTs) were analyzed in this study. Because gene annotation of most of the genes and ESTs of our in-house array was lacking, gene ontology and pathway analyses were performed manually according to information available on the PubMed database.

Preliminary analysis of the microarray data indicates that the expression level of 669 genes and ESTs in B6 osteoblasts (360 upregulated and 309 downregulated) was significantly affected at 4 hours after the 30-min shear stress. In contrast, the same shear stress altered the

expression level of 474 genes and ESTs in C3H osteoblasts (212 upregulated and 262 downregulated). Seventy-two genes and ESTs were upregulated in both B6 and C3H osteoblasts, while 80 genes and ESTs were downregulated in both osteoblasts. One gene was upregulated in B6 osteoblasts but downregulated in C3H osteoblasts. Similarly, another gene was downregulated in B6 osteoblasts but upregulated in C3H osteoblasts. Because B6 but not C3H osteoblasts responded osteogenically to the shear stress, we expected that at least some of the genes whose expression was affected only in B6 osteoblasts are involved in the differential response mechanotransduction pathway.

Further gene groupings and pathway analyses of known mouse genes (done manually) showed that the expression of at least 51 known mouse genes were significantly upregulated and the expression of at least 20 known mouse genes were significantly downregulated in response to the shear stress in osteoblasts of both C3H and B6 mice (Tables 1& 2). It is noted that many growth factor and receptor genes were upregulated. However, because C3H osteoblasts failed to show an osteogenic response to shear stress, these shear stress responsive genes are either upstream to the "defect" of the mechanotransduction mechanisms that prevented an osteogenic effect in C3H osteoblasts or are not directly involved in the mechanotransduction mechanisms.

Table 1: Known Mouse Genes Upregulated In Osteoblasts of Both Mouse Strains List of genes in which expression level increased more than two-fold after application of shear stress as compared to control cells isolated from B6 and C3H mice.

Growth Factors
TGF-β1
VEGF-D
Pro-IGF-II
Osteogenic protein (OP)-2
BMP 8b
PDGF A
Growth Factor Receptors
BMP receptor
Thyroid hormone receptor
PTH/PTHrp receptor
Estrogen receptor β
Fibronectin receptor β
Cytokines
IL-1 precursor
IL-1α
Cytokine Receptors
Oncostatin M receptor β
IFN-g receptor
55-kDa TNF receptor
Resorption genes
MMP3
RANKL

Protein Degradation genes ubiquitin-conjugating enzyme HR6A IGFBP5 peptidase DBA/2J delta proteasome subunit proteasome subunit, a type 2 (Psm2)
Structural genes chromatin structural protein
Transcription Factors TFIIIA/TRAF domain M-twist Id2 GATA-binding protein Dermo-1 (twist-related bHLH protein) Hox-7.1 protein (Msx-1)
Signaling Proteins Ran (GTPase) GNA01 G protein RPS3a serum/glucocorticoid-dependent protein kinase (SGK) Calcium-binding protein Cab-45a PTB-associated splicing factor Era (G-protein)-like 1 (Eral1) pleckstrin homology (Sec7 and coil domain 3 (Pscd3)
Protein and RNA Synthesis U2-snRNP b ribosomal protein L23 Robophorin ribosomal protein L27 polynucleotide kinase 3'-phosphatase Spermidine/spermine N1-acetyl transferase
Others 25(OH)-vitamin D 24-hydroxylase a-Amylase-2 Sepiaterin reductase T-complex testis expressed 1 Myocardium phospholipid hydroperoxide glutathione peroxidase Emerin (Emd) SCID complementing gene

Table 2: Known Mouse Genes Downregulated In Osteoblasts of Both Mouse Strains. List of genes in which expression level decreased more than two-fold after application of shear stress as compared to control cells isolated from B6 and C3H mice.

Structural genes
SYNAPSIN I (Syn1)
Cytoplasmic g-actin gene
Cytokines
Ly6/neurotoxin 1 (Lynx1)
Transcription Factors
Transcription factor-like 1 (Tcfl1)
Signaling Proteins
Putative seven pass transmembrane protein (Tm7sf1)
Apoptotoic genes
MA-3 (apoptosis-related gene)
Others
Hippocampal amyloid precursor
Transcription elongation factor A
DNAse-2
Nucleophosmin 1 (Npm1)
Cytochrome b-245 b
APEX nuclease
Sui 1 homolog
Smoothelin, alternatively spliced gene
Complement component C3, a and b subunits
Mcdc21 protein
EIG 180 mRNA for ethanol induced gene product
Protein disulfide isomerase
Protein synthesis elongstion factor Tu (eEF-Tu, eEF-1α

We are interested in obtaining information about mechanotransduction pathways. Because B6 osteoblasts, but not C3H osteoblasts, responded to shear stress, we focused on the identity of known genes that were upregulated in response to the shear stress only in B6 osteoblasts. Thus, further analysis of the data show that many of these genes were growth factors and receptors, signaling proteins, transcription factors, and genes associated with cell proliferation and differentiation, and genes associated with cell proliferation and transport (Table 3). These genes are known to be associated with cell proliferation and differentiation. Thus, these findings are consistent with an osteogenic response to shear stress in B6 osteoblasts.

Table 3. A partial list of known genes whose expression was upregulated in B6 osteoblasts only in response to the shear stress. List of genes in which expression level increased more than two-fold after application of shear stress as compared to control cells isolated from B6 mice.

Growth Factors
FGF-1
Wnt-5a
FGF6
IGFBP5
PDGF-C
keratocyte growth factor (mKGF/FGF-7)

BMP-4 TGF-β2
Growth Factor Receptors IGF-I receptor Alternatively spliced growth hormone receptor/binding protein BMP2/4 type II receptor Estrogen related receptor α
Cytokines Oncostatin M Endothelial monocyte activating polypeptide 2
Cytokine Receptors IL-6 receptor IL-8 receptor
Apoptosis gene Stannin neurotrophin receptor interacting factor (Zfp110) Caspase 6 B-cell leukemia/lymphoma 10 (Bcl10) TR2L Ret finger protein (Rfp)
Transcription Factors c-fos Lymphoid enhancer factor 1 (Lef-1) Leucine rich repeat (in FLII) interacting protein 1 (LRRFLP1) Necdin Zinc finger protein 228 (Zfp228) High mobility group protein 2 Upsteam binding protein 1 Ring finger protein 25 Zinc finger protein 68 (Zfp68) Deltex2deltaE p47-Phox MDM2 binding protein Placental specific homeobox 1 (Psx1) DLX-1 Mesoderm posterior 2 (Mesp2) Nucleosome assembly protein-like 1 Retinoid binding protein 7 Cystein rich protein (Csrp) c-Jun Recombining binding protein suppressor of hairless (RBPSUH) Nuclear receptor coactivator 1 Nonamer binding protein High mobility group protein 14 Ets-related transcription factor (Etv5) Transcriptional factor E3

Myocyte enhancer factor 2A (MEF2) Glucocorticoid receptor interacting protein (GRIP) Retinoic acid receptor γ
Signaling Proteins Big MAP kinase 1a (BMK1), alternatively spliced (Erk5) RPS3a Heat shock 70 protein (Hsc70) IL6 signal transducer (gp130) Soluble acid phosphatase 1 (Acp1) MEK kinase 3 Dual specificity protein phosphatase 10 CDC28 protein kinase 1 14-3-3 sigma protein MAP kinase-interacting serine/threonine kinase 2 G-protein coupled receptor kinase 6-D
Protein Degradation genes Antileukoproteinase 1 Plasminogen Hyaluronidase 2 Extracelluar proteinase inhibitor TIMP-2
Protein and RNA synthesis genes Fibrillarin (Fbl) Ribosomal proteins S6, S16, S21, L21, L29, and L27A RNA polymerase 1-1 U2 SnRPA1 Translation initiation factor 3 Transcription elongation factor TFIIS.h Transcriptional regulator protein Orotidine-5'-monophosphate decarboxylase
Transport genes Soluble carrier family 16 (monocarboxylic acid transporters) member 1 (Slc16a1) Nuclear pore complex glycoprotein p62 Ceroid-lipofuscinosis, neuronal 8 (Cln8) Connexin 31 Vacuolar ATPase subunit C Carbonic anhydrase 4 Bet3 homolog ATPase, H+ transporting, lysosmal (vacuolar proton pump) Solute carrier family 2 (facilitated glucose transporter), member 4 ATP-binding cassette 1, sub-family A, member 1 (Abca1) Potassium channel Kv4.2

Others
Axin
25(OH) vitamin D 1,α hydroxylase
Gelsolin
Myogenin
Pap7
Sca10
Xrcc1
Sacsin
Tex292
Osmotic stress protein 94 (Osp94)
CD9 antigen
Serine palmitoyltransferase
Cd164 antigen
Tm4sf6
3-b hydroxysteroid dehydrogenase
Vamp8
Ermap

To obtain information about potential mechanotransduction pathways, we performed a manual inspection of potential involvement of various signal transduction pathways. The preliminary evaluation of global gene expression profiling suggested the potential involvement of four signal transduction pathways, namely the canonical Wnt pathway, the GH/IGF-I pathway, the estrogen receptor pathway, and the TGFβ/BMP pathway, in the mechanotransduction mechanism leading to an osteogenic response in B6 mice (Table 4-7).

Table 4: Shear Stress Upregulates Genes In The Canonical Wnt Pathway. List of genes of the canonical Wnt pathway in which expression level increased more than two-fold after application of shear stress as compared to control cells isolated from B6 mice.

Wnt Pathway
Wnt-5a
lymphoid enhancer factor 1 (Lef-1)
Axin
β-Catenin

Table 5: Shear Stress Upregulates Genes In The Growth Hormone/IGF Pathway. List of genes of Growth Hormone/IGF pathway in which expression level increased more than two-fold after application of shear stress as compared to control cells isolated from B6 mice. Genes in red letters were upregulated in osteoblasts of both B6 and C3H mice; and genes in black letters were upregulated only in osteoblasts of B6 mice.

The Growth Hormone/IGF Pathway
Growth hormone receptor/binding protein
pro-IGF-II
IGF-I receptor
IGFBP5
MEK kinase 3
14-3-3 σ protein
Low molecular weight dual-specificity protein phosphatase
Big MAPK1/Erk5 (B6 only).
Dual specificity protein phosphatase 10
c-Fos/c-Jun

Table 6: Shear Stress Upregulates Genes In The Estrogen Receptor Pathway. List of genes of Estrogen Receptor pathway in which expression level increased more than two-fold after application of shear stress as compared to control cells isolated from B6 mice. Genes in red letters were upregulated in osteoblasts of both B6 and C3H mice; and genes in black letters were upregulated only in osteoblasts of B6 mice.

The Estrogen Receptor Pathway
Estrogen receptor β
Estrogen receptor α
Nuclear receptor coactivator 1 (NCOA1)
Retinoic acid receptor γ
Glucocorticoid receptor interacting protein (GRIP)

Table 7: Shear Stress Upregulates Genes In The TGF-β/BMP Pathways. List of genes of TGF- β /BMP Pathways in which expression level increased more than two-fold after application of shear stress as compared to control cells isolated from B6 mice. Genes in red letters were upregulated in osteoblasts of both B6 and C3H mice; and genes in black letters were upregulated only in osteoblasts of B6 mice.

The TGF- β/BMP Pathways
TGF-β1
BMP 8b
BMP receptor
BMP-4
TGF-β2
BMP2/4 type II receptor
Necdin
MEF2
DLX-1

Table 8. Gene expression changes in the canonical Wnt pathway genes after fluid flow shear stress on osteoblasts isolated from B6 mice by microarray and Real Time PCR. * Fold of increases compared to corresponding static controls after normalization against β- actin expression level.

Gene	Microarray		Real - time PCR	
	Fold ± SD*	p	Fold ± SD*	p
β-Catenin	2.35 ± 0.019	< 0.01	2.96 ± 0.746	< 0.01
Wnt 5a	1.85 ± 0.017	< 0.05	1.68 ± 0.135	< 0.01
LEF-1	1.62 ± 0.034	< 0.05	2.79 ± 0.486	< 0.01
Axin	1.69 ± 0.037	< 0.05	3.48 ± 0.822	<0.01

To further confirm and better evaluate the role of canonical Wnt signaling pathway in mechanical strain induced cell proliferation in osteoblasts from these two inbred strains of mice, we measured the level of expression of β-catenin, LEF-1, axin, and Wnt5a in response to shear strain using real time PCR in the osteoblasts isolated from C3H and B6 mice. For this, shear strain of 20 dynes/cm^2 was applied to the bone cells from these two strains for 30 minutes. RNA was extracted after 4 hours and expression levels of β-catenin, LEF-1, axin and Wnt5a were measured using real time RTPCR. As shown in Table 8, significant increase in the expression levels of β-catenin, LEF-1, axin, and Wnt5a were seen in B6 bone cells subjected to shear strain as compared to control cells. In case of C3H cells, no change was observed in the levels of these genes in response to shear strain.

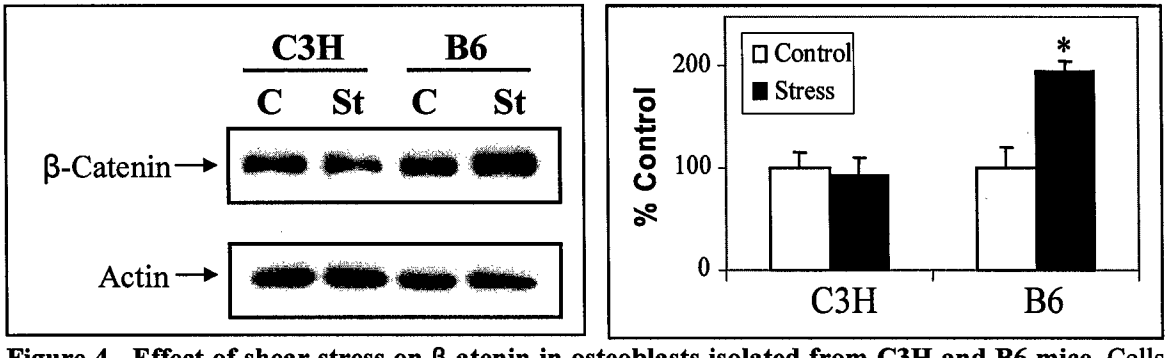

Figure 4. Effect of shear stress on β-atenin in osteoblasts isolated from C3H and B6 mice. Cells were subjected to fluid flow of 20 dynes/cm^2 for 30 minutes. **(Left):** Cell lysates were immunoblotted with anti- β-Catenin and anti-actin antibodies. **(Right):** The graph represents the densitometric measurements of β-Catenin levels from western blots normalized by actin.

In order to further confirm the microarray and real time PCR results, β-catenin expression level in response to shear strain was measured in C3H and B6 osteoblasts by Western blot. Figure 4 shows that shear stress did not have any significant effect on the expression level of β-

catenin in C3H bone cells. However, the same shear stress induced a significant increase (~ 2 fold) in the β-catenin level in B6 osteoblasts.

To gain further insight into genetic basis for difference in loading signal in response to shear stress between other pair of inbred mice strains, we isolated bone cells from 129J and Balb/c mice. These cells were subjected to fluid flow shear stress of 20 dynes/cm^2 for 30 minutes. After four hours, RNA was extracted and analyzed for quality and quantity using bioanalyzer and nanodrop. Microarray will be performed in the future to identify the genes in which the expression level increased more than two-fold when subjected to shear stress as compared to no stress in these two strains.

This preliminary genome-wide gene expression profiling study suggests that at least four well known signal transduction pathways, namely the GH/IGF-I pathway, the estrogen receptor pathway, the canonical Wnt pathway, and the TGF-β/BMP signaling pathway, are involved in the molecular mechanisms of the osteogenic response to the mechanical loading. Past studies from others have provided evidence for the involvement of the estrogen receptor and IGF-I pathways in mediating the osteogenic response to mechanical loading. These findings are consistent with these previous studies. However, our findings of the potential involvement of the canonical Wnt pathway and TGF-β/BMP pathway are novel and have not been previously reported in other studies. More importantly, these studies also raise the strong possibility that the "defect" in C3H osteoblasts responsible for the lack of an osteogenic response to the fluid shear stress compared to B6 osteoblasts occurs upstream to these four signaling pathways. Our further studies will address the relationship between these four signaling pathways in the mechanotransduction mechanism and attempt to identify the "defect" that is responsible for the lack of an osteogenic response to fluid shear stress in C3H osteoblasts.

Key Research Accomplishments:

1. We compared the phenotypic differences between 129J and Balb/c mice in response to fluid flow shear strain and found that osteoblasts isolated from Balbc mice were significantly responsive to shear strain in terms of cell proliferation and differentiation. On the other hand, osteoblasts isolated from 129J mice were unresponsive to the same shear strain.
2. We evaluated strain-induced tyrosine phosphorylation levels of key signaling proteins in 129J and Balbc mice and found that the fluid flow shear stress-induced phosphorylation of Erk1/2 and integrin expression in these cells and found that shear strain induced a significant increase in the integrin β1expression as well as the phosphorylation levels of Erk1/2 in Balb/c bone cells. In contrast, no change was observed in either integrin β1 expression or phosphorylation levels of Erk1/2 in 129J bone cells in response to the steady fluid flow.
3. Global gene expression profiling 4 hrs after a 30-min shear stress revealed that the expression of a large number of genes associated with various anabolic signaling pathway and cell metabolic pathways was upregulated in B6 osteoblasts, but not in C3H osteoblasts.
4. A preliminary inspection of the differential gene expression profiles between B6 osteoblasts and C3H osteoblasts revealed potential involvement of four anabolic signal transduction pathways, namely the canonical Wnt pathway, the IGF-I pathway, the ER pathway, and the BMP pathway, in the mechanotransduction mechanism.

Reportable Outcomes:

1. Sonia Kapur, David J. Baylink, and K.-H. William Lau (2003) Fluid shear stress (a mechanical strain mimic) synergizes with IGF-I on human osteoblast proliferation through upregulation of the IGF-I signaling pathway. Mol Biol Cell 14 (Suppl), 281a, abstract # 1567, at the Annual Meeting of American Society of Cell Biology in San Francisco, California.
2. K.-H. William Lau, Sonia Kapur, and David J. Baylink. (2004) Global application of expression profiling reveals potential involvement of the Wnt, IGF-I, Estrogen Receptor (ER), and BMP/TGFβ pathways in C57BL/6J (B6) but not C3H/HeJ (C3H) mouse osteoblasts in response to fluid shear stress. J Bone Miner Res 19 (Suppl 1), S79, abstract # F264, at 26th Annual Meeting of American Society for Bone and Mineral Research. Seattle, Washington.

Conclusions:

1. These findings provide compelling in vitro evidence that genetics play an important role in determining the bone formation response to mechanical loading.
2. Comparison of global gene expression profiling pattern in osteoblasts of a mouse strain that responds to mechanical stimulation (i.e., B6 osteoblasts) with that in osteoblasts of a mouse strain that does not respond to mechanical stimulation (i.e., C3H osteoblasts) revealed two novel signal transduction pathways (i.e., the canonical wnt pathway and the TGF-β/BMP pathway) that previously have not been identified to be involved in the mechanotransduction mechanism.
3. These findings strongly suggest that the genetic difference (or "defect") that is responsible for the differential response in B6 osteoblasts and C3H osteoblasts occurs upsteam to the IGF-I, estrogen receptor, canonical wnt, and TGFβ/BMP signaling pathways.

References:

1. Lanyon LE 1987 Functional strain in bone tissue as an objective, and controlling stimulus for adaptive bone remodelling. J Biomech, 20:1083-1093.
2. Hillsley MV, and Frangos, JA 1994 Bone tissue engineering: the role of interstitial fluid flow. Biotech Bioeng, 43:573-581.
3. Kodama Y, Umemura Y, Nagasawa S, Beamer WG, Donahue LR, Rosen CR, Baylink DJ, and Farley JR 2000 Exercise and mechanical loading increase periosteal bone formation and whole bone strength in C57BL/6J mice but not in C3H/HeJ mice. Calcif Tissue Int, 66:298-306.
4. Akhter MP, Cullen DM, Pedersen EA, Kimmel DB, and Recker RR 1998 Bone response to in vivo mechanical loading in two breeds of mice. Calcif Tissue Int, 63:442-449.
5. Kapur S, Baylink DJ, and Lau K-HW 2003 Fluid flow shear stress stimulates human osteoblast proliferation and differentiation through multiple interacting and competing signal transduction pathways. Bone, 32:241-251.
6. Kapur S, Chen S-T, Baylink DJ, and Lau K-HW 2004 Extracellular signal-regulated kinase-1 and -2 are both essential for the shear stress-induced human osteoblast proliferation. Bone, 35:535-534.

Report Period: May, 2004 – May, 2005

Molecular Genetic Studies of Bone Mechanical Strain – In Vivo Studies

Introduction:

It is well known that mechanical stimulus is one of the important factors in the development and maintenance of skeletal tissues (1). *In vivo*-increased mechanical stress on bone tissue changes the bone density and morphology, resulting in an increased bone mass, whereas lack of mechanical stress leads to a rapid bone loss as evidenced by immobilization and bed rest studies (2). Thus, physical exercise has been used as a strategy in humans to maintain bone mass and prevent osteoporosis. Recent studies (3) in humans have shown that the bone anabolic response to a given mechanical load is highly variable with some individuals exhibiting robust bone formation while others respond modestly. A similar variation has been observed in some animal models, such as B6 and C3H mouse strains, in which the same degree of *in vivo* loading (4, 5) caused extremely different responses in total vBMD and bone size between these two strains. This great variation in skeletal response in human and mice is largely determined by genetic factors.

To identify the genes and pathways that contribute to the observed variation in bone anabolic response, various approaches such as microarray, gene knock out, and QTL (Quantitative trait loci) can be used. We use the QTL technique to identify critical regions in the chromosomes that are important in mediating loading response. This approach has been used extensively to study the genetic characteristics of bone and several quantitative trait loci have been mapped for the skeletal phenotypes such as BMD (total volumetric bone mineral density) (6), bone strength (7), femoral length, etc. in inbred strains.

Body:

In the present study, we used B6 and C3H as two optimal mouse strain pairs for our QTL study because B6 mice showed a 15% increase in BMD while C3H exhibited no change in response to mechanical stress. To our knowledge, the genetic contribution for this difference in the mechanical adaptation observed between B6 and C3H strains has not yet been analyzed *in vivo*. We therefore crossed these two strains of mice to produce 329F2 female mice, which were given mechanical loading using a four-point bending device at 9N load 2Hz for 36 cycles at 10-weeks. Change in the bone parameters were measured in live animals using pQCT (Peripheral quantitative computerized tomography) after 12 days loading. Genome wide scan was performed and mechanosensitive QTLs that co-segregate with the phenotype were identified using MapQTL program.

Technical Objectives:

Our goals for the next twelve months of the funding period are as follows:

1) To cross two strains of mice (a poor responder strain and a good responder strain) to produce F1 mice.
2) To intercross F1 mice from these two mouse strains to produce approximately 300 F2 mice.
3) To begin phenotyping the 300 F2 mice with our newly validated phenotype (i.e. real-time PCR of bone marker genes).
4) To begin genotyping the 300 F2 mice.
5) To determine the fate of new bone gained during 2 weeks of mechanical loading (i.e. to determine how long the bone density and/or bone strength gained during 2

weeks of mechanical loading is maintained after termination of 4-point bending).

6) To determine if the load applied to increase optimal anabolic response causes micro cracks in loaded bone.

Specific Objective 1: To cross two strains of mice (a poor responder strain and a good responder strain) to produce F1 mice.

In the previous report, we demonstrated that the B6 mouse is a good responder to mechanical loading and C3H is a poor responder in terms of BMD response. We therefore selected these two inbred strains of mice for our QTL study to localize the genetic regions responsible for increasing bone's anabolic response to mechanical stress. We used 20 female B6 and 10 male C3H mice with two females and one male in each cage, giving a total of 10 cages, to produce 100 F1s (a mix of male & female).

Specific Objective 2: To intercross F1 mice from these two strains to produce about 300 F2 mice.

A population of 329 F2 female mice was generated from 100 F1s (brother-sister mating). We used female mice for our study in the F2 population for three reasons: 1) There was no difference in the bone response to mechanical loading between the sexes in the parental strains (B6 and C3H mice); 2) The males are aggressive and territorial compared to females; and 3) All our previous experiments to establish the phenotypic difference between the B6 and C3H mice to mechanical load were carried out in females.

Specific Objective 3: To begin phenotyping the 300 F2 mice with our newly validated phenotype.

The F2 animals, after reaching 10-weeks, were mechanically loaded for 12 days using four-point bending according to our optimized regimen (9N load at 2Hz, 36 cycles). We used halothane [95% Oxygen and 5% Halothane] for 2-3 minutes to anesthetize the mice and performed mechanical loading while the mice were anesthetized. Prior to loading and while the mice were anesthetized, we used the ankle of the tibia that sits on the lower secondary immobile point as a reference which allowed us to position the loading region of the tibia similarly for each mouse. The right tibia was used for loading and the left tibia was used as an internal control. Two days after the last loading regimen, changes in the bone parameters were measured *in vivo* in the loaded vs unloaded tibia using the pQCT system from Stratec XCT Research. The mice were anesthetized using a solution of sterile water, ketamine (16.6 mg/mL), and xylazine (3.3 mg/mL). The mice were weighed and the ketamine/xylazine solution was injected in cubic centimeters (ccs) based on the gram weight of the mice [gram weight multiplied by 0.0036 (0.06 mg ketamine/g mouse, 0.012 mg xylazine/g mouse)]. The bone measurements were then taken using pQCT while the mice were anesthetized and afterwards the mice recovered from the anesthetsia near a heat source. To minimize the measurement errors caused by positioning of the tibia for pQCT, we used the tibia-fibular junction as the reference line in all F2 mice. We selected two-slices (1mm intervals) that were 4 mm proximal from the tibia-fibular junction for pQCT measurement. The reasons for selecting the two slices were as follows: 1) this region corresponds to the loading zone; 2) To complete pQCT scanning of more than two slices would take 25 minutes and longer for one mouse; 3) Since we are performing *in vivo* pQCT, straight positioning of the tibia in our scout view was very important for measuring the transverse-cross section accurately, which also consumes time; and 4) Long duration of ketamine/xylazine

anesthesia can lead to death in the mice, which would have reduced the number of mice in our F2s.

After the pQCT measurements, the mice were sacrificed for isolation of following tissues: a) livers were collected and stored in -80°C for DNA extraction; b) tibias were collected, and stored at -80°C for extracting RNA to perform real time PCR for candidate genes to use as phenotype for expression QTLs. The overall duration of time to complete the four-point bending experiments was approximately 8 months, which includes: 1) 1 month and 15 days to generate 100 F1 offspring; 2) The F1s mice were housed for 4-weeks and were weaned to perform the sister-brother mating; and 3) 2 months to generate 329 F2 offspring from 100 F1s. The F2 mice were kept in house for 3–5 months until they reached 10-weeks and then mechanical loading using four-point bending was performed.

We next analyzed the pQCT data for the changes in the bone parameters such as vBMD, mBMD and bone size in the unloaded and loaded bones of F2 animals. We used two thresholds that have been selected based on preliminary studies. A 180-730 mg/cm^3 threshold was used to measure total area, total mineral content, periosteal circumference, and endosteal circumference in the loaded vs. unloaded bones. A 730-730-mg/cm^3 threshold was used to measure cortical thickness, total volumetric density, and material bone mineral density. The data obtained from pQCT measurements were tested for statistical significance using Statistica software (8) to investigate: a) Heritability index for bone phenotypes; b) the distribution of phenotypes in the F2 populations; c) if anabolic response of bone induced by mechanical load is dependent upon the body weight or bone size in the F2 population.

a) Heritability index for bone phenotypes

We used a formula that allows us to calculate the heritability index of each phenotype without the F1 data. The formula is provided below:

$$H = \frac{Vf2 - \frac{1}{2}[Vp1+Vp2]}{Vf2}$$

H= stands for heritability index
Vf2 = stands for variation of phenotype in the F2 population
Vp1= stands for variation of phenotype in the parent 1
Vp2= stands for variation of phenotype in the parent 2
½ = corresponds to 50% variation of phenotypes in both parents

We therefore applied this formula for the following phenotypes in the F2 population to calculate the heritability index and the results are as follows:

a) vBMD (Total volumetric Bone Mineral Density)

$$H = \frac{12.59 - \frac{1}{2}[1.50 + 2.87]}{12.59} = 82\%$$

b) mBMD (Material Bone mineral Density)

$$H = \frac{1.74 - \frac{1}{2}[0.08 + 0.94]}{1.74} = 70\%$$

c) Bone size (Periosteal Circumference)

$$H = \frac{77 - \frac{1}{2}[11.37 + 10.36]}{77} = 86\%$$

In this formula, Vp1 corresponds to C3H mice and Vp2 corresponds to B6 mice. We used five mice in each parent group and 329 F2 mice to perform this calculation.

b) Phenotype distribution in the F2 population

Mechanical loading by four-point bending resulted in increased vBMD, mBMD, and bone size in most of the F2 animals. These three phenotypes (vBMD, mBMD, and bone size), major determinants of bone strength, showed a continuous distribution with a heritability of 70-80% in the F2 population (**Fig 1**). All these three phenotypes showed variable bone response to mechanical loading in terms of vBMD (-6 to+20%), mBMD (-5 to+5%), and PC (-10% to+40%) in the F2 population suggesting that mechanical load induced bone response is a complex trait controlled by several genes.

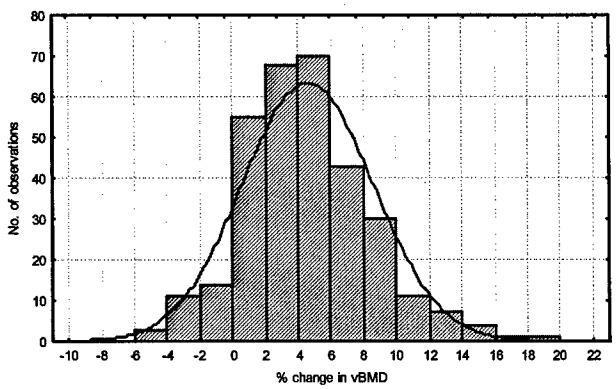

(a)

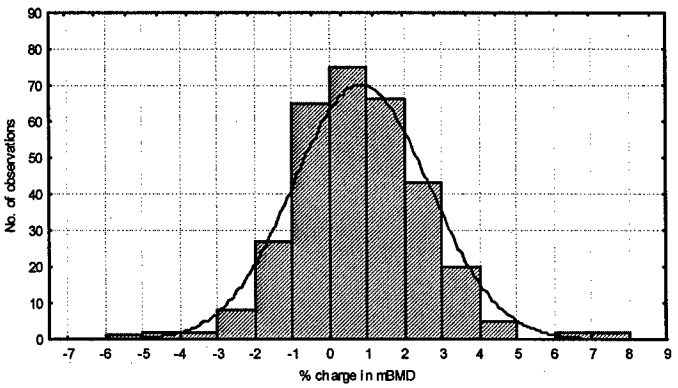

(b)

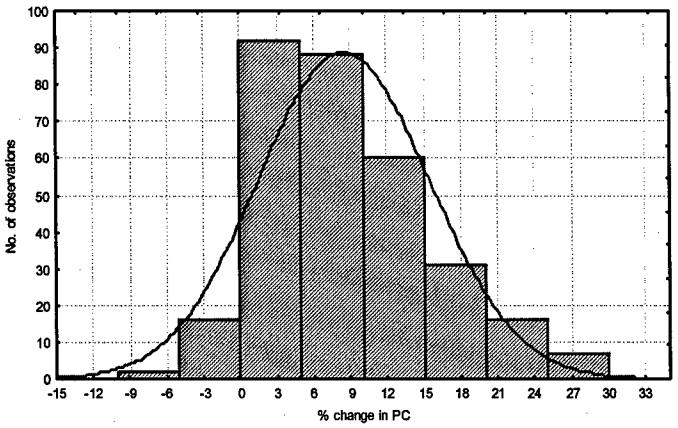

(c)

Figure 1. Distribution of percentage changes for (a) vBMD, (b) mBMD, and (c) PC in the F2 population after two weeks of four-point bending. The x-axis represents the percentage change ('–'indicates reduction) and y-axis represents the number of observations (mice). vBMD, volumetric bone mineral density; mBMD, material bone mineral density; PC, periosteal circumference. The solid line represents theoretical normal distribution. Based on kolmogorov-smirnov test, vBMD, mBMD, and PC show normal distribution (n=329).

c) Correlation of bone size (unloaded bones) and body weight with percent changes in vBMD and mBMD.

We next correlated percentage changes of vBMD and mBMD in response to four-point bending with body weight and unloaded bone size in the F2 population to determine if the anabolic response of bone mediated by mechanical load is dependent on the weight of the animal and size of the bone. We found mechanical load-induced bone phenotype (vBMD and mBMD) showed no correlation with the bone size (unloaded bones) of the F2 population suggesting that the increase in BMD is independent of bone size. (**Fig 2**).

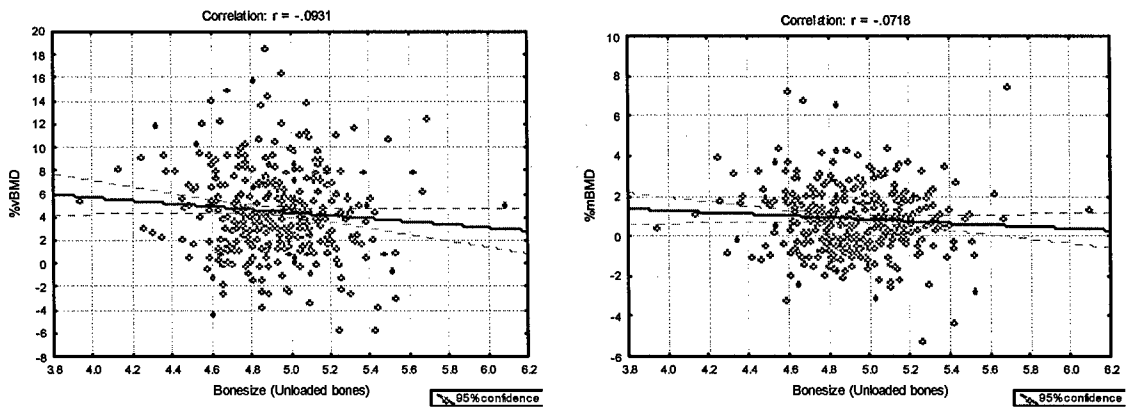

(a) (b)

Figure 2. Correlation of bone size (unloaded bones) with the percentage change in the (a) vBMD and (b) mBMD of the F2 population after mechanical loading. The x-axis represents bone size (periosteal circumference) and y-axis represents percentage change in the vBMD and mBMD. N=329

Simultaneously, the changes in the vBMD, mBMD, or PC induced by mechanical loading did not show significant correlations with body weight in the F2 population (**Fig 3**). This finding suggests that mechanical loading-induced bone responses in the F2 population are unrelated to changes in body weight and bone size.

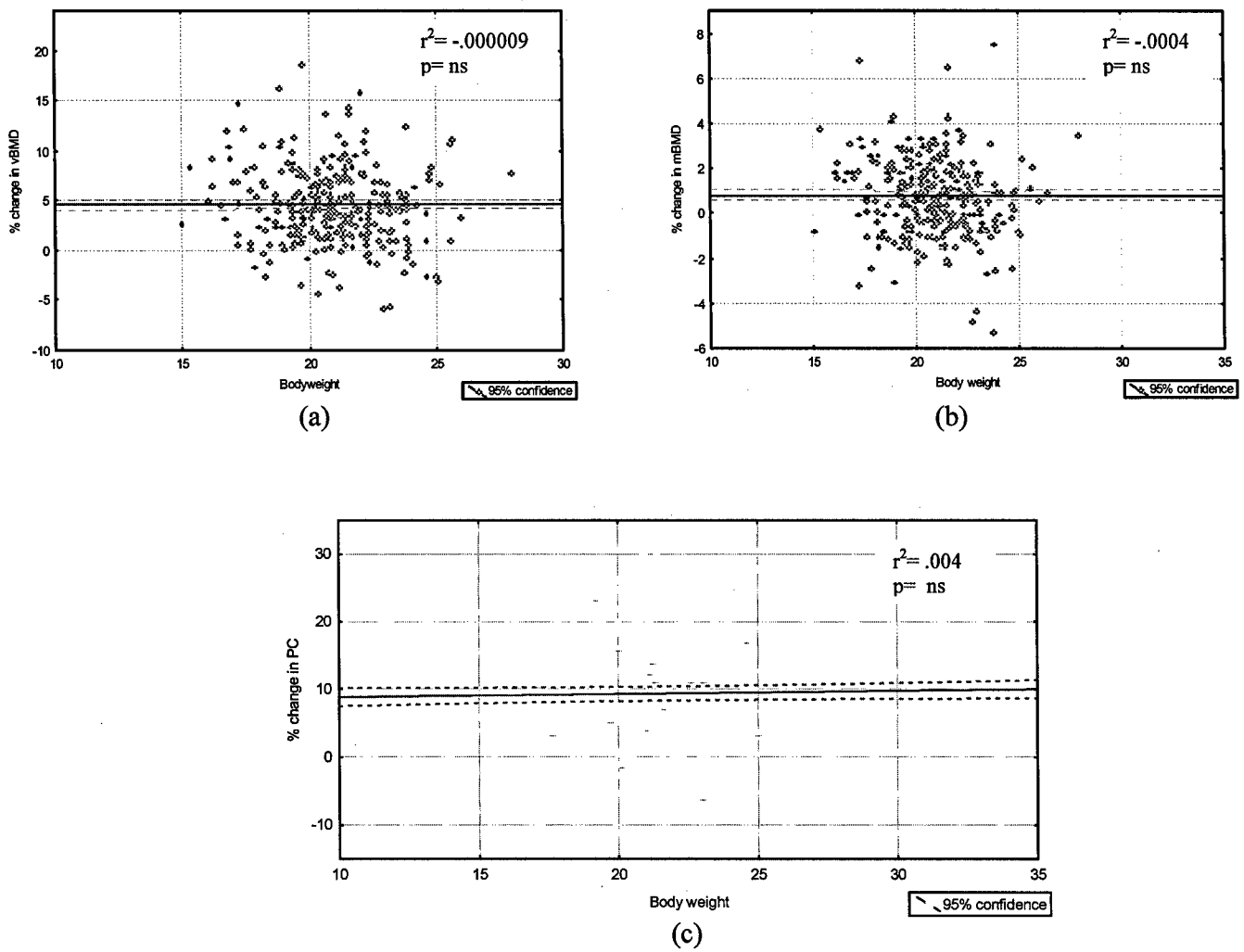

Figure 3. Correlation of body weight with percentage change in the (a) vBMD, (b) mBMD, and (c) PC of F2 population after mechanical loading. The x-axis represents body weight and the y-axis represents percentage change in the bone phenotypes. ns: not significant, vBMD, Total volumetric bone mineral density; mBMD, Material bone mineral density; PC, Periosteal circumference. N=329

In our QTL study, we have also proposed to use expression changes of genes as our newly validated phenotype for identifying chromosomal regions linked to mechanical loading.

This allows us to validate our QTLs obtained from the pQCT measurements. Accordingly in the F2 populations, after *in vivo* measurement of bone parameters, mice were sacrificed and tibias were collected for extracting RNA.

4) Improvement in the RNA extraction protocol

In our preliminary study we encountered several problems in extracting RNA from a single bone, including prior reproducibility of the technique and variability in quality between the samples. The variation in quality of RNA between samples could influence gene expression changes measured by real time PCR. We used a Qiagen Kit (RNeasy Lipid Tissue RNA extraction kit) with modification to extract high quality and quantity of RNA from bone (**Fig.4**). The optimized protocol for extracting RNA from tibias of F2 population is mentioned below.

A Qiagen lipid RNA extraction kit [Qiagen, Valencia, CA] was used to extract RNA from bones with the following modification. After euthanization, tissues were removed from test mice and stored with RNA later (a chemical that prevents degradation of RNA) at -80°C. The autoclaved mortar and pistol were washed twice prior to our extraction, using DEPC water and cooled with liquid nitrogen (This kept the bone RNA from degrading while in the mortar). At this point, 4-6mm bone was added and liquid nitrogen was added three times until it froze. This caused the bone to become brittle and easier to achieve a fine powder. Approximately 1ml of Trizol was added to each sample and ground until it became a finer powder. This fine bone powder were removed from the cold mortar using a sterile razor blade and transferred quickly to a fresh 1.5 ml RNase free tube. Chloroform (200 µl) was added to each sample, and each sample was shaken (up & down) for 15 seconds and incubated at room temperature for 3 minutes (This step is highly important because long duration of incubation and forceful shaking degrade the RNA). The samples were then centrifuged at 12,000 g for 15 minutes and the aqueous layer was removed carefully to a fresh tube after centrifugation. Approximately 700 µl of ethanol was added to the fresh samples and shaken gently (up & down) for 15 seconds. The samples were then transferred to a spin column and the RNA was purified according to the manufacturer's instructions. Quality and quantity of RNA were analyzed using Bio-analyzer and Nano-drop instrumentation [Agilent].

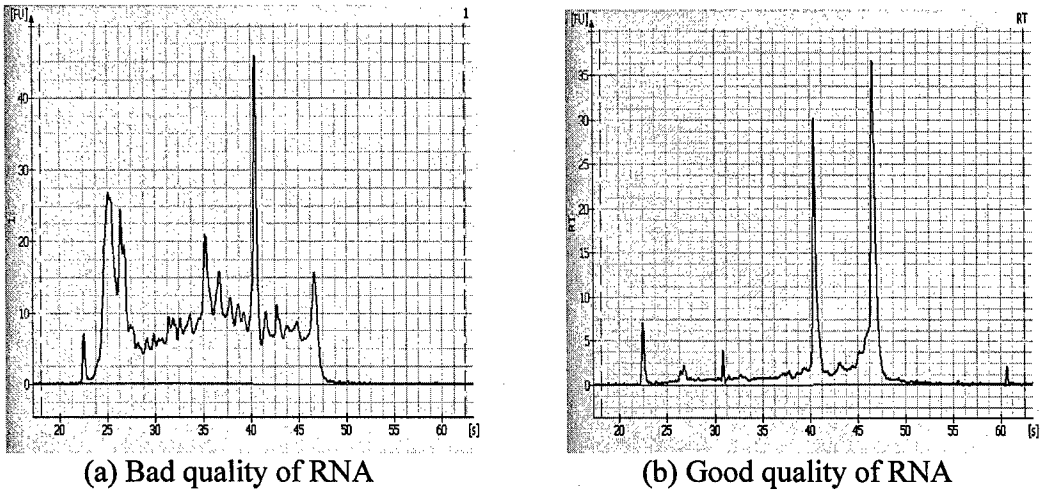

(a) Bad quality of RNA (b) Good quality of RNA

Figure 4. Quality of the RNA extracted from bone.
'a' represents poor quality of RNA extracted from marrow-fleshed bone with old protocol. 'b' represents

good quality of RNA extracted from 4-6mm bone with altered protocol.

In all F2 mice, the RNA was extracted from the 4-6mm region of tibia, which represents the loading zone. Presently, we have extracted RNA from 100 mice and the rest 229 are in progress. After completing RNA extraction from the F2 populations, real time PCR will be performed using bone marker genes. Using the Ct-values of the bone gene and genotype data, loci that segregate with phenotypes will be identified by the MapQTL program/Pseudomarker program.

Specific Objective 4: To begin genotyping the 329 F2 mice.

We extracted DNA from the liver of each F2 mouse using a qiagen DNA extraction kit. The quality and quantity of the extracted DNA was measured by nano-drop and bio-analyzer.

120 Polymerase chain reaction primers (9) will be purchased from Applied Biosystems to perform the genotyping on the F2 population. All these markers were chosen depending upon the position on the chromosome in an effort to distribute then at <15cM to generate a complete genome wide scan. A list of markers is shown in **Table-1.** To proceed faster and restrict the usage of more chemicals in our genotyping reaction, we have optimized the PCR reactions (Eppendorf reagents were used) and running conditions to perform multiplexed (3-4 micro satellite markers) in a single electrophoretic lane.

Table-1 shows a list of genotyping markers for the B6-C3H intercrosses and the estimate PCR product size

Markers	cM	Product size
D1MIT64	0	87-118
D1MIT430	6.6	116-136
D1MIT169	12	215-229
D1MIT236	25.1	81-115
D1MIT380	37.2	117-148
D1MIT215	47	147-165
D1MIT60	59	270-310
D1MIT495	69.9	144-173
D1MIT102	75.4	87-103
D1MIT106	83.1	94-120
D1MIT113	91.8	206-228
D1MIT150	99.5	118-154
D1MIT17	110.4	170-190
D2MIT1	2.2	195-239
D2MIT242	28.4	124-144
D2MIT66	48.1	246-284
D2MIT395	55.7	131-177
D2MIT285	72.1	103-169
D2MIT145	84.2	118-160
D2MIT148	91.8	117-217
D3MIT203	9.8	234-267
D3MIT67	20.8	231-245

D3MIT57	40.4	154-184
D3MIT320	50.3.2	91-117
D3MIT147	59	253-277
D4MIT193	12	127-155
D4MIT268	21.9	103-157
D4MIT9	39.3	202-245
D4MIT28	45.9	240-256
D4MIT251	66.7	72-110
D4MIT256	82	77-107
D5MIT146	0	89-117
D5MIT387	10.9	186-194
D5MIT201	28.4	98-117
D5MIT277	40.4	253-283
D5MIT425	54.6	191-211
D5MIT247	73.2	167-179
D5MIT143	82	95-115
D6MIT274	10.9	95-115
D6MIT209	21.9	139-180
D6MIT284	30.6	193-204
D6MIT36	40.4	197-215
D6MIT14	63.4	156-181
D7Mit21	0	259-297
D7Mit294	5.5	170-177
D7Mit228	16.4	187-206
D7Mit71	53.6	134-226
D8MIT63	13.1	209-257
D8MIT178	35	168-191
D8MIT211	50.3	161-199
D8MIT88	60.1	131-149
D8MIT49	68.9	206-236
D9MIT2	13.1	173-196
D9MIT97	24	149-181
D9MIT336	33.9	150-172
D9MIT355	49.2	94-129
D9MIT151	69.9	109-145
D10MIT213	6	238-270
D10MIT86	12	214-226

D10MIT115	33.9	85-146
D10MIT95	50.3	174-208
D10MIT233	63.4	107-137
D11MIT2	4.4	109-137
D11MIT231	14.2	67-103
D11MIT86	25.1	91-105
D11MIT285	49.2	92-129
D11MIT333	69.9	81-113
D11MIT214	77.6	146-178
D12Mit103	1.1	170-196
D12Mit59	9.8	82-128
D12Mit60	13.1	94-124
D12Mit143	29.5	134-164
D12Mit16	50.3	247-261
D13Mit56	2.2	192-288
D13Mit275	7.7	111-127
D13Mit19	14.2	160-182
D13Mit13	21.9	144-154
D13Mit144	35	135-150
D13Mit260	45.9	180-204
D14Mit201	12	115-139
D14Mit174	17.5	131-145
D14Mit82	28.4	72-90
D14Mit39	38.3	247-283
D14Mit68	45.9	142-168
D14Mit263	52.5	112-131
D14Mit228	55.7	135-199
D15Mit80	4.4	149-162
D15Mit252	9.8	288-310
D15Mit143	19.7	88-142
D15Mit67	29.5	151-181
D15Mit107	41.5	135-187
D15Mit159	49.2	249-285
D15Mit161	65.6	264-292
D16Mit131	6.6	173-213
D16Mit169	36.5	238-318
D16Mit189	40.4	177-206
D16Mit153	45.9	77-103

D17Mit51	14.2	131-157
D17Mit180	25.1	84-111
D17Mit93	39.3	155-177
D17Mit1	50.3	316-230
D18Mit64	0	159-179
D18Mit12	9.8	93-115
D18Mit91	19.7	124-152
D18Mit186	30.6	76-132
D18Mit48	35	165-181
D18Mit144	38.3	182-193
D19Mit68	3.3	110-126
D19Mit28	9.8	152-168
D19Mit88	24	143-155
D19Mit17	33.9	69-109
D19Mit33	45.9	233-327
DXMIT81	12	211-229
DXMIT68	20.8	138-148
DXMIT64	31.7	162-182
DXMIT172	40.4	205-219
DXMIT223	59	185-191

Key Research Accomplishments:

1. We have completed mechanical loading in the F2 populations of B6 and C3H intercrosses.
2. Changes in the bone parameters (loaded vs. unloaded) were measured and analyzed using pQCT for three phenotypes (vBMD, mBMD, and bone size) in the F2 populations.
3. All these three phenotypes showed normal distribution in the F2 population, which demonstrate that multiple loci harboring several genes are influencing the bone response to mechanical stress.
4. We have ordered the primers from ABI to perform the genotyping in the F2 populations.
5. We optimized a method to extract good quality of RNA from 4-6mm bone.

Reportable Outcomes:

1. Chandrasekhar K, Mohan S, Oberholtzer S and Baylink DJ. Mechanical loading induced gene expression and BMD changes are different in two inbred mouse strains. Accepted in Journal of Applied Physiology, 2005.

Conclusions:

1. Bone response to a standard mechanical loading can be divided into at least three different phenotypes (changes in bone size, vBMD and mBMD). All these three phenotypes in our study showed Gaussian distribution with a heritability of 75-85%, suggesting that bone

response is a complex trait controlled by multiple genetic loci.

References:

1. Umemura Y, Baylink DJ, Wergedal JE, Mohan S, Srivastava AK. 2002 A time course of bone response to jump exercise in C57BL/6J mice. J Bone Miner Metab, 20(4):209-15.
2. Kodama Y, Dimai HP, Wergedal J, Sheng M, Malpe R, Kutilek S, Beamer W, Donahue LR, Rosen C, Baylink DJ et al. 1999 Cortical tibial bone volume in two strains of mice: effects of sciatic neurectomy and genetic regulation of bone response to mechanical loading. Bone; 25(2):183-90.
3. Dalsky GP, Stocke KS, Ehsani AA, Slatopolsky E, Lee WC, Birge SJ. 1988 Weight Bering exercise training and lumbar bone mineral content in postmenopausal women. Ann Intern Med, 108:824-828.
4. Akhter MP, Cullen DM, Pedersen EA, Kimmel DB, Recker RR. 1998 Bone response to *in vivo* mechanical loading in two breeds of mice. Calcif Tissue Int; 63(5):442-9.
5. Chandrasekhar K, Mohan S, Oberholtzer S and Baylink DJ. 2005 Mechanical loading induced gene expression and BMD changes are different in two inbred mouse strains. Accepted J of Applied Phys.
6. Beamer WG, Shultz KL, Donahue LR, Churchill GA, Sen S, Wergedal JR, Baylink DJ, Rosen CJ. 2001 Quantitative trait loci for femoral and lumbar vertebral bone mineral density in C57BL/6J and C3H/HeJ inbred strains of mice. J Bone Miner Res. Jul; 16(7):1195-206.
7. Li X, Masinde G, Gu W, Wergedal J, Mohan S, Baylink DJ.2002 Genetic dissection of femur breaking strength in a large population (MRL/MpJ x SJL/J) of F2 Mice: single QTL effects, epistasis, and pleiotropy. Genomics. May, 79(5):734-40.
8. StatSoft, Inc. 2003. STATISTICA (data analysis software system), version 7.1 www.statsoft.com
9. http://www.cidr.jhmi.edu/mouse/mouse.html and http://www.appliedbiosystems.com/

Molecular Genetic Studies of Bone Mechanical Strain – In Vitro Studies

Introduction:

The interstitial fluid flow through the lacunar/canalicular spaces generated by the strains exerted by mechanical loading produces strains in the mineralized matrix of bone creates a shear stress at surfaces of osteoblasts and osteocytes lining these spaces. This shear stress then generates biochemical signals that transducer to the nucleus of bone cells to exert biological effects (1). Therefore, fluid flow shear stress has been used by our laboratory as well as other laboratories as a surrogate in vitro model for mechanical loading. We have developed a Cytodyne flow chamber system for the fluid shear stress model and used to investigate the mechanism(s) whereby the shear stress transduces biochemical signals from the membrane to the nucleus is commonly referred to as the mechanotransduction mechanism (2,3).

A major objective of this work was to identify essential signaling pathways that are involved in the mechanotransduction mechanism to produce the osteogenic response. Consequently, during this reporting period, we used the Cytodyne flow chamber system to identify signaling pathways and their components that play a role in the mechanotransduction pathway.

Body:

Our microarray analysis for differential global gene expression profiles between C57BL/6J (B6) osteoblasts and C3H/HeJ (C3H) osteoblasts suggests the involvement of at least four osteogenic signal transduction pathways in the mechanotransduction mechanism. These four pathways are the GH/IGF-I pathway, the estrogen receptor pathway, the canonical wnt pathway, and the TGF-β/BMP pathway. Accordingly, the work for the reporting period focused on confirming the role of these pathways in the mechanotransduction pathway. The first specific objective will focus on the IGF-I pathway. For this study we used human TE85 osteosarcoma cells. The second specific objective addresses the role of each of the remaining three pathways using corresponding specific inhibitors. Osteoblasts derived from B6 mice will be used for work in specific objective #2.

Technical Objective:

To continue *in vitro* studies to identify signaling proteins that show differential responses to mechanical loading in osteoblasts.

1) Identify key signaling protein/s that are regulated by tyrosine phosphorylation in osteoblasts from inbred strains of mice consistent with their response to mechanical strain.
2) Evaluate the role of select candidate protein/s on osteoblast cell response to mechanical strain by using a specific inhibitor of tyrosine phosphorylation of a candidate protein or by using osteoblasts from mice lacking a corresponding functional gene (i.e., knock out mice for candidate protein).

Specific Objective 1. To identify key signaling protein/s that are regulated by tyrosine phosphorylation in osteoblasts from inbred strains of mice consistent with their response to mechanical strain.

We focus on the IGF-I signaling pathway first for the following two reasons: 1) bone growth factors function as autocrine and paracrine mediators of bone formation (4). We believe that the mechanism whereby mechanical stimulation of osteoblast proliferation and activity should involve bone growth factors and corresponding signaling pathways. In this regard, IGF-I is one of the most abundant bone growth factors (4). Loading increases bone cell production of IGF-I (5, 6). The signaling pathway of IGF-I involves Erk1/2 activation, which is essential for mechanical stimulation of bone cell proliferation and activation (3). It has been suggested that that the bone cell mitogenic response to mechanical strain is mediated by the IGF-I receptor (IGF-IR) (7). 2) There is evidence mechanical loading might have a permissive role in the IGF-I mitogenic action in bone, as skeletal unloading induces resistance to IGF-I with respect to bone formation (8). Accordingly, unloading blocked the ability of IGF-I to stimulate bone formation in the rat. IGF-I administration stimulates bone formation in the loaded bone, but not in unloaded bone (8, 9).

In these studies, human TE85 osteoblastic cells were subjected to a steady fluid shear stress of 20 dynes/cm^2 for 30 min followed by 24-hr incubation with osteogenic doses of IGF-I (0 to 50 ng/ml). IGF-I significantly increased the cell proliferation (~1.5 to 2.5 fold, $p< 0.01$, ANOVA) of human osteoblasts in a dose-dependent manner (Fig. 1A). The 30-minutes steady shear stress at 20 dynes/cm^2 alone also significantly ($p<0.01$) increased [^{3}H]thymidine incorporation (by 70%) compared to the corresponding static control cells. The combination of shear stress and the test doses of IGF-I produced much greater than additive stimulations (~ 3.5

to 5.5 fold) of each treatment alone (Figure.1A). Two-way ANOVA indicates a highly significant interaction between the shear stress and IGF-I ($p<0.001$). These findings suggest that there is a synergistic interaction between IGF-I and fluid shear stress in the stimulation of human bone cell proliferation.

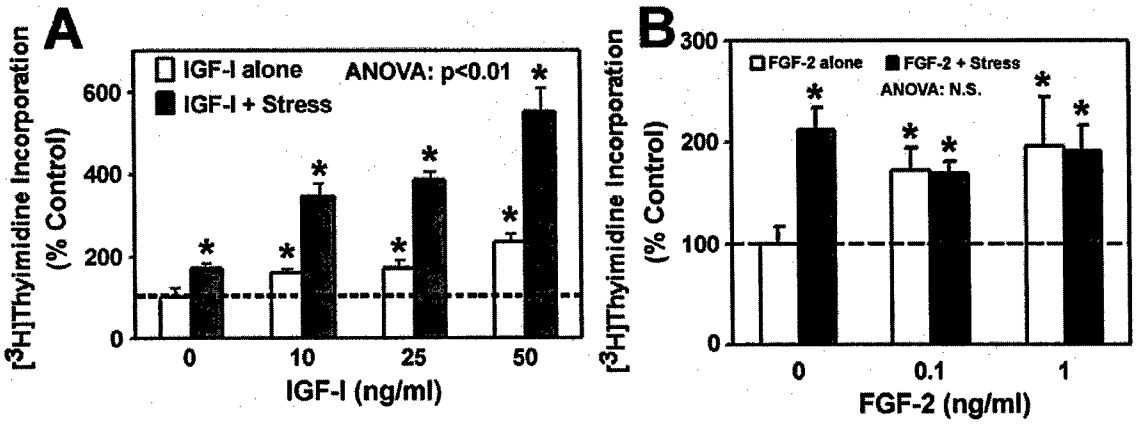

Figure 1. Interaction between IGF-I (A) or FGF-2 (B) and fluid shear stress on the proliferation of TE85 osteosarcoma cells. The effect of IGF-I or FGF-2 at the indicated concentrations with (filled bars) or without (open bars) a 30-min steady shear stress of 20 dynes/cm^2 on TE85 cell proliferation was assessed by measuring [3H]thymidine incorporation 24-hr later. Results are shown as mean ± SD (n=6). *$p<0.01$ (compared to the static control).

To test if the synergistic interaction between shear stress and IGF-I on human bone cell proliferation is a general feature between bone cell growth factors and shear stress, we evaluated if shear stress would also synergistically enhance the mitogenic activity of FGF-2 (another potent bone cell growth factor) in TE85 cells. Fig. 1B shows that FGF-2 alone significantly and dose dependently ($p<0.01$) stimulated the TE85 cell proliferation (by ~1.5-fold to 2-fold). The combined treatment of the shear stress and FGF-2 yielded no further enhancement (p=N.S., two-way ANOVA) than FGF-2 alone, indicating that the synergistic interaction between shear stress and IGF-I is not universal to all bone growth factors.

Because the mitogenic action of IGF-I is mediated through Erk1/2 activation, and fluid shear stress also activates Erk1/2 in osteoblasts, we investigated the effect of shear stress and/or IGF-I (or FGF-2) on Erk1/2 phosphorylation (an index of Erk1/2 activation). Fig. 2A confirms that IGF-I alone at the test doses significantly and dose dependently ($p<0.01$, one-way ANOVA) increased the pErk1/2 level (by ~1.2 to 5-fold) in TE85 cells. The 30-min steady shear stress alone also significantly ($p<0.01$) increased the pErk1/2 level (by ~2.5-fold). The combination of shear stress and IGF-I treatment produced a synergistic ($p<0.01$, two-way ANOVA) enhancement (up to 12-fold) in Erk1/2 phosphorylation. Fig. 2B indicates that the mitogenic doses of FGF-2 (0.1 and 1 ng/ml) alone also markedly and significantly increased the pErk1/2 levels in TE85 cells ($p<0.01$, one-way ANOVA). In contrast to IGF-I, the combination treatment of shear stress and FGF-2 did not result in a further increase in the pErk1/2 level compared to the FGF-2 treatment alone (p=N.S., two-way ANOVA). These findings further support the conclusions that the synergistic interaction between shear stress and IGF-I on bone cell proliferation is mediated through synergistic enhancement of IGF-I-dependent activation of the

Erk1/2 mitogenic signaling pathway and that the synergy between shear stress and IGF-I on human bone cell proliferation is not shared by FGF-2.

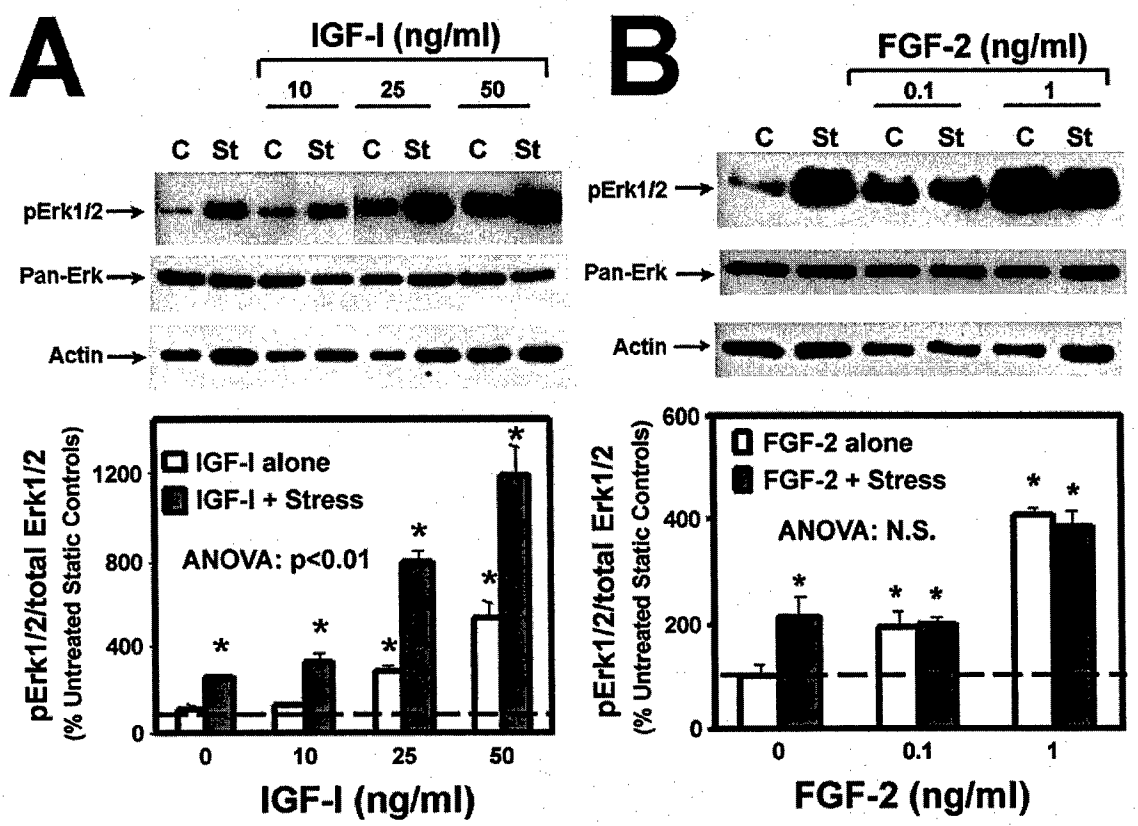

Figure 2. Interaction between IGF-I (A) or FGF-2 (B) and fluid shear stress on Erk1/2 phosphorylation in TE85 cells. Top panels show representative western blots of phoshporylated Erk1/2 (pErk1/2). Each blot was stripped and rebloted against anti-pan-Erk and anti-actin antibodies for loading controls. Bottom panels summarized the results of three separate repeat experiments. Results are shown as mean ± SD. *p<0.01 (compared with no addition control).

To further evaluate if Erk 1/2 activation is essential for the synergy between IGF-I and shear stress, we next determined the effect of U0126 (a specific inhibitor of MEK1) on the shear stress and/or IGF-I induced cell proliferation and Erk1/2 phosphorylation. Fig. 3A shows that pretreatment with U0126 at 10 μM completely blocked the IGF-I-mediated as well as the shear stress-induced TE85 cell proliferation. It also completely abolished the synergistic enhancement of IGF-I and shear stress. Fig. 3B shows that U0126 pretreatment completely blocked the shear stress as well as IGF-I induced phosphorylation of Erk1/2 confirming that both shear stress and IGF-I effects on cell proliferation are mediated by Erk 1/2 pathway and that the synergy between IGF-I and shear stress involve Erk 1/2 activation. These findings also indicate that the synergy between shear stress and IGF-I led to activation of bone cell proliferation occurs upstream to the Erk1/2 activation.

We next tested whether the synergy between IGF-I and shear stress occurs prior to or after the phosphorylation of IGF-IR receptor. Figure 4 shows that IGF-I significantly and dose dependently increased the phosphorylation levels of IGF-IR (~ 2 to 3.5 fold p<0.01) in the human osteoblasts *in vitro*. Shear stress alone also increased the phosphorylation levels of IGF-

IR (~ 2.5 fold, $p<0.01$). Again the combination of IGF-I and shear stress led to a synergistic enhancement in the IGF-IR phosphorylation (~ 8 fold, $p<0.01$).

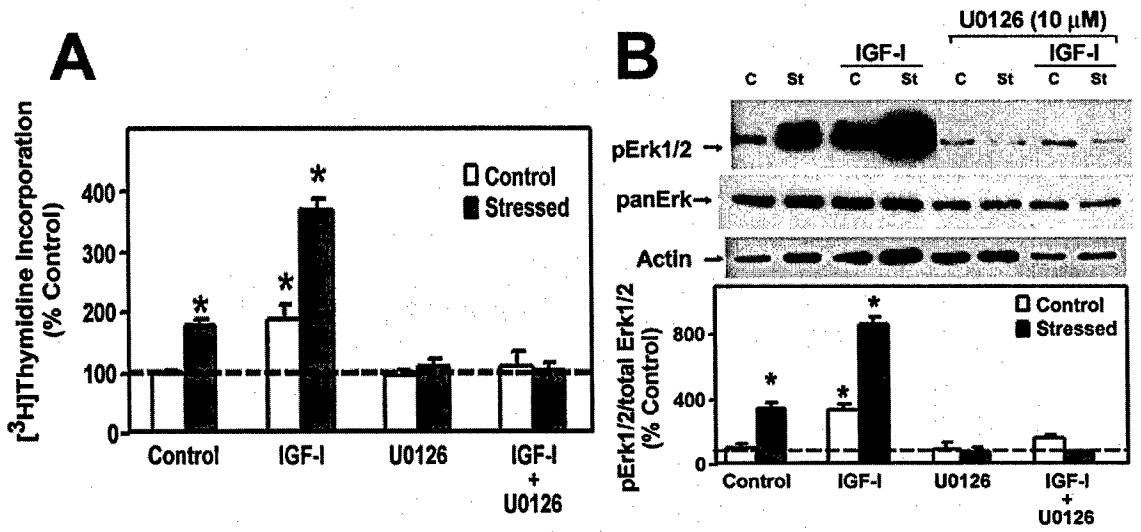

Figure 3. Effects of U0126 (a specific inhibitor of the Erk signaling pathway) on the stimulation of cell proliferation (A) and Erk1/2 protein-tyrosine phosphorylation (B) mediated by IGF-I and/or shear stress in TE85 cells. TE85 cells were pretreated with 10 μM U0126 overnight before subjecting to the shear stress and/or IGF-I treatments. A shows the effects of U0126 on [3H]thymidine incorporation in response to the 30-min steady shear stress of 20 dynes/cm2 and/or 10 ng/ml IGF-I. Top panel of B shows a representative western blot of pErk1/2. Each blot was stripped and rebloted against anti pan-Erk and antiactin antibodies for loading controls. Bottom panel of B summarized the results of three separate repeat experiments. Results are shown as mean ± SD. *$p<0.01$ (compared with no addition control).

Because shear stress synergistically enhanced IGF-IR phosphorylation, which is initiated by the binding of IGF-I to IGF-IR, we next assessed whether the synergistic enhancement between IGF-I and shear stress was due to an increase in IGF-I binding to IGF-IR. Figure 5 shows that 30-min steady 20 dynes/cm^2 shear stress slightly but significantly ($p<0.05$) enhanced the binding of IGF-I to IGF-IR. However, this effect was too small to explain for the large synergic interaction between IGF-I and shear stress on IGF-IR phosphorylation, Erk1/2 activation, and/or cell proliferation.

Because shear stress activates integrin pathway, we evaluated whether integrin activation is involved in the synergy by measuring the effect of echistatin (integrin receptor antagonist) on [^{3}H]thymidine incorporation and IGF-IR phosphorylation in response to shear stress with or without IGF-I in human osteoblasts. As shown in figure 6A, echistatin reduced basal cell proliferation by 60%, but slightly but not significantly reduced the mitogenic response to shear stress as compared to the control. However, echistatin completely abolished the mitogenic effect of the IGF-I and also that of the combination treatment of shear stress and IGF-I. Similarly, echistatin also completely abolished the basal, shear-stress, or IGF-I-induced IGF-IR phosphorylation (Fig. 6B). These findings suggest that the synergy between IGF-I and shear stress on the proliferation and that on IGF-IR phosphorylation level may involve integrin activation.

Recent studies suggest that IGF-IR activation in response to IGF-I binding led to

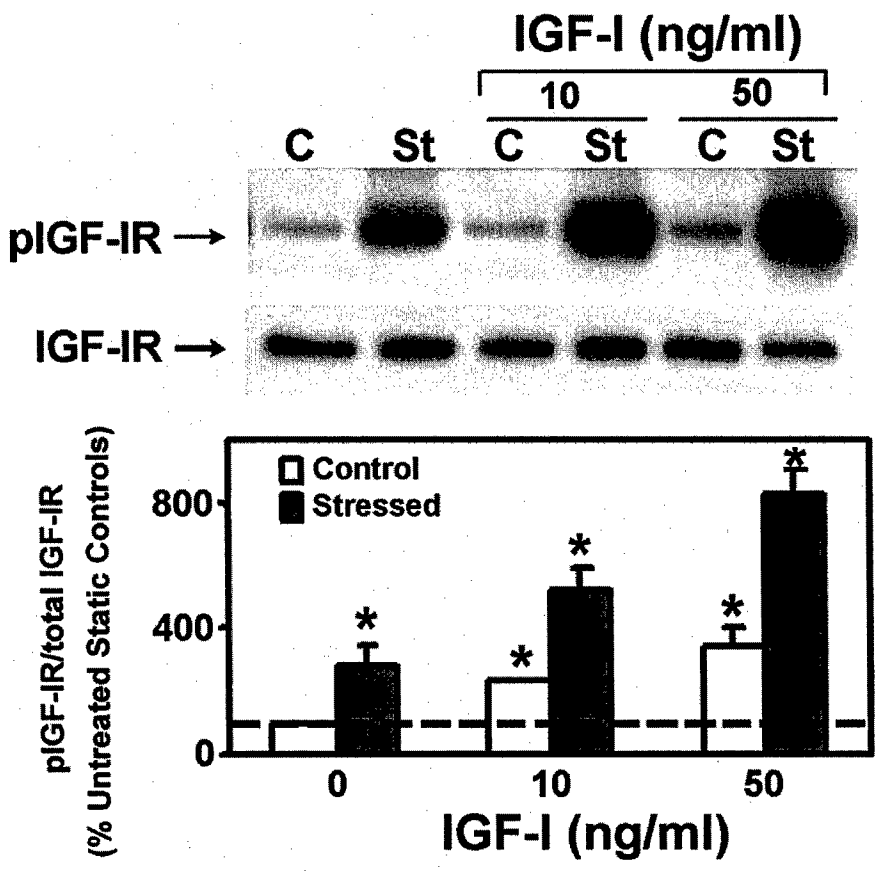

Figure 4. Interaction between IGF-I and fluid shear stress on IGF-I receptor (IGF-IR) phosphorylation in TE85 cells. Top panel shows a representative western blot of phosphorylated IGF-IR (pIGF-IR). The blot was stripped and reblotted against an anti-IGF-IR antibody for loading controls. Bottom panels summarized the results of three separate repeat experiments. Results are shown as mean ± SD. *p<0.01 (compared with no addition control).

recruitment of SHP2 to the IGF-IR. SHP2 would then dephosphorylate IGF-IR, terminating the activation of IGF-I signaling pathway. However, activation of the integerin pathway results in recruitment of SHP2 away from the IGF-IR complex, leading to the sustained IGF-IR phosphorylation and activation of IGF-I pathway (10). Consequently, we next evaluated the effect of IGF-I and/or shear stress on the relative amounts of SHP-2 associated with integrin β3 or with IGF-IR. Figure 7 shows that shear stress, IGF-I, and the combination each significantly enhanced the recruitment of SHP-1 to integrin β3 and away from IGF-IR.

We also determined whether the synergistic interaction could also involve integrin dependent recruitment of the related SHP-1 away from the IGF-IR. Figure 8 shows that fluid shear stress, IGF-I, and the combination treatment each also significantly enhanced the recruitment of SHP-1 to integrin β3 and away from the IGF-IR. However, the effects of fluid shear stress on the recruitment of SHP-2 away from the IGF-IR appeared to be bigger than those on the SHP-1 recruitment. These findings suggest that the synergy between IGF-I and shear stress at least in part involves the integrin-dependent inhibition of SHP-mediated IGF-IR dephosphorylation by recruiting away the SHP-1 and SHP2 from the phosphorylated IGF-IR

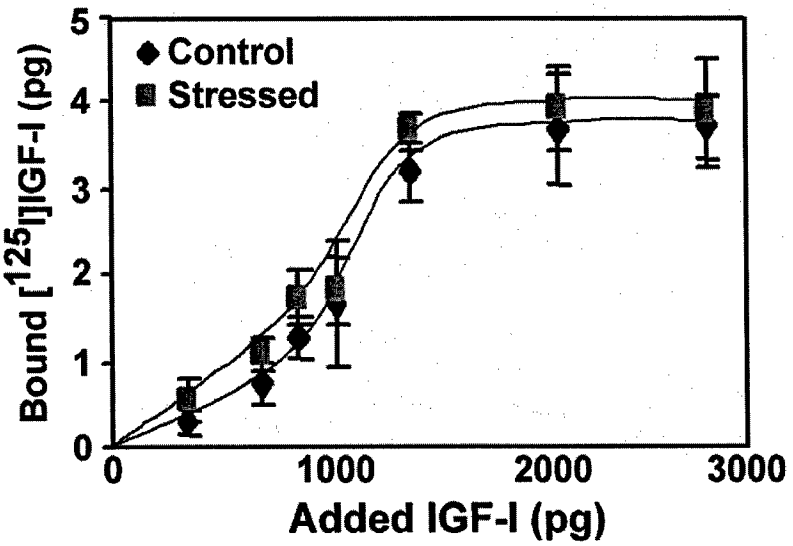

Figure 5. Effects of fluid shear stress on specific binding of IGF-I to IGF-IR in TE85 cells. The binding of IGF-I to surface IGF-IR of TE85 cells was performed by measuring the receptor bound [125I]IGF-I. Total and non-specific IGF-I binding was determined in the absence and presence of 100 X non-radioactive "cold" IGF-I, respectively. Specific binding of IGF-I to IGF-IR was calculated by subtracting the nonspecific binding from the total binding. Only specific binding is shown in this figure. The filled squares were cells receiving the shear stress; whereas the filled diamonds were the corresponding static controls.

These results demonstrated for the first time that a 30-min steady fluid shear stress of 20 dynes/cm^2 in human osteoblastic cells enhanced synergistically the mitogenic action of IGF-I through an up-regulation of the Erk1/2-mediated IGF-I mitogenic signaling pathway. Accordingly, these findings substantiated the results of our preliminary microarray studies indicating that the mechanotransduction pathway might involve the IGF-I signaling pathway. Consequently, it appears that mechanical loading not only plays a permissive role in the osteogenic actions of IGF-I, but also interacts synergistically with the IGF-I signaling pathway to promote bone formation. More importantly, our findings that the disintegrin echistatin completely abolished the synergy on IGF-IR and bone cell proliferation and the previous finding that unloading-related resistance to IGF-I is mediated through down-regulation of integrin expression (9) together raise the strong possibility that the synergy between shear stress and IGF-I on bone cell proliferation involves integrin activation.

Our findings that shear stress, IGF-I, and the combination treatment increased the relative amount of SHP-2 that was associated with integrin β3 and that each also reduced the relative amount of SHP-2 co-immunoprecipitated with IGF-IR are consistent with the hypothesis that the shear stress-mediated recruitment of SHP-2 to activated integrins and away from IGF-IR may be responsible for the synergy between shear stress and IGF-IR to promote bone cell proliferation. We also found that shear stress, IGF-I, and the combination treatment also increased the relative amount of the integrin β3-associated SHP-1 and reduced the relative amount of IGF-IR-associated SHP-1. This suggests that SHP-2 and the related SHP-1 are both involved in the IGF-I signaling mechanism as well as in the synergy between shear stress and IGF-I in enhancing the overall IGF-IR phosphorylation and activation.

The effect of unloading on recruitment of SHP-2 and/or SHP-1 to integrins has not been assessed previously. Thus, it is unclear at this time whether or not the unloading-induced resistance to IGF-I may also involve a reduction of SHP-2 and/or SHP-1 recruitment to integrins.

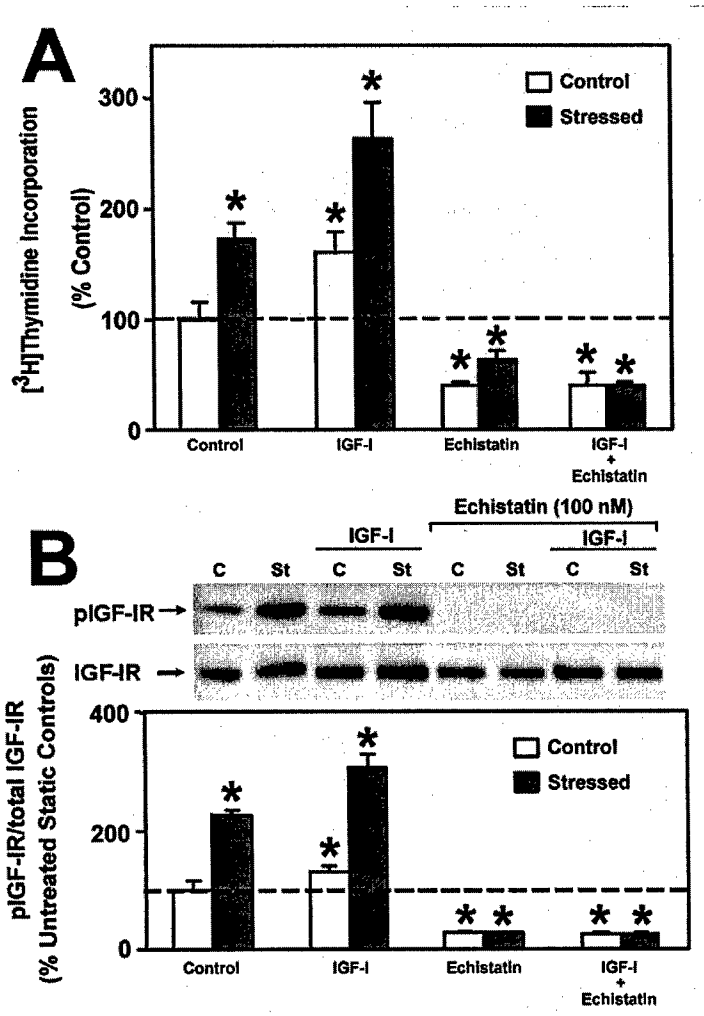

Figure 6. Effect of echistatin on the synergy between IGF-I and shear stress with respect to cell proliferation (A) and IGF-IR phosphorylation (B). TE85 cells were pretreated with 100 nM echistatin overnight prior to the 30-min shear stress and/or the IGF-I treatment. In A, cell proliferation was measured by [3H]thymidine incorporation. In B, the IGFIR phosphorylation level was determined by Western analysis. Top panel shows a representative western blot of pIGF-IR. The blot was stripped and reblotted against an anti-IGF-IR antibody. Bottom panels summarized the results of three separate repeat experiments. Results are shown as mean ± SD. *$p<0.01$ (compared with no addition control).

However, because unloading down-regulated integrin expression in osteoblasts and because SHP-2 recruitment to integrins is essential for IGF-I signaling, it is likely that the reduced integrin recruitment of SHP-2 and/or SHP-1 in response to unloading-mediated down-regulation of the integrin pathway could also play a pivotal role in the permissive effect of mechanical loading on the IGF-I anabolic action in bone.

Specific Objective 2: To evaluate the role of select candidate protein/s on osteoblast cell response to mechanical strain by using a specific inhibitor of tyrosine phosphorylation of a candidate protein or by using osteoblasts from mice lacking a corresponding functional gene.

Work in the first specific objective has clearly demonstrated the involvement of the IGF-I signaling pathway in the mechanotransduction mechanism. Thus, the aim of this specific objective was to assess the potential involvement of the other three pathways, namely the canonical wnt pathway, the estrogen receptor pathway, and the TGF-β/BMP pathway in the mechanotransduction mechanism. The approach used in this work was to evaluate the effect of a specific inhibitor of each of these three pathways on the shear stress-induced osteoblast proliferation. Since all of these signaling pathways in B6 osteoblasts appear to be responsive to fluid shear stress, B6 osteoblasts were used in these studies.

To study if the canonical Wnt/β-catenin pathway is involved in the mechanical signaling,

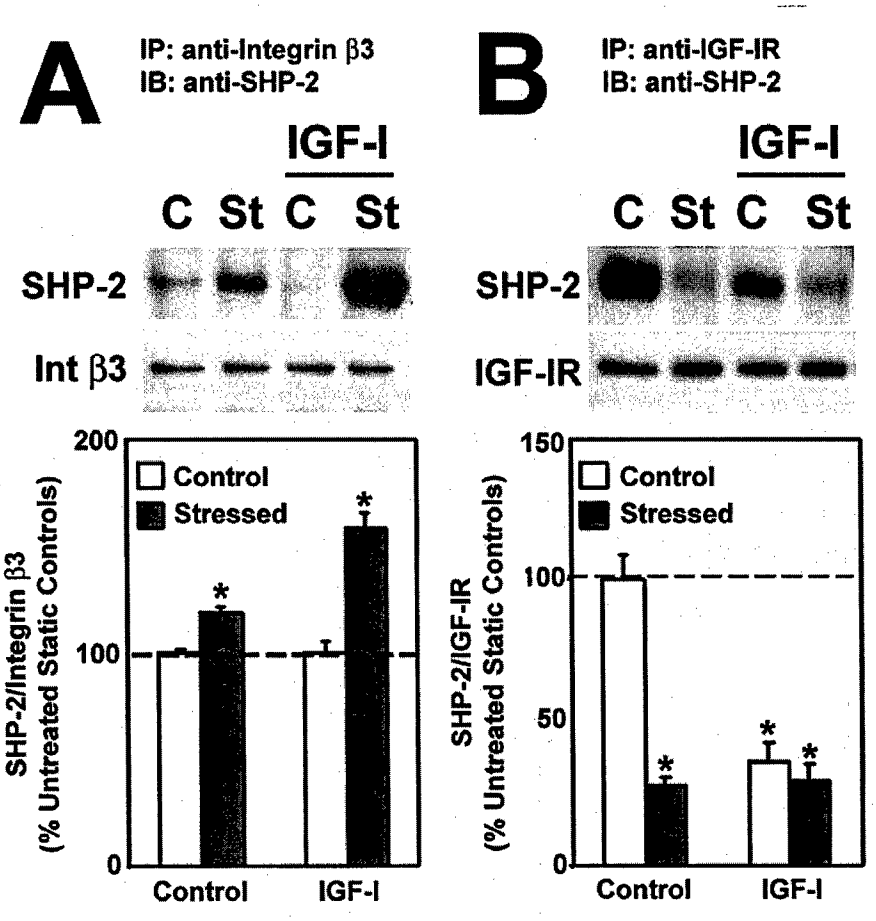

Figure 7. Effect of IGF-I or shear stress on recruitment of SHP-2 to integrin β3 or to IGF-IR. The recruitment of SHP-2 to integrin β3 and away from IGF-IR was assessed by measuring the relative amounts of SHP-2 co-immunoprecipitated with integrin β3 (A) or with IGF-IR (B). The amounts of immunoprecipitated SHP-2 were normalized against the corresponding levels of immunoprecipitated integrin β3 and IGF-IR, respectively. Top panels show representative Western immunoblots against SHP-2 or integrin β3 and IGF-IR, respectively. Bottom panels summarize the results as percentage of respective untreated control (mean ± SD) of 4 replicate experiments. *p<0.01.

we evaluated if endostatin (a specific inhibitor of the canonical Wnt pathway) would inhibit the shear stress-induced β-catenin expression and if endostatin would also abolish the shear stress induced cell proliferation of B6 osteoblasts. The effect of endostatin on the shear stress-induced β-catenin gene expression was assessed by real-time PCR. As shown in Table 1, the fluid shear stress-induced gene expression of β-catenin was completely blocked by treatment of 10 μg/ml endostatin. When the effect of endostatin on the shear stress-induced [^{3}H]thymidine incorporation (an index of cell proliferation) was assessed, endoststatin only partially but significantly ($p<0.002$) blocked the fluid flow-induced increase in [^{3}H]thymidine incorporation (Figure 9).

Table 1. Effect of endostatin pretreatment on shear strain induced β-catenin expression in B6 osteoblasts. Cells isolated from B6 mice were pretreated with 10μg/ml endostatin for 24 hours and subjected to shear strain of 20 dynes/cm^2 for 30 minutes. RNA was extracted 4 hours later and Real Time PCR was performed for β-catenin levels. The fold changes were defined in relative to the expression level of osteoblasts not subjected to shear strain.

Gene	Fold Change (Strain vs. Control)

	Without ES	With ES
β-Catenin	2.96	0.06

Since our previously studies have demonstrated that Erk1/2 activation is essential for the mechanotransduction mechanism (3), we next evaluated the effect of endostatin pretreatment on Erk1/2 activation in B6 osteoblasts to further test whether the canonical wnt pathway is important for the osteogenic response to mechanical loading. As shown in figure 10, similar to that in shear stress-induced cell proliferation, endostatin partially but significantly abolished the fluid flow-induced increase in the phosphorylation of Erk1/2.

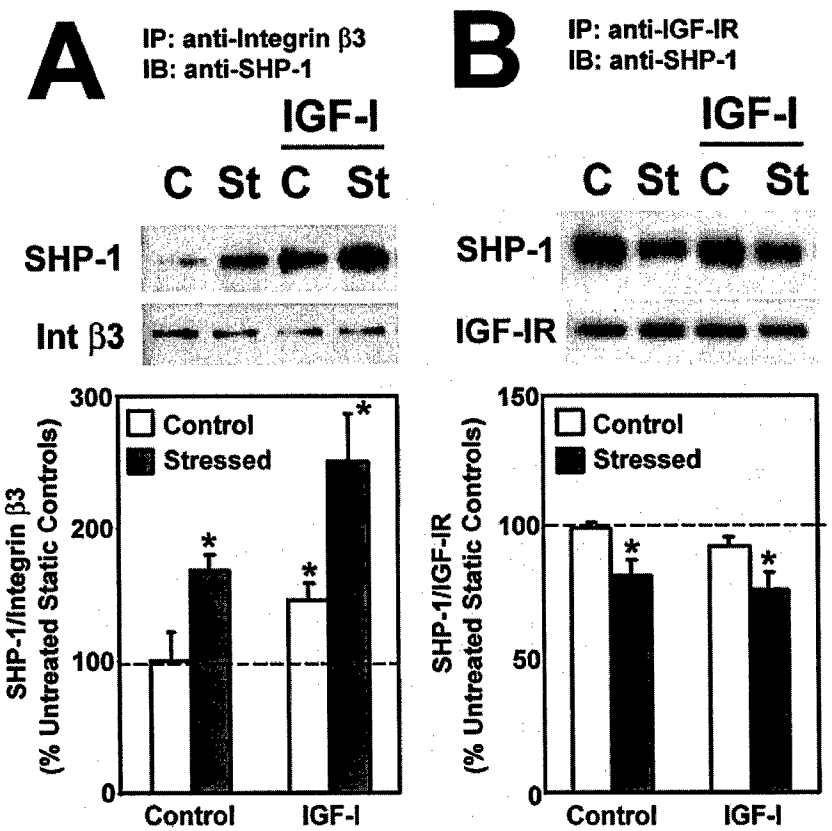

Figure 8. Effect of IGF-I or shear stress on recruitment of SHP-1 to integrin β3 or to IGF IR. The recruitment of SHP-1 to integrin β3 and away from IGF-IR was assessed by measuring the relative amounts of SHP-1 co-immunoprecipitated with integrin β3 (A) or with IGF-IR (B). The amounts of immunoprecipitated SHP-1 were normalized against the corresponding levels of immunoprecipitated integrin β3 and IGF-IR, respectively. Top panels show representative Western immunoblots against SHP-1 or integrin β3 and IGF-IR, respectively. Bottom panels summarize the results as percentage of respective untreated control (mean ± SD) of 4 replicate experiments. *$p<0.01$.

These preliminary inhibitor findings provide strong circumstantial evidence that the canonical wnt pathway is at least in part involved in the mechanotransduction mechanism. Our results also suggest that the wnt pathway is upstream to the Erk1/2 activation. However, an intriguing and potential important observation is that endostatin at 15 μg/ml, while it completed abolished the shear stress-induced β-catenin gene expression, was only partially inhibited the shear stress-mediated activation of Erk1/2 and bone cell proliferation. The significance of this observation remains to be determined. However, it raises the strong possibility that

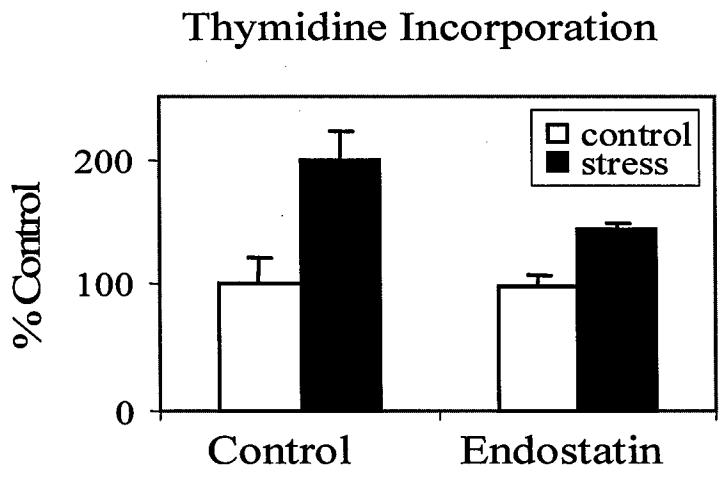

Figure 9: Effect of endostatin pretreatment on shear strain induced cell proliferation in osteoblasts isolated from B6 mice. Cells were pretreated with 10 μg/ml endostatin for 24 hours and subjected to shear strain of 20 dynes/cm^2 for 30 minutes. [^{3}H]thymidine incorporation was measured after 24 hours.

the wnt pathway is not absolutely essential for the shear stress-mediated bone cell proliferation.

We next tested whether the estrogen receptor (ER) signaling pathway is involved in the mechanotransduction mechanism of osteoblasts. Previously studies by Lanyon and his co-workers have clearly established the important role of estrogen receptor in the mediation of mechanical stimulation of bone cell proliferation and bone formation (7). Our approach to assess the role of the estrogen receptor signaling pathway was to evaluate the effects of a specific inhibitor of estrogen receptor (ICI182780) in B6 osteoblasts on the shear stress-induced bone cell proliferation (i.e., [^{3}H]thymidine incorporation). In these studies, primary B6 osteoblasts were pretreated with 200 nM of ICI182780 for 24 hours prior to the 30-min shear stress of 20 dynes/cm^2. The effect of ICI182780 pretreatment on [^{3}H]thymidine incorporation was then evaluated.

As shown in Figure 11, ICI182780 completely abolished the shear stress-induced cell

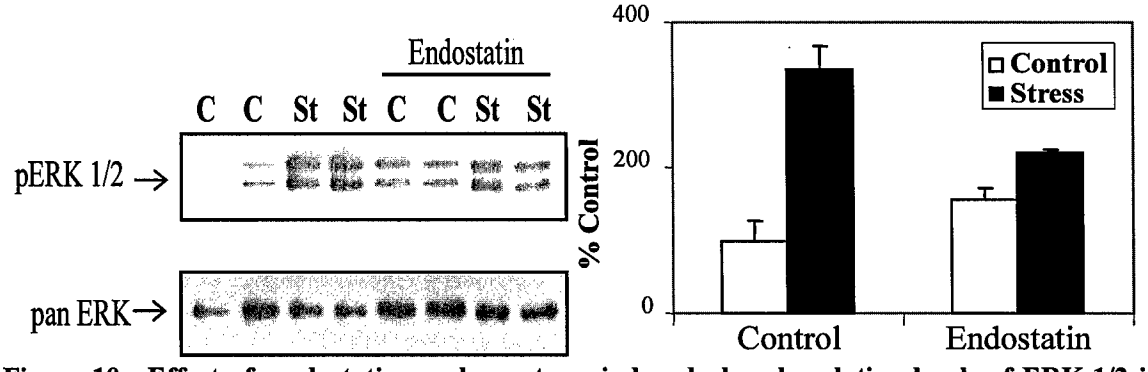

Figure 10. Effect of endostatin on shear stress induced phosphorylation levels of ERK 1/2 in osteoblasts isolated from B6 mice. Cells were pretreated with 10μg/ml endostatin for 24 hours and subjected to shear strain of 20 dynes/cm^2 for 30 minutes. (Left): Cell lysates were then prepared and immunoblotted with a phospho-specific anti-pan ERK antibodies. The blot was stripped and reblotted with anti-pan ERK to normalize the protein loading. (Right): The graph represents the densitometric measurements of pERK 1/2 levels from western blots normalized by pan ERK.

proliferation in B6 osteoblasts. Further, when the effect of ICI182780 on the phosphorylation levels of Erk1/2 was studied, we found that similar to cell proliferation, ICI182780 completely abolished the shear stress-induced Erk1/2 activation as well in B6 osteoblasts (Figure 12), indicating that the ER signaling pathway is involved in the mechanotransduction mechanism in B6 osteoblasts.

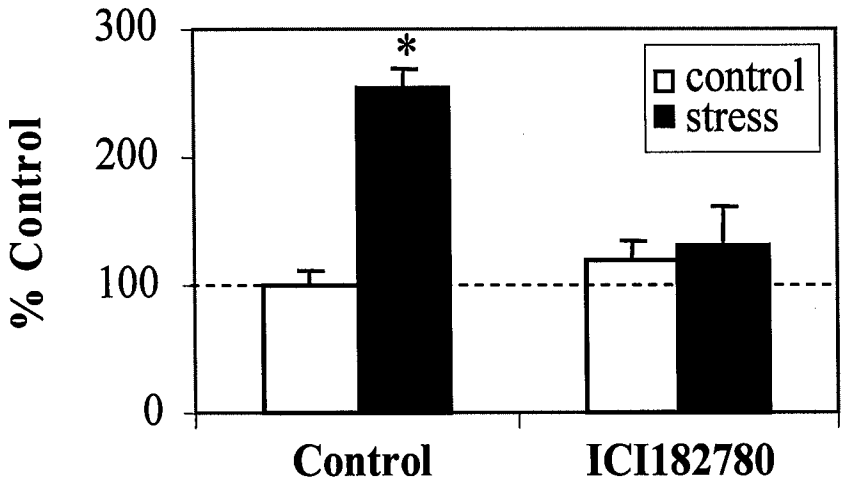

Figure 11: Effect of ICI182780 pretreatment on shear strain induced cell proliferation in osteoblasts isolated from B6 mice. Cells were pretreated with 200nM ICI182780 for 24 hours and subjected to shear strain of 20 dynes/cm^2 for 30 minutes. [3H]thymidine incorporation was measured after 24 hours. *p<0.001.

Our preliminary findings based on the inhibitor of ER signaling pathway strongly support the work of Lanyon and co-workers that ER signaling pathway is essential for the mediation of the mechanical stimulation of bone cell proliferation, since blocking the activation of the ER signaling pathway by ICI182780 completely abolished the shear stress-mediated Erk1/2 activation and bone cell proliferation. These findings also suggest that the ER pathway is also upstream to the Erk1/2 activation.

Finally, to test whether the BMP signaling pathway is involved in the mechanotransduction mechanisms in B6 osteoblasts, we pre-treated B6 osteoblasts with 300 ng/ml of noggin (a specific inhibitor of the BMP pathway) for 24 hrs prior to the 30-min shear

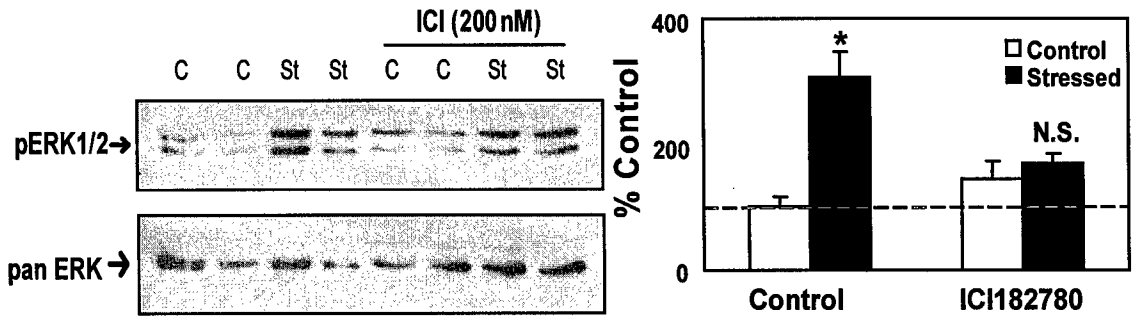

Figure 12. Effect of ICI182780 on shear stress induced phosphorylation levels of ERK 1/2 in osteoblasts isolated from B6 mice. Cells were pretreated with 200nM ICI182780 for 24 hours and subjected to shear strain of 20 dynes/cm^2 for 30 minutes. (Left): Cell lysates were then prepared and immunoblotted with a phospho-specific anti-pan ERK antibodies. The blot was stripped and reblotted with anti-pan ERK to normalize the protein loading. (Right): The graph represents the densitometric measurements of pERK 1/2 levels from western blots normalized by pan ERK. *p<0.001

stress at 20 dynes/cm^2. The effects of noggin pretreatment on the shear stress-induced stimulation of [^{3}H]thymidine incorporation (Figure 13) and Erk1/2 activation (Figure 14) were then evaluated. As shown in figure 13, the noggin treatment completely inhibited the shear stress induced increase in the cell proliferation in B6 osteoblasts.

Similarly, the noggin treatment completely blocked the fluid shear stres-induced increase in the phosphorylation levels ok Erk1/2. These results strongly indicate that the BMP signaling pathway is involved in the mechanotransduction mechanism in B6 osteoblasts.

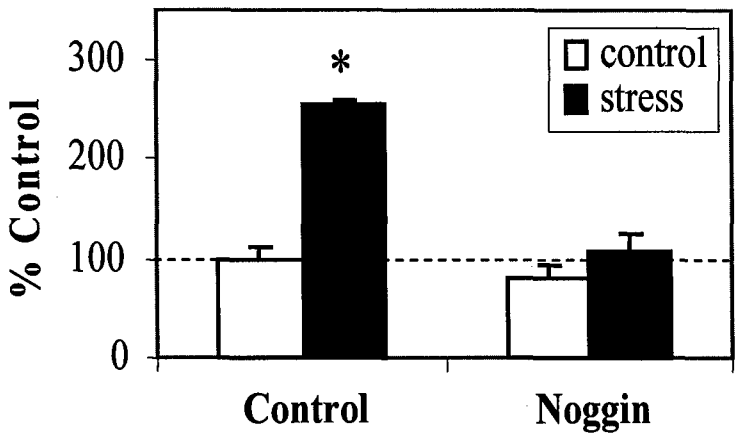

Figure 13: Effect of Noggin pretreatment on shear strain induced cell proliferation in osteoblasts isolated from B6 mice. Cells were pretreated with 300 ng/ml of noggin for 24 hours and subjected to shear strain of 20 dynes/cm^2 for 30 minutes. [^{3}H]thymidine incorporation was measured after 24 hours. *p<0.001.

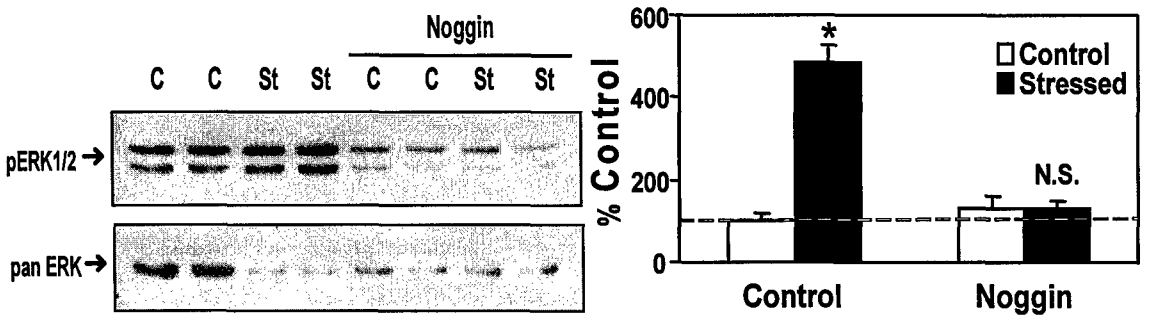

Figure 14. Effect of Noggin on shear stress induced phosphorylation levels of ERK 1/2 in osteoblasts isolated from B6 mice. Cells were pretreated with 300ng/ml of noggin for 24 hours and subjected to shear strain of 20 dynes/cm^2 for 30 minutes. (Left): Cell lysates were then prepared and immunoblotted with a phospho-specific anti-pan ERK antibodies. The blot was stripped and reblotted with anti-pan ERK to normalize the protein loading. (Right): The graph represents the densitometric measurements of pERK 1/2 levels from western blots normalized by pan ERK. *p<0.001.

Key Research Accomplishments:

1. We have provided the first evidence for a synergistic interaction between shear stress and IGF-I in stimulation of osteoblastic proliferation.
2. This study also provides strong evidence that the synergy involves the integrin-dependent upregulation of IGF-IR phosphorylation through an inhibition of SHP-mediated IGF-IR dephosphorylation.

3. Studies with specific inhibitors of respective signaling pathways confirm the potential role of the canonical Wnt pathway, the BMP pathway, and the estrogen receptor pathway in the mechanotransduction mechanism.

Reportable Outcomes:

1. Sonia Kapur, Subburaman Mohan, David J. Baylink, and K.-H. William Lau (2005) Fluid shear stress synergizes with IGF-I on osteoblast proliferation through integrin-dependent activation of IGF-I mitogenic signaling pathway. ***J Biol Chem.*** 280, 20163-20170
2. K.-H. William Lau, Sonia Kapur, and David J. Baylink.(2004) Fluid shear stress synergizes with IGF-I on osteoblast proliferation through integrin-dependent activation of IGF-I receptor. ***J Bone Miner Res*** 19 (Suppl 1), S151, abstract # SA263, at 26th Annual Meeting of American Society for Bone and Mineral Research. Seattle, Washington.
3. Lau K-HW, Kapur S, Mohan S, and Baylink DJ (2005) Fluid shear stress synergizes with IGF-I on osteoblast proliferation through integrin-dependent upregulation of IGF-I receptor phosphorylation levels. ***Transactions to the 51st Annual meeting of Orthopaed Res Soc*** abstract # 845, at the 51st Annual meeting of Orthopaedic Research Society, Washington, DC..

Conclusions:

1. These studies have confirmed our previous conclusion that the mechanotransduction mechanism is complex and is consisted of multiple anabolic signal transduction pathways. Most importantly, this work has identified at least two previously unknown pathways, namely the canonical Wnt pathway and the BMP pathway.
2. Our studies with the IGF-I signaling pathway have clearly demonstrated that not only the mechanotransduction mechanism is comprised of multiple anabolic signaling pathways, these anabolic pathways could interact synergistically with each other to promote bone cell proliferation and bone formation.
3. We have dissected the mechanism of interaction between two such pathways, namely the IGF-I and integrin pathway, and shown that the interaction between these two pathways involved recruitment of SHP-2 and/or SHP-1 to the IGF-IR. However, the nature of interaction between other pathways remains to be determined.

References:

1. Hillsley MV, and Frangos, JA (1994) Bone tissue engineering: the role of interstitial fluid flow. Biotech Bioeng 43:573-581.
2. Kapur S, Baylink DJ, and Lau K-HW (2003) Fluid flow shear stress stimulates human osteoblast proliferation and differentiation through multiple interacting and competing signal transduction pathways. Bone 32:241-251.
3. Kapur S, Chen S-T, Baylink DJ, and Lau K-HW (2004) Extracellular signal-regulated kinase-1 and -2 are both essential for the shear stress-induced human osteoblast proliferation. Bone 35:535-534.
4. Mohan S, and Baylink DJ (1991) Bone growth factors. Clin Orthop Relat Res 263:30-48.
5. Lean JM, Jagger CJ, Chambers TJ, and Chow JW (1995) Increased insulin-like growth factor I mRNA expression in rat osteocytes in response to mechanical stimulation. Am J Physiol 268:E318-E327.

6. Mikuni-Takagaki Y, Suzuki Y, Kawase T, and Saito S (1996) Distinct responses of different populations of bone cells to mechanical stress. Endocrinology 137:2028-2035.
7. Cheng MZ, Rawlinson SC, Pitsillides AA, Zaman G, Mohan S, Baylink DJ, and Lanyon LE (2002) Human osteoblasts' proliferative responses to strain and 17 β-estradiol are mediated by the estrogen receptor and the receptor for insulin-like growth factor I. J Bone Miner Res 17:593-602.
8. Sakata T, Halloran BP, Elalieh HZ, Munson SJ, Rudner L, Venton L, Ginzinger D, Rosen CJ, and Bikle DD (2003) Skeletal unloading induces resistance to insulin-like growth factor I on bone formation. Bone 32:669-680.
9. Sakata T, Wang Y, Halloran BP, Elalieh HZ, Cao J, and Bikle DD (2004) Skeletal unloading induces resistance to insulin-like growth factor-I (IGF-I) by inhibiting activation of the IGF-I signaling pathways. J Bone Miner Res 19:436-446.
10. Clemmons DR, and Maile LA (2005) Interaction between insulin-like growth factor-I receptor and αVβ3 integrin linked signaling pathways: cellular responses to changes in multiple signaling inputs. Mol Endocrinol 19:1-11.

Appendices

1. Chandrasekhar Kesvan, Subburaman Mohan, Susanna Oberholtzer and David J Baylink. (2004) Evidence that BMD response to mechanical loading (ML) in vivo is caused by acute up-regulation of both bone formation (BF) genes and down regulation of bone resorption (BR) genes. ASBMR 26th Annual Meeting, Washington State Convention & Trade Center, Seattle, WA, USA.

2. Chandrasekhar Kesavan, David J Baylink, Jon Wergedal and Subburaman Mohan (2004) Inbred mouse strain development variations in the skeletal adaptive response to four-point bending evidence for involvement of different genetic mechanisms. ASBMR 26th Annual Meeting, Washington State Convention & Trade Center, Seattle, WA, USA. 1

3. Chandrasekhar Kseavan, Subburaman Mohan, Jon Wergedal and David J Baylink (2004) Bone anabolic response to a mechanical load is a complex trait and involves bone size, material bone density (mBMD) and volumetric bone density (vBMD) phenotypes. ASBMR 26th Annual Meeting, Washington State Convention & Trade Center, Seattle, WA, USA

4. Sonia Kapur, David J. Baylink, and K.-H. William Lau (2003) Fluid shear stress (a mechanical strain mimic) synergizes with IGF-I on human osteoblast proliferation through upregulation of the IGF-I signaling pathway. Mol Biol Cell 14 (Suppl), 281a, abstract # 1567, at the Annual Meeting of American Society of Cell Biology in San Francisco, California.

5. K.-H. William Lau, Sonia Kapur, and David J. Baylink. (2004) Global application of expression profiling reveals potential involvement of the Wnt, IGF-I, Estrogen Receptor (ER), and BMP/TGF pathways in C57BL/6J (B6) but not C3H/HeJ (C3H) mouse osteoblasts in response to fluid shear stress. J Bone Miner Res 19 (Suppl 1), S79, abstract # F264, at 26th Annual Meeting of American Society for Bone and Mineral Research. Seattle, Washington.

6. Chandrasekhar K, Mohan S, Oberholtzer S and Baylink DJ. Mechanical loading induced gene expression and BMD changes are different in two inbred mouse strains. Accepted in Journal of Applied Physiology, 2005.

7. Sonia Kapur, Subburaman Mohan, David J. Baylink, and K.-H. William Lau (2005) Fluid shear stress synergizes with IGF-I on osteoblast proliferation through integrin-dependent activation of IGF-I mitogenic signaling pathway. J Biol Chem. 280, 20163-20170

8. K.-H. William Lau, Sonia Kapur, and David J. Baylink.(2004) Fluid shear stress synergizes with IGF-I on osteoblast proliferation through integrin-dependent activation of IGF-I receptor. J Bone Miner Res 19 (Suppl 1), S151, abstract # SA263, at 26th Annual Meeting of American Society for Bone and Mineral Research. Seattle, Washington.

9. K-H William Lau, Sonia Kapur, Subburaman Mohan, and David J Baylink (2005) Fluid shear stress synergizes with IGF-I on osteoblast proliferation through integrin-dependent upregulation of IGF-I receptor phosphorylation levels. Transactions to the 51st Annual meeting of Orthopaed Res Soc abstract # 845, at the 51st Annual meeting of Orthopaedic Research Society, Washington, DC.

Evidence that the BMD response to mechanical loading *in vivo* is caused by acute up-regulation of both bone formation genes and down regulation of bone resorption genes

Chandrasekhar Kesavan, Subburaman Mohan, Susanna Oberholtzer and David J. Baylink

Musculoskeletal Disease Center, JLP VA Medical Center, Loma Linda, CA 92357, USA.

The increase in bone mass in response to skeletal loading is an important adaptive response. It is likely that regulation of both osteoblast and osteoclast cell functions are involved in producing an optimal response to a given skeletal load. In order to evaluate the osteoblast and osteoclast cell response to mechanical input, we tested the hypothesis that *in vivo* mechanical loading by 4-point bending leads to an acute reduction in the expression of bone resorption genes besides the anticipated increase in the expression of bone formation marker genes. We, therefore, measured expression changes by real time PCR in 12 genes that relate to bone formation (BF) and resorption (BR) at 2, 4, 8 and 12 days of training in 10-week old C57Bl/6J mice. A 9N load at 2Hz (36 cycles) was applied on right tibia by a four point bending device and the left tibia was used as an internal control. 12 days of loading caused a highly significant ($p<0.001$) increase in BMC (33%), volumetric BMD (14%), and total area (26%), as measured by pQCT in the loaded bone compared to corresponding unloaded bone. Measurement of gene expression changes by real time PCR at day 2 showed significant ($p<0.01$) change in the down-regulation of bone resorption makers MMP-9 and TRAP by 2 and 4-fold with no change in the expression of formation genes compared to control. Four days of loading caused down regulation of bone resorption genes MMP-9, TRAP, and Sodium-potassium pump by 3, 5, and 2-fold respectively ($p<0.0001$). In contrast, the expression of type-I collagen and bone sialoprotein was increased by 2-fold as expected. After 8 days of loading, the expression of TRAP was decreased by 3-fold while expression of type-I collagen, alkaline phosphatase (ALP), bone sialoprotein (BSP) and osteocalcin (OC) was increased by 3-fold. Surprisingly, the expression level of bone resorption marker genes increased after 12 days of loading (MMP-9 by 12 fold and TRAP by 7.5 fold) which may reflect loading-induced increase in remodeling. In contrast, expression of type-I collagen, BSP, ALP and OC increased by 4.2, 8, 6 and 4-fold, respectively ($p<0.001$). In order to determine if gene expression change can be used as a surrogate for bone anabolic response, we determined the correlation between expression levels and BMD changes. Accordingly, we found cortical density measured by pQCT showed significant correlation with bone sialoprotein ($r=0.66$) measured by Real Time PCR. In conclusion, our data indicates that: 1) Mechanical loading by 4-point bending caused a dramatic increase in both size and volumetric BMD after 12 days; 2) The expression levels of bone formation genes were increased throughout the loading period; 3) This is the first report that demonstrates acute reduction in bone resorption marker genes in response to loading. 4); The increase in expression of bone resorption genes at day 12 may indicate loading induced remodeling of bone; and 5) Our findings demonstrate the usefulness of gene expression changes as surrogate markers for bone anabolic response to mechanical loading.

Introduction

Mechanical stress is an important determinant of the structural and functional integrity of the skeletal system. A number of *in vivo* studies on rats, mice, turkeys, and humans using histology and pQCT have shown that mechanical loading promotes bone formation and unloading leads to loss of bone (1,2,3). *In vitro* studies using fluid flow have shown that mechanical stimulation increases osteoblast proliferation and differentiation by involving one or more signaling pathways such as integrins, nitric oxide, and cyclo-oxygenase. Furthermore, it has been also well shown that mechanical stimulation inhibited formation and activity of osteoclast by decreasing RANKL (4). Although these *in vitro* studies provide evidence that both osteoblasts and osteoclasts respond to mechanical strain, it is not known if osteoblast and osteoclast cell functions are involved in producing an acute response to a given skeletal loading *in vivo*. In order to evaluate the osteoblast and osteoclast cell response to mechanical input, we tested the hypothesis that *in vivo* mechanical loading by 4-point bending leads to acute reduction in the expression of bone resorption genes besides the anticipated increase in the expression of bone formation marker genes. To test this hypothesis, we choose 10-week old female C57BL/6J mice as our *in vivo* mouse model and 4-point bending as our *in vivo*-loading device. We carried out time course studies of mechanical loading using the 4-point bending device and changes in the bone response were measured by using Real Time PCR and pQCT (Peripheral Quantitative Computerized Tomography).

Material and Methods

Animals: 9-week old female C57BL/6J (B6) inbred mice were purchased from the Jackson Laboratory (Bar Harbor, ME, USA) and housed at the Animal Research facility of the JL Pettis VA Medical Center (Loma Linda, CA) for 1 week prior to use for loading experiments.

In vivo loading model: We used a 4-point bending method developed by Dr.Recker and his collaborator (5) as our *in vivo* loading regimen. The loading protocol consists of 9N loads at 2Hz frequency for 36 cycles and the training is once per day. The right tibia is used for loading while the left tibia is used as an internal control. The mice are trained for 6 days/ week with 1 day of rest for 2-weeks. Before the training, the mice were given halothane anesthesia [95% Oxygen and 5% Halothane] for 2-3 minutes and while anesthetized the loading is performed. After 48 hrs last loading regimen, on the 15^{th} day, mice sacrificed and the tibias collected. The tibias are stored in 70% ethanol until pQCT is performed. In the other set of mice, tibias are collected, stored in RNA later (Ambion) at –80 °C until RNA extraction is performed.

Gene Expression Analysis: Total RNA extracted from the loaded region of tibia using Lipid Qiagen RNA extraction protocol. Quality and quantity of RNA was analyzed using Bioanalyzer and Nana-drop (Agilent). 200ng of RNA was reverse transcribed using Invitrogen Superscript. Real time PCR (ABIPRISM, Foster City, California, USA) was used as a method to measure the changes in the expression of bone related genes in response to 4-point bending between loaded and unloaded bones. The data were normalized using b-actin and fold change was calculated using ABI $2^{-\Delta\Delta}$Ct formula. The primers for the bone marker genes were designed using Vector NTI program.

Bone parameters: Geometrical properties of loaded and unloaded tibias were measured by using peripheral quantitative computed tomography (pQCT) method from Stratec XCT 960M (Norland Medical System, Ft.Atkinson, WI).

Statistical analysis: Data are presented as Means ± SD. Students T-test was used to compare the difference due to loading using the percentage obtained from loaded versus unloaded bones. Results were considered significantly different for $p<0.05$.

Table-1. Fold change in the mRNA expression of (a) bone formation and (b) resorption genes in response to 2, 4, 8, and 12 days of 4-point bending in 10-week old female B6 mice.

(a) Bone Formation genes

Duration of loading	Genes	$\Delta\Delta$Ct ± SD	Fold change	P-value
2-days (N=6)	Type-I Collagen	0.78 ± 0.61	0.54	0.76
	Bone sialoprotein	0.66 ± 0.97	0.47	0.82
	Alkaline Phosphotase	0.89 ± 0.60	0.31	0.69
	Osteocalcin	0.46 ± 0.94	1.0	0.97
4-days (N=5)	Type-I Collagen	1.02 ± 0.29	2.04	0.03
	Bone sialoprotein	1.03 ± 0.37	2.04	0.006
	Alkaline Phosphotase	0.53 ± 0.39	1.4	0.18
	Osteocalcin	0.12 ± 1.02	1.0	0.73
8-days (N=5)	Type-I Collagen	1.93 ± 0.25	3.84	0.00001
	Bone sialoprotein	1.89 ± 1.1	3.71	0.003
	Alkaline Phosphotase	1.53 ± 0.73	2.88	0.001
	Osteocalcin	1.45 ± 0.97	2.72	0.01
12-days (N=7)	Type-I Collagen	2.06 ± 0.25	4.18	0.000001
	Bone sialoprotein	3.01 ± 0.19	7.82	0.00000002
	Alkaline Phosphatase	2.55 ± 0.43	5.86	0.0000005
	Osteocalcin	2.01 ± 0.34	4.03	0.0005

(b) Bone Resorption genes

Duration of loading	Genes	$\Delta\Delta$Ct ± SD	Fold change	P-value
2-days (N=6)	MMP-9	1.98 ± 0.76	-4.25	0.007
	TRAP	1.14 ± 0.90	-2.07	0.006
4-days (N=5)	MMP-9	1.98 ± 0.53	-3.2	0.002
	TRAP	1.68 ± 0.76	-5.56	0.004
	Na-K pump	2.47 ± 0.39	-2	0.008
	Cathespin K	0.93 ± 0.87	-1.9	0.07
8-days (N=5)	MMP-9	0.28 ± 1.0	1.2	0.2
	TRAP	1.61 ± 1.0	-3.06	0.007
	Na-K pump	0.10 ± 1.2	0.92	0.34
	Cathespin K	1.14 ± 0.93	0.45	0.12
12-days (N=7)	MMP-9	2.91 ± 0.35	12	0.00000003
	TRAP	3.61 ± 0.53	7.5	0.000000008
	RANK-L	2.65 ± 0.37	5	0.00001
	OPG	0.47 ± 0.33	1	0.81

Interpretation:

1) Mechanical loading applied by 4-point bending caused acute change in the expression of bone resorption markers as observed by down regulation of MMP-9 and TRAP at day 2.
2) The expression of type-I collagen and bone sialoprotein were increased after 4-days of mechanical loading while those of MMP-9, TRAP, and Na-K pump were decreased.
3) The magnitude of change in the expression of bone formation genes was greater at 12 days of training compared to other time points.
4) Surprisingly, expressions of bone resorption markers genes were increased after 12 days of training.
5) Our data suggest that mechanical loading influences both osteoblast and osteoclast acutely.

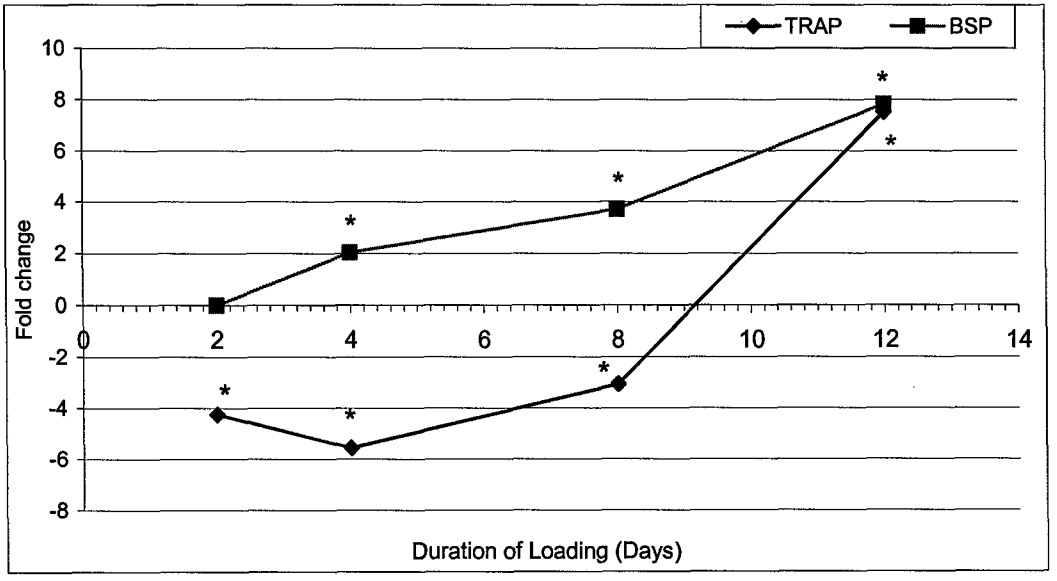

Fig.1. Changes in the expression of bone sialoprotein and TRAP in response to a time course of mechanical loading. The x-axis corresponds to varying time points and the y-axis represents mean fold change measured by real time PCR.
*N=5-7, *p<0.01*

Interpretation:

1) The expression of BSP increased as the duration of loading was increased. An significant fold increases in BSP expression was seen after 12 days of loading.
2) The expression of TRAP was decreased by 5-fold after 4 days of loading and was increased by 7.5 fold after 12 days.
3) These data suggest that bone formation and bone resorption parameters are influenced acutely by 4-point bending.

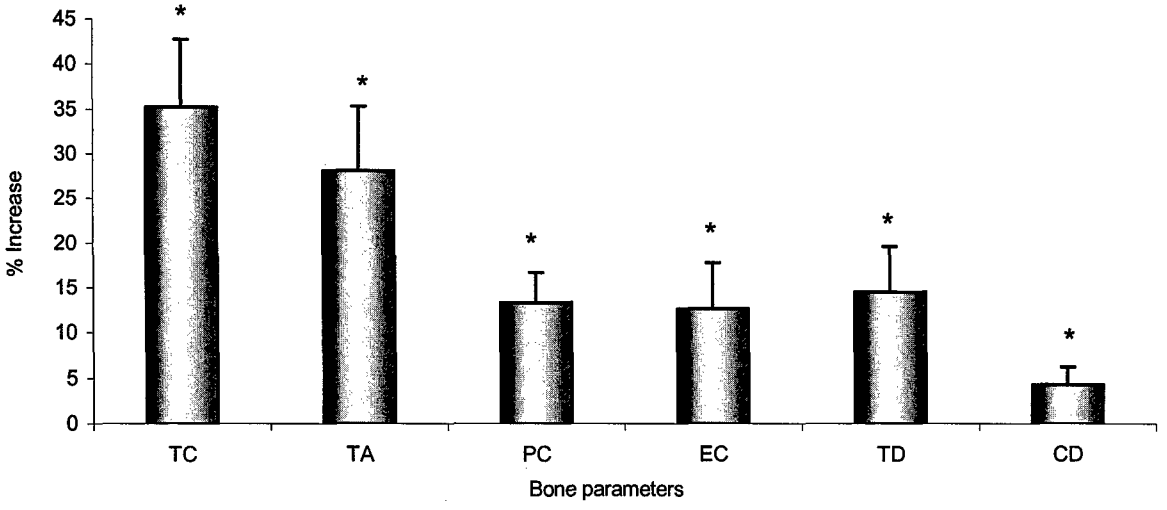

Fig.2. Changes in bone parameters in response to 12 days of 4-point bending measured by *in vivo* pQCT in the tibia of 10-week old female B6 mice.

The data shown here is the percentage that corresponds to the loading zone of tibia [Include slices 6-9] mean ± SD (N=9). P-values are calculated using t-test by comparing the loaded and unloaded bones. The y-axis represents percentage increase and x-axis represents bone parameters TC-Total content; TA-Total area; PC-periosteal circumference; EC-Endosteal circumference; TD-Total Density; CD-Cortical Density.
*N=9, *p<0.001 vs. corresponding unloaded bones*

Interpretation:

1) 12 days of loading increased total content by 35%, which was reflected by increase in total area.
2) Both periosteal and endosteal circumference were increased after loading.
3) A dramatic increase of 15% and 4% in vBMD and mBMD was seen after 12 days of loading.

Table-2. Correlation between pQCT and Real time PCR data from tibia

	Total Density	Periosteal circumference	Endosteal circumference	Cortical Content	Total Mineral Content	Cortical Density
Type-I collagen	-0.11	-0.14	0.04	-0.58	-0.45	0.04
Bone sialoprotein	0.54	-0.36	-0.35	0.07	-0.17	0.66[a]
Alkaline phosphotase	0.25	-0.10	0.03	-0.28	-0.17	0.22
Osteocalcin	0.43	-0.48	-0.34	-0.42	-0.47	0.35

For Real time PCR N=9, [a]$p<0.05$

Same mouse tibia was used for pQCT measurement and mRNA quantitation obtained from 12 days of 4-point bending in 10-week old female B6 mice.

Interpretation:

1) Of the various genes tested, BSP showed the strongest correlation with bone parameters measured by pQCT. This data is consistent with expression changes measured by real time PCR which showed that BSP has the greatest fold change of all genes tested.
2) These findings suggest that expression phenotypes can be used as surrogates for the measuring the bone response to loading.

Conclusions

1) Mechanical loading by 4-point bending caused a dramatic increase in both size and volumetric BMD after 12 days.
2) The expression levels of bone formation genes were increased throughout the loading period.
3) This is the first report that demonstrates acute reduction in bone resorption marker genes in response to loading.
4) The increase in expression of bone resorption genes at day 12 may indicate loading induced remodeling of bone.
5) Our findings demonstrate the usefulness of gene expression changes as surrogate marker for bone anabolic response to mechanical loading.

Acknowledgements

This work was supported by Assistance Award No. DAMD17-03-2-0021. The U.S. Army Medical Research Acquisition Activity, 820 Chandler Street, Fort Detrick MD 21702-5014, is the awarding and administering acquisition office. The information contained in this publication dose not necessarily reflects the position or the policy of the government, and no official endorsement should be inferred. All work was performed in facilities provided by the Department of Veterans Affairs.

References:

1. Robling AG, Hinant FM, Burr DB, Turner CH 2002. *J Bone Miner Res* 17:1545-1554.
2. Umemura Y, Baylink DJ, Wergedal JE, Mohan S, Srivastava AK 2002, J *Bone Miner Metab* 20(4):209-15
3. Y.Kodama, Y.Umemura, S.Nagasawa, W.G.Beamer, L.R.Donahue, C.R.Rosen, D.J.Baylink and J.R.Farley 2000. *Calcif Tissue Int* 66:208-306.
4. Rubin J, Murphy T, Nanes MS, Fan X 2000. *Am J Physiol Cell Physiol* 278: C1126-C1132.
5. M.P.Akther, D.M. Cullen, E.A. Perdersen, D.B.Kimmel, R.R.Recker 1998. *Calcif Tissue Int* 63:442-449.

Inbred Mouse Strain Dependent Variations in the Skeletal Adaptive Responses to 4-Point Bending: Evidence for Involvement of Different Genetic Mechanisms.

Chandrasekhar Kesavan, David J. Baylink, Jon E. Wergedal and Subburaman Mohan
Musculoskeletal Disease Center, JLP VA Medical Center, Loma Linda, CA 92357, USA.

One of the most fundamental features of skeletal tissue is its adaptive response in the amount of bone tissue present and the configuration of this tissue in response to mechanical loads. The present study was undertaken to test the hypotheses that: 1) different inbred strains of mice would show variable responses to a given mechanical load; and 2) within these mouse strains, the mechanisms involved in these adaptive interactions to mechanical loads would be variable. We compared bone anabolic response to 4-point bending in four different, commonly used inbred strains of mice (C57BL/6J [B6], DBA, C3H/HeJ [C3] and Balb/c). A 9N load (except for Balb/c, in which 8N was used since 9N caused fractures) at 2Hz for 36 cycles was applied for 12 days on right tibia and left tibia as an internal control. Two days after the last loading, skeletal changes were evaluated by pQCT. A dramatic 15.7% and 10.8% increase in total vBMD ($P<0.0001$) was seen in C57BL/6J and DBA/J mice after 12 days of loading. While vBMD increased by 3% ($P<0.05$) in Balb/c, no increase in vBMD was seen in C3H mice (-0.5%) after the same duration of training. We subsequently performed dose response studies (6, 7, 8, and 9 N load) using B6 as good responder and C3H as poor responder strain. While 4-point bending caused a dose-dependent increase in BMD in B6, it did not cause a BMD increase in C3 mice at any of the four loads tested. The lack of BMD response in C3H mice cannot be explained on the basis of differential mechanical strain since strain gage measurements revealed a slightly higher mechanical strain in C3 mice compared to B6 mice at all four loads tested. Four-point bending increased endosteal circumference in a dose-dependent manner in both B6 and C3 mice in a similar manner with no difference in slopes (B6=y: 5.891x -34.44,C3H- y: 5.859x -32.44,$p>0.05$). On the contrary, the increase in periosteal circumference in response to 4-point bending was greater in B6 mice compared to C3 mice (B6=y: 5.3x-29.58, C3H=y: 2.98x-14.23, $p<0.05$). Conclusions: 1) the increase in BMD by 4-point bending is variable in four strains tested, from no response to 15.7% increase in BMD after 2 weeks; 2) in B6 mice, 4-point bending increased both periosteal and endosteal circumference in a dose-dependent manner; 3) in C3 mice, there was an impaired periosteal response, but the magnitude of increase at the endosteum was similar to that of the B6 mice; and 4) because the C3 mice responded as well as the B6 mice to the endosteum, it follows that the impairment in responsive in C3 mice is not due to an overall decrease in detection of the mechanical signal and, accordingly, different genetic mechanisms may regulate periosteal and endosteal responses to mechanical loading.

Introduction

It is now well demonstrated that bone tissue responds to mechanical stress with adaptive changes in mass and structure. Numerous studies in humans have shown that mechanical loading induces new bone formation and increases bone mineral density, while disuse of bone results in bone loss. Thus, physical exercise has been used as a strategy in increasing the bone mass and maintenance of skeletal integrity to prevent incidence of osteoporosis and related fractures in men and women. Consistent with these observations in humans, animal studies using many *in vivo* loading models have demonstrated that skeletal integrity is largely dependent upon the amount of mechanical input. Recent studies have also shown that the magnitude of increase in bone mass is variable given the same amount of mechanical stress, with some individuals exhibiting robust bone response and others responding modestly. In terms of the mechanisms that contribute to variation in anabolic response to loading among different individuals, others and we have found evidence that the variation in response to loading is partially under the influence of genetic factors (1,2). To further understand the mechanisms involved in the different adaptive interactions to mechanical loads, we tested the hypotheses that: 1) different inbred strains of mice would show variable responses to a given mechanical load; and 2) within these mouse strains, the mechanisms involved in these adaptive interactions to mechanical loads would be variable. To test these hypotheses, we used inbred strains with diverse genetic backgrounds to evaluate the effects of 4-point bending on bone parameters.

Materials and methods

Animals: 9-week old female Balb/c, DBA/J, C57BL/6J (B6), and C3H/HeJ (C3H) inbred mice were purchased from the Jackson Laboratory and housed at the Animal Research facility at the JL Pettis VA Medical Center (Loma Linda, CA) for one week prior to use.

In vivo loading model: We used a 4-point bending method developed by Dr.Recker and his collaborators as our *in vivo* loading regimen (3). The loading protocol consists of 9N loads at 2Hz frequency for 36 cycles and the training is once per day. The right tibia is used for loading while the left tibia is used as an internal control. The mice are trained for 6 days/ week with 1 day of rest for 2-weeks. After 48 hrs of the last loading regimen, the mice were euthanized, the tibias collected and stored at 70°C prior to analysis. Before the training, the mice were given halothane anesthesia [95% Oxygen and 5% Halothane] for 2-3 minutes and while anesthetized the loading was performed.

Experiment-I: We performed mechanical loading using the 4-point bending device on varying inbred strains of 10-week old mice.

Experiment-II: We performed varying doses of load (6, 7, 8 and 9N) on 10-week old B6 and C3H mice using the 4-point bending device for 12 days.

Strain measurement: The amount of mechanical strain resulting from the applied forces on bone was measured using strain gages (Micro-Measurement Group, Raleigh, NC) at different loads.

Bone parameters measurement: Geometrical properties of loaded and unloaded tibias were measured by peripheral quantitative computed tomography (pQCT) method from Stratec XCT 960M (Norland Medical System, Ft.Atkinson, WI).

Statistical analysis: Data are presented as Means ± SD. ANOVA (Newman-Keuls test) and Student's t-test was used to compare the difference due to loading between the strains using the percentage obtained from loaded versus unloaded bones. Results were considered significantly different for $p<0.05$.

Results

Table-I. Changes in bone parameters [measured by pQCT] in response to 12 days of 4-point bending at 9N load in 10-week old female Balb/c, B6, DBA/J, and C3H mice.

Bone parameters	Balb/c[#]	C3H	DBA/J	B6
Total Content	14.03 ± 4.7[a]	19.17 ± 6.14[a]	48.37 ± 2.85[a b]	47.83 ± 6.0[a b]
Total area	13.04 ± 1.89[a]	26.45 ± 10.85[a]	33.56 ± 6.00[a]	43.5 ± 13[a]
Periosteal circumference	6.22 ± 0.92[a]	12.3 ± 4.8[a]	18.50 ± 7.15[a b]	19.5 ± 5.6[a b]
Endosteal circumference	5.75 ± 2.33[a]	20.35 ± 9.9[a]	16.81 ± 12.85[a]	23.0 ± 8.8[a]
Total density	2.97 ± 1.8	-0.45 ± 1.75	10.82 ± 5.50[a b]	15.67 ± 6.7[a b]
Cortical density	0.80 ± 1.35	-1.45 ± 1.08	2.72 ± 2.12[a]	4.00 ± 2.0[a c]

The values represent % increase in the loaded bone compared to unloaded bone and are mean ± SD of 6 animals for each strain. [#]8N was applied on Balb/c since some of the tibias fractured at 9N.

[a]$p<0.05$ vs. unloaded bones.

[b]$p<0.05$ between Balb/c and C3H

[c]$p<0.05$ between Balb/c, DBA/J, and C3H

Interpretation:

1) Four-point bending induced significant changes in the bone parameters of Balb/c, C3H, DBA/J, and B6 after 12 days mechanical loading.
2) The magnitude of change in the total density and periosteal circumference was variable between mouse strains in response to loading.
3) Cortical density increased in B6 and DBA strains, but not in C3H and Balb/c strains.
4) These data demonstrate adaptive response to loading is highly variable between inbred strains of mice.

Fig.1. Changes in bone parameters in response to varying magnitude of loads applied by 4-point bending in 10-week old female B6 and C3H inbred strains of mice.

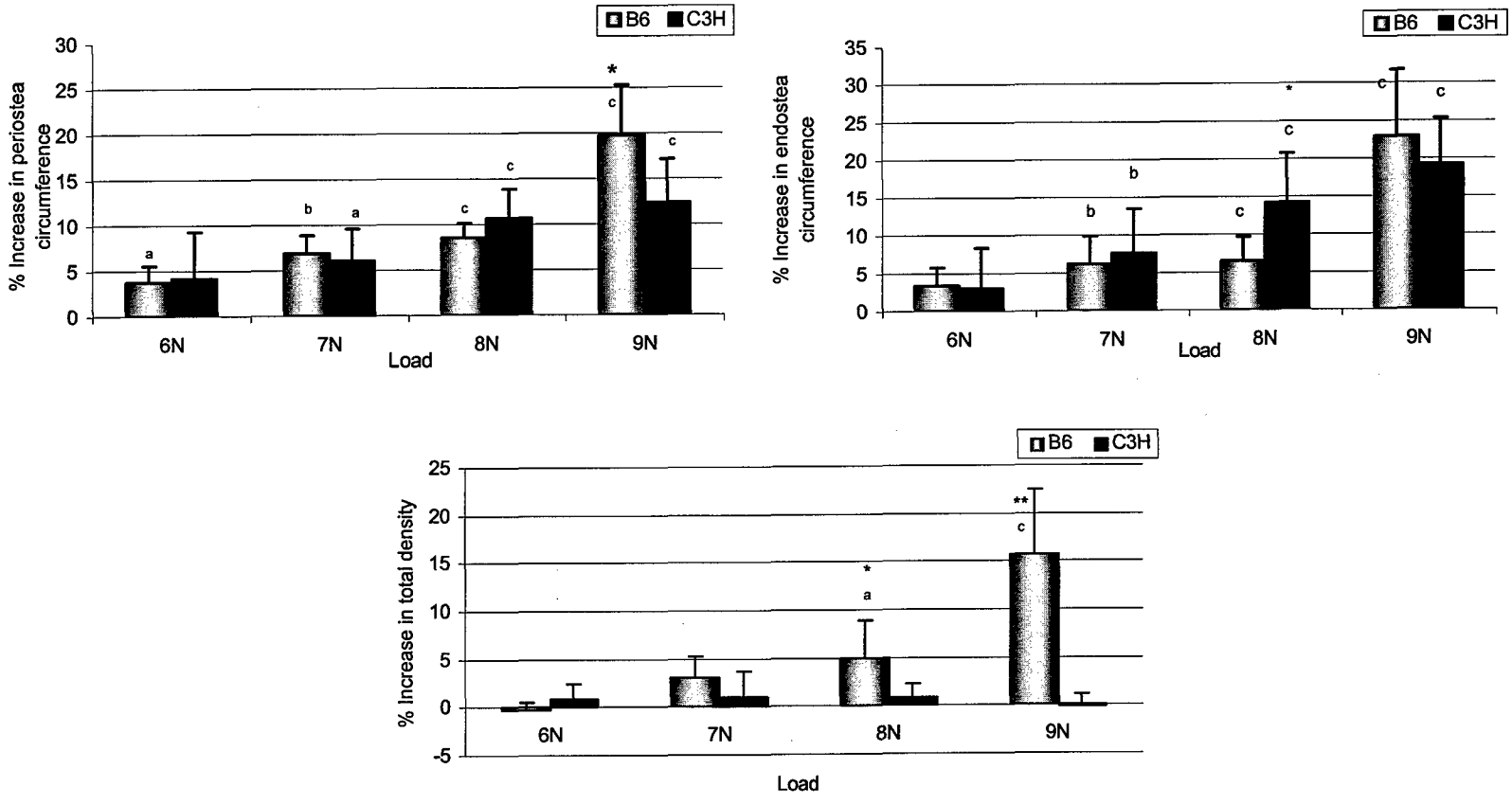

The values shown are the mean ± SD of the percentage increase in the tibia [loaded vs unloaded tibia (Includes slices 6-9)] of the same mouse. *[a]p<0.05, [b]p<0.01, [c]p<0.001, vs. corresponding unloaded bones, *p<0.05 and **p<0.001 between the strains. N=6 for each load in both strains*

Interpretation:

1) Both periosteal and endosteal circumference increased due to 4-point bending in both B6 and C3H mice. However, the increase in periosteal circumference was significantly greater at 9N in B6 mice compared to C3H mice.
2) Four-point bending caused a dose-dependent increase in total volumetric bone mineral density in B6, but not in C3H mice.

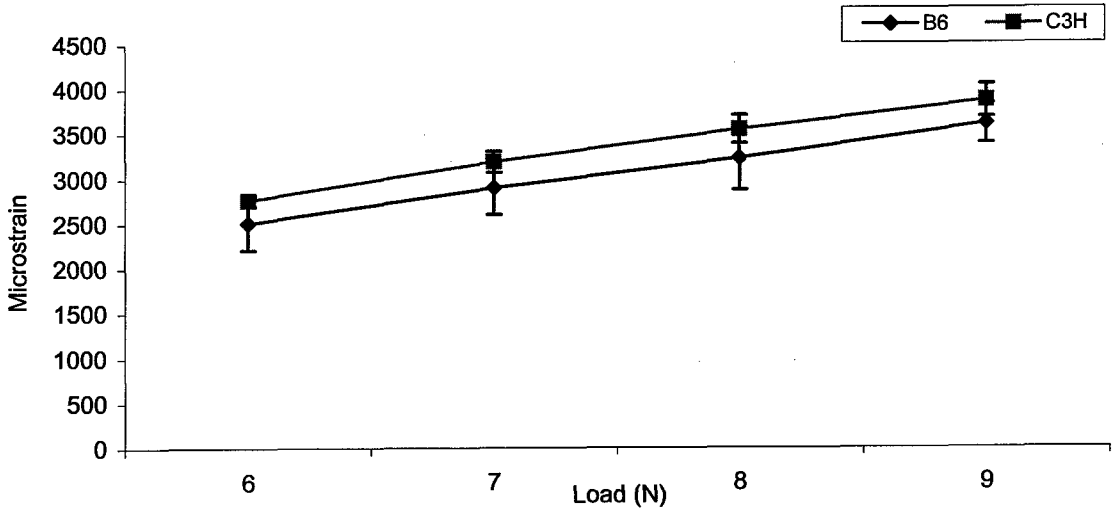

Fig.2. Mechanical strain produced by varying magnitude of loads applied by 4-point bending in the tibia of 10-week old B6 and C3H mice using strain gage. The values are mean ± SD. *N=5 in each load*

Interpretation:

1) The amount of mechanical strain produced by 4-point bending increased with an increase of load in both B6 and C3H mice.

2) Consistent with the slightly smaller periosteal circumference in C3H, the amount of strain was slightly larger in C3H compared to B6.
3) The lack of vBMD response in C3H at 8N and 9N load could not be explained due to a differential mechanical strain between B6 and C3H strains.

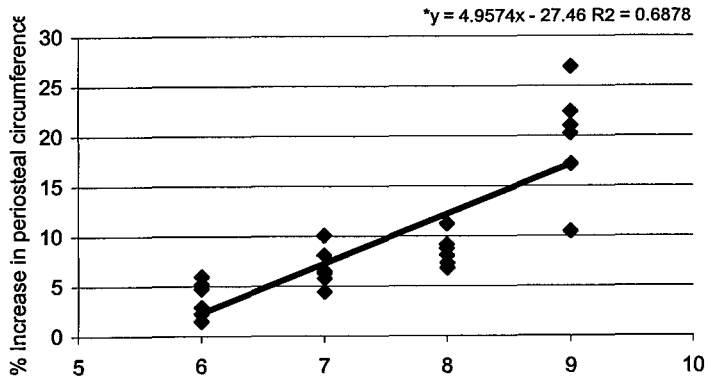

a) Periosteal circumference (B6)*

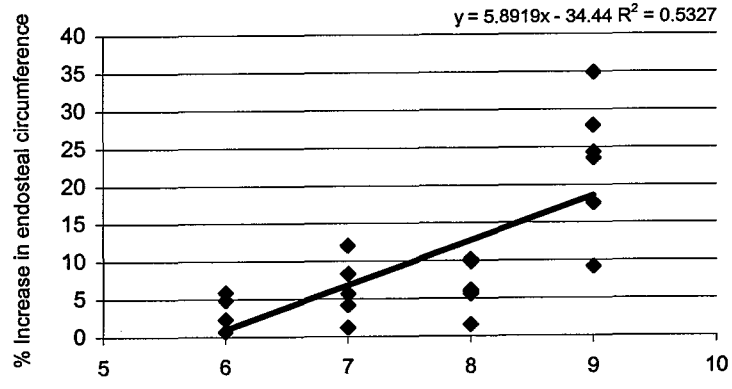

b) Endosteal circumference (B6)

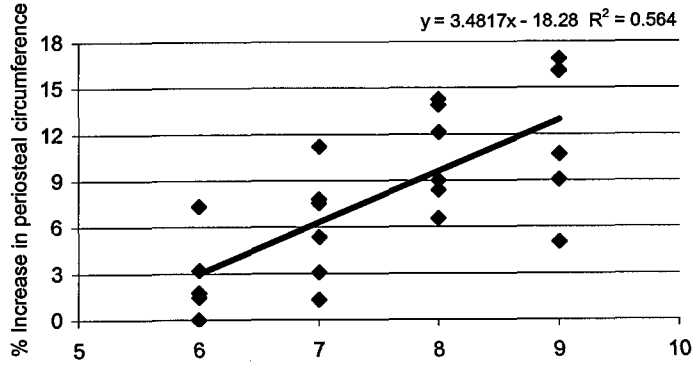

c) Periosteal circumference (C3H)

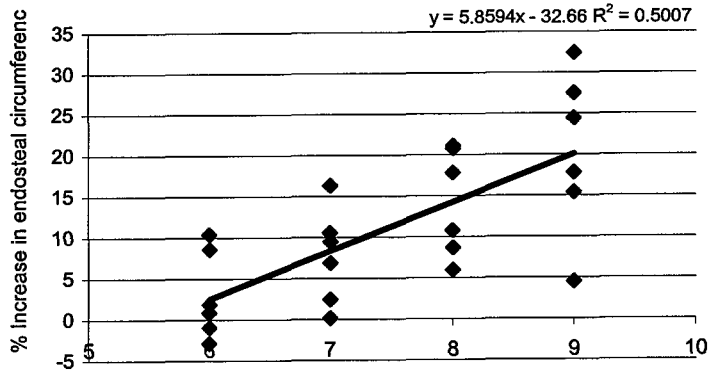

d) Endosteal circumference (C3H)

Fig.3. Regression slope of periosteal and endosteal response to varying magnitudes of loads applied by 4-point bending in 10-week old B6 and C3H female mice. The x-axis represents varying magnitude of loads and y-axis represents percentage increase.
*N=6 in each load, *p<0.05 between C3H periosteal circumference*

Interpretation:

1) The periosteal and endosteal circumference increased with an increase in magnitude of loads in both B6 and C3H mice.
2) The regression slope of periosteal circumference was significantly greater in B6 mice compared to C3H mice in response to varying loads.
3) However, there was no difference in the slope of endosteal circumference between B6 and C3H mice in response to varying loads.
4) These data suggest that there is a genetic effect on the periosteal but not the endosteal response to mechanical loads.

Conclusions:

1) The increase in BMD by 4-point bending is variable in four strains tested, from no response to 15.7% increase in BMD after 2 weeks; 2) in B6 mice, 4-point bending increased both periosteal and endosteal circumference in a dose-dependent manner; 3) in C3 mice, there was an impaired periosteal response, but the magnitude of increase at the endosteum was similar to that of the B6 mice; 4) because the C3 mice responded as well as the B6 mice to the endosteum, it follows that the impairment in responsiveness to C3 mice is not due to an overall decrease in detection of the mechanical signal and, accordingly, different genetic mechanisms may regulate periosteal and endosteal responses to mechanical loading.

Acknowledgements

This work was supported by Assistance Award No. DAMD17-03-2-0021. The U.S. Army Medical Research Acquisition Activity, 820 Chandler Street, Fort Detrick MD 21702-5014, is the awarding and administering acquisition office. The information contained in this publication dose not necessarily reflects the position or the policy of the government, and no official endorsement should be inferred. All work was performed in facilities provided by the Department of Veterans Affairs.

References:

1. Y. Kodama, Y.Umemuram S.Nagasawa, W.G.Beamer, L.R.Donahue, C.R.Rosen, D.J.Baylink, J.R.Farley 2000. Cal.Tiss.Int 66:306.

2. Y. Kodama, H.P.Dimai, J.Wergedal, M.Sheng, R.Malpe, S.Kutilek, W.G.Beamer, L.R.Donahue, C.R.Rosen, D.J.Baylink and J.R.Farley 1999. *Bone* 25 No.2, 183-190.
3. M.P.Akther, D.M. Cullen, E.A. Perdersen, D.B.Kimmel, R.R.Recker 1998. *Calcif Tissue Int* 63:442-449.

Bone anabolic response to a mechanical load is a complex trait and involves bone size, material bone density (mBMD), and volumetric bone density (vBMD) phenotypes.

Chandrasekhar Kesavan, Subburaman Mohan, Jon E. Wergedal, David J. Baylink.
JLP Veterans Medical Center/Loma Linda University, Loma Linda, CA, USA.

Different mouse strains show large variations in the change in BMD in response to the same mechanical load, suggesting that bone response to mechanical loading is genetically regulated. To test the hypothesis that the mechanical load response is a complex trait, we first applied 4-point bending to the tibia to evaluate the response in six different strains of mice in order to select the two strains with the most different response. These strains were C3H/HeJ (C3), the poor responder, and C57BL/6J (B6), the good responder. These two parents were used to produce 300 F2 mice. The 4-point bending method utilized a 9N load (3500 ue, upper limit of physiological strain) at 2Hz for 36 cycles and was applied for 12 days. Two days after the last load, skeletal changes were evaluated by pQCT. In these F2 mice, all three phenotypes (changes in bone size, mBMD and vBMD) showed Gaussian distributions, consistent with complex traits. Heredity indexes ranged from 86-70%. The vBMD data demonstrated that some F2 mice had decreased bone density in response to the load whereas other mice gained as much as 20% in vBMD of the tibia. The other phenotypes ranged from -5 to +5% for mBMD, and -10 to +30% for bone size in the F2 mice. Cortical BMD reflects material bone mineral density (mBMD) since vascular canal volume in our sampling site is too low to alter cortical BMD (less than 1% of the bone volume). Our data on BMD of bone formed prior to loading indicates for the first time that mechanical load increases mBMD. We next determined if the magnitude of bone anabolic response to 4-point bending is dependent on body size. None of the three phenotypes were positively correlated with body weight. Furthermore, there was no significant difference between the bone size (unloaded bones) and the degree of change in vBMD in response to loading. These data demonstrate that a differential anabolic response cannot be explained by differences of applied mechanical strain in the F2 mice or to differences in body size. Summary: 1) Anabolic response to a standard mechanical load can be divided into at least three different phenotypes (change in bone size, vBMD, and mBMD). 2) These three phenotypes show a Gaussian curve in the B6/C3H F2 mice consistent with a complex trait controlled by several genes. 3) Bone size and vBMD changes are dependent upon new bone formation, found to be exceedingly variable in our F2 mice. However, the mBMD phenotype, a measurement of mineral density in preexisting bone, implies that there is a mechanism to increase mBMD materials density i.e. the bone quality can adapt to a large mechanical load. Conclusion: This study shows genetic environmental adaptive interactions in bone of a remarkable magnitude.

Introduction

It is now well acknowledged that skeletal development and increase in bone anabolic response are largely dependent upon mechanical stimulation. Several *in vivo* studies in rats, mice and turkeys using pQCT and histology have shown that bone mass increases in response to mechanical loading. It has also been well demonstrated using cell culture models that mechanical stimulation activates many signaling pathways such as integrins, FAK, NO, etc., resulting in increased osteoblast proliferation, differentiation, and activity. Thus, physical exercise has been used as a therapeutic strategy for improving the bone mass and bone quality to prevent osteoporosis/fracture in humans. Recent studies have shown that bone response is variable; although the same amount of mechanical stress is applied, some individuals exhibit robust bone formation while others respond poorly. Accordingly, in our previous studies we have identified two inbred mouse strains that vary in their peak bone density and display a considerable difference in the bone response to mechanical loading. The B6 mice have a low bone density and showed good response, while the C3H mice with high bone density showed poor adaptation to mechanical stimuli (1,2). These findings are consistent with results of jump studies by Umemura, et al, and 4-point bending by Recker, et al, (3). In terms of mechanisms that contribute to this variation in bone response to loading, others and we have shown that variation is largely influenced by genetic factors. In order to identify these genetic factors, we hypothesize that bone responses induced by mechanical loading are controlled by multiple genes. One of the approaches commonly employed for identifying the candidate genes in complex traits is QTL mapping. In the present study, we generated F2 mice by crossing two inbred strains of mice that exhibited an extreme difference in the bone response to loading, and examined the phenotypic changes and distribution in an attempt to establish the mouse model for further studies.

Materials and methods

Animals: 5-week old female C57BL/6J (B6) and male C3H/HeJ (C3H) inbred mice were purchased from the Jackson Laboratory and housed at the Animal Research facility at the JL Pettis VA Medical Center (Loma Linda, CA). These two inbred strains were crossed to produce a population of 300 F2 mice. At 10-weeks, each F2 mouse was used for mechanical loading using the optimized loading regimen.

In vivo loading model: We used a 4-point bending method developed by Dr.Recker and his collaborators as our *in vivo* loading regimen (3). The loading protocol consisted of a 9N load at 2Hz frequency for 36 cycles and the training was conducted once per day. Before the training the mice were given halothane anesthesia [95% Oxygen and 5% Halothane] for 2-3 minutes and while anesthetized the loading was performed. The right tibia was used for loading while the left tibia was used as an internal control. The mice were trained for 6 days/ week for 2-weeks. 48hrs after the last loading regimen, on the 15^{th} day in vivo pQCT was performed and later the mice were sacrificed, tibias collected and stored in RNA later at –80° C for RNA extractions.

Bone parameters measurement: Geometrical properties of loaded and unloaded tibias were measured by peripheral quantitative computed tomography (pQCT) using a Stratec XCT 960M (Norland Medical System, Ft.Atkinson, WI).

Heritability Calculation: We used a Vf2 –1/2[Vp1 +Vp2]/Vf2 formula to calculate the heritability of the phenotypes in the F2 population.

Statistical analysis: Percentage change in the bone phenotypes was calculated by subtracting the loaded bone values from the unloaded bone values and divided by unloaded bone values. Phenotypic distributions were plotted using the percentage change by Statistica software.

Results

Distribution of percentage change values for vBMD, mBMD, and PC

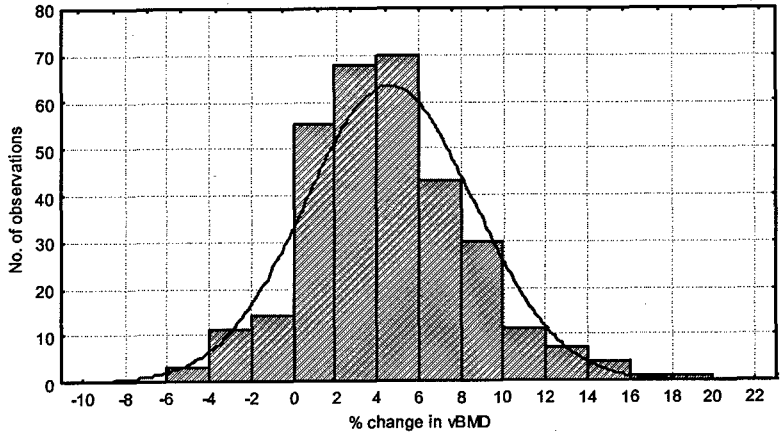

(a)

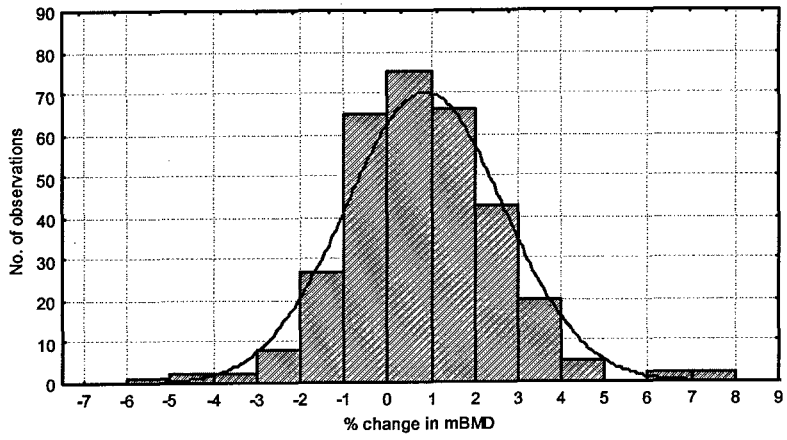

(b)

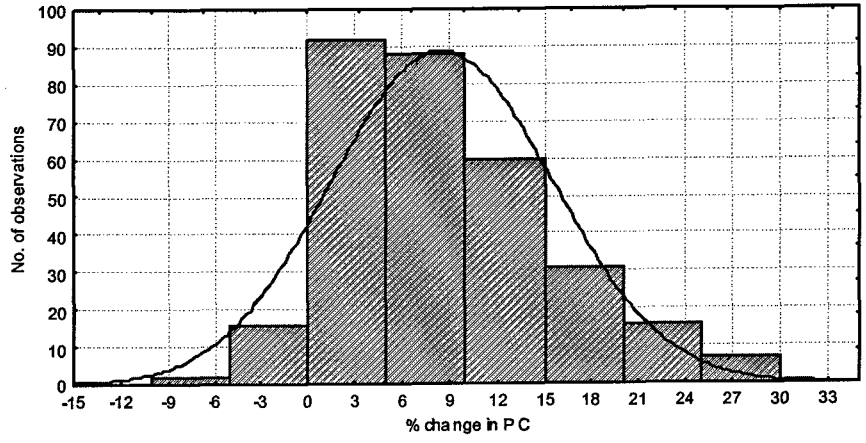

(c)

Fig.1. Distribution of percentage changes in (a) vBMD, (b) mBMD, and (c) PC response in the F2 population after two weeks of 4-point bending. The x-axis represents the percentage change ('–' Indicates reduction) and y-axis represents the number of observations (mice). vBMD, volumetric bone mineral density; mBMD, material bone mineral density; PC, periosteal circumference. The solid line represents theoretical normal distribution. Based on kolmogorov-smirnov test, vBMD, mBMD, and PC show normal distribution.

Interpretation:

1) Cyclic loading of the tibia resulted in increased vBMD, mBMD, and PC in most animals.
2) The vBMD, mBMD, and PC values showed a Gaussian distribution in the F2 population.
3) All three phenotypes induced by mechanical loading showed 70-80% heritability.
4) There was a variable bone response to mechanical loading in terms of vBMD (-6 to +20%), mBMD (-5 to +5%) and PC (-10% to +40%) in the F2 population.
5) The increase in cortical density (mBMD) reflects an increase in true mineral density because the vascular canal volume in our sampling sites was too low to alter cortical BMD [(less than 1%), data not shown].
6) These findings suggest that mechanical load induced bone response is a complex trait controlled by several genes.

Percentage change of vBMD, mBMD, and PC is unrelated to body weight

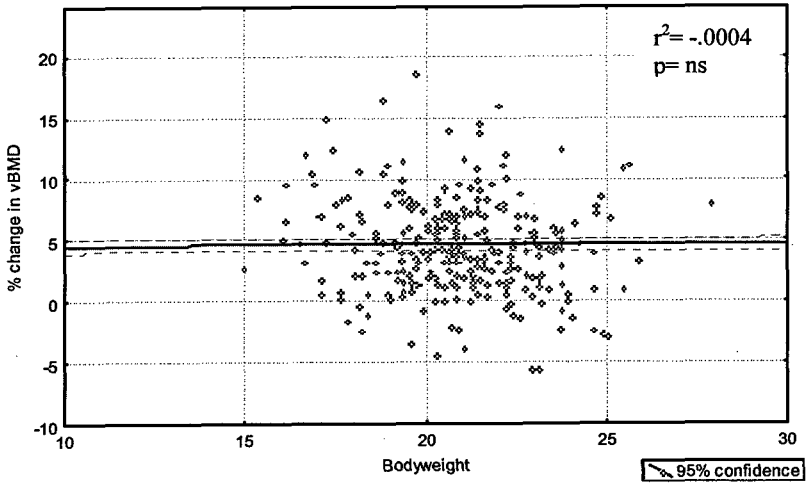

(a)

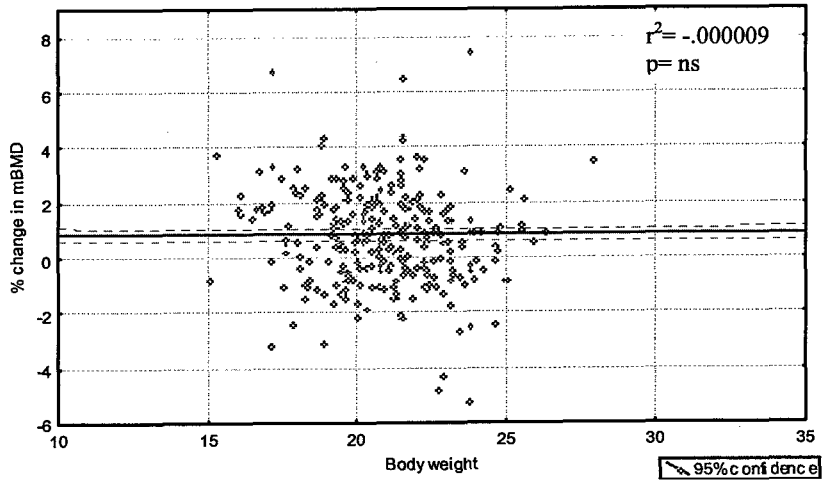

(b)

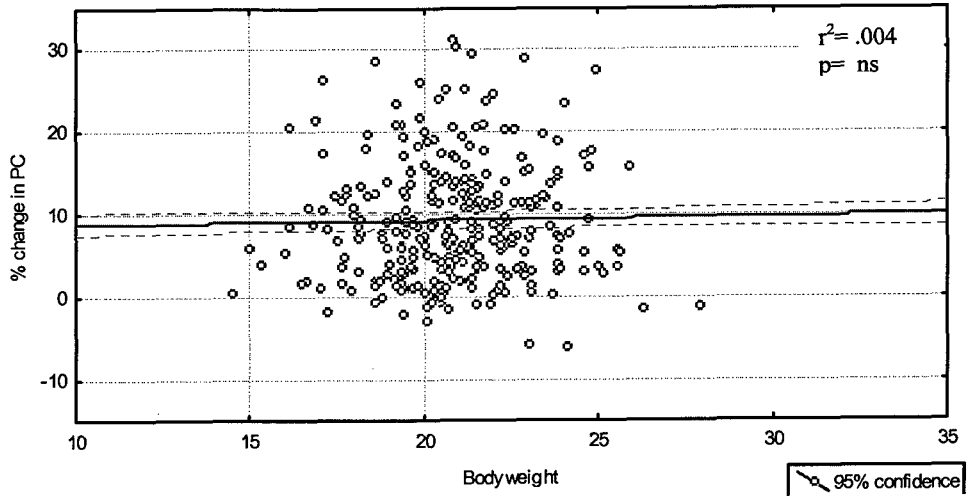

(c)

Fig.2. Correlation of body weight with percentage change in the (a) vBMD, (b) mBMD, and (c) PC of F2 population after mechanical loading. The x-axis represents body weight and the y-axis represents percentage change in the bone phenotypes. ns: not significant.

Interpretation:

1) The changes in the vBMD, mBMD, or PC induced by mechanical loading did not show significant correlations with body weight in the F2 population.
2) This finding suggests that mechanical loading-induced bone responses in the F2 population are unrelated to changes in body weight.

Percentage change of vBMD and mBMD is inversely related to bone size

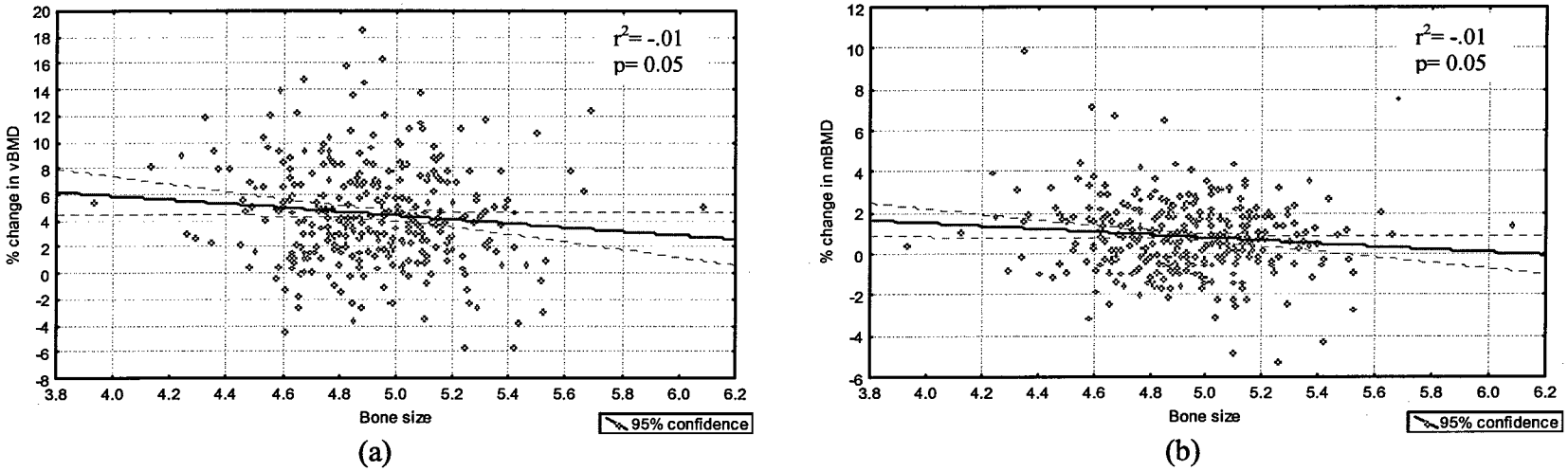

Fig.3. Correlation of bone size (unloaded bones) with the percentage change in the (a) vBMD and (b) mBMD of the F2 population after mechanical loading.

Interpretation:

1) We found mechanical load-induced bone phenotypes (vBMD and mBMD) showed an inverse correlation with the bone size of the F2 population.
2) Because bone size in the F2 population varied by as much as 20%, we anticipated that the amount of strain would vary in different F2 mice. Accordingly, we predicted a significant negative correlation between BMD response vs. bone size. The weak correlation between BMD change and bone size suggests that variation in bone size contributes only minimally (1%) to variation in BMD response.

Summary

1) Anabolic response to a standard mechanical load produces at least three different phenotypes (change in bone size, vBMD, and mBMD).
2) These three phenotypes show a Gaussian distribution in the B6/C3H F2 mice consistent with a complex trait controlled by several genes.
3) Bone size and vBMD changes are dependent upon new bone formation, found to be exceedingly variable, in our F2 mice. However, the mBMD phenotype, a measurement of mineral density in preexisting bone, implies that there is a mechanism to increase mBMD material density i.e. the bone quality can adapt to a large mechanical load.

Conclusion

1) The response to mechanical loading is variable and dependent upon the allele structure of multiple genes.

Acknowledgements

This work was supported by Assistance Award No. DAMD17-03-2-0021. The U.S. Army Medical Research Acquisition Activity, 820 Chandler Street, Fort Detrick MD 21702-5014, is the awarding and administering acquisition office. The information contained in this publication dose not necessarily reflects the position or the policy of the government, and no official endorsement should be inferred. All work was performed in facilities provided by the Department of Veterans Affairs.

References:

1) Kodama Y, Dimal HP, Wergedal J, Sheng M, Malpe R, Kutilek S, Beamer W, Donahue LR, Rosen C, Baylink DJ and Farley J 1999. *Bone* 25(2):183-190.
2) Kodama Y, Umemura Y, Nagasawa S, Beamer WG, Donahue LR, Rosen CR, Baylink DJ and Farley JR 2000. *Calcif Tissue Int* 66:208-306.
3) Akhter MP, Cullen DM, Pedersen EA, Kimmel DB, Recker RR 1998. *Calcif Tissue Int* 63(5):442-9.

Fluid Shear Stress (a Mechanical Strain Mimic) Synergizes with IGF-I on Human Osteoblast Proliferation Through Upregulation of the IGF-I Signaling Pathway

S. Kapur, D. J. Baylink, K. W. Lau; Musculoskeletal Disease Center, Jerry L. Pettis Mem VAMC, Loma Linda, CA

Presentation Number: 1567

Poster Board Number: B30

Mechanical strain increases osteoblast proliferation and bone formation. Recent studies suggested that mechanical strain has a permissive role in the IGF-I mitogenic action in osteoblasts. This study tested the hypothesis that mechanical strain interacts with the IGF-I pathway in the stimulation of osteoblast proliferation. Human osteoblasts were subjected to steady shear stress of 20 dynes/cm^2 for 30 min followed by 24-hr incubation with IGF-I (1 to 50 ng/ml) or vehicle. Parallel cells without the stress were the controls. [^{3}H]Thymidine incorporation (TdR) was measured as an index of proliferation. IGF-I increased TdR (1.5- to 2.5-fold, $p<0.01$) in a dose-dependent manner. Shear stress alone increased TdR by 70% ($p<0.01$). The combination of shear stress and IGF-I produced stimulation in TdR (3.5- to 5.5-fold) much greater than the additive effects of each treatment alone. ANOVA suggests a synergistic interaction. The same shear stress did not enhance the FGF-2-induced osteoblast proliferation, suggesting that the interaction may be specific for IGF-I. To assess the effects on the IGF-I signaling pathway, the phosphorylation levels of Erk1/2 and IGF-I receptor (IGF-IR) were determined by western analyses. IGF-I significantly and dose-dependently increased the phosphorylation level of Erk1/2 (1.2- to 5.3-fold) and IGF-IR (2- to 4-fold). The shear stress alone increases the phosphorylation Erk1/2 and IGF-IR (2-fold each). The combination treatment resulted in synergistic enhancements in both Erk1/2 and IGF-IR phosphorylation (up to 12-fold for Erk1/2 and 8-fold for IGF-IR). While treatment with FGF-2 caused 4-fold increase in Erk1/2 phosphorylation, the combined treatment of shear stress and FGF-2 induced no further enhancement. In summary, mechanical stress interacts synergistically with the IGF-I signaling pathway in osteoblast proliferation and this interaction may be unique to the IGF-I pathway.

Global Application of Expression Profiling Reveals Potential Involvement of the Wnt, IGF-I, Estrogen Receptor (ER), and BMP/TGFβ Pathways in C57BL/6J (B6) But Not C3H/HeJ (C3H) Mouse Osteoblasts In Response to Fluid Shear Stress

K. H. W. Lau, S. Kapur, D. J. Baylink. Musculoskeletal Disease Center, Jerry L. Pettis Mem VAMC, Loma Linda, CA, USA.

Presentation Number: SA264

Our previous studies indicate that, while B6 inbred mice responded to in vivo mechanical loading with an increase in bone formation; C3H mice showed no such response. In this study, we tested the hypothesis that this inbred mouse differential response would be present in vitro in response to shear stress. We found that a steady fluid shear stress of 20 dynes/cm^2 for 30 min, while significantly increased (by 2-fold, $p<0.001$) thymidine incorporation and ALP specific activity in B6 osteoblasts (ob), had no effects on either parameter in C3H ob, confirming that osteogenic responses to mechanical strains are genetically regulated. We next applied global gene expression profiling 4 hr after the 30-min shear stress in an attempt to identify signaling pathways to account for the differential shear stress response in ob from these 2 inbred strains of mice. RNAs isolated from C3H and B6 ob (4 replicates each) were analyzed by microarray with our in-house chips (containing 5,500 gene fragments). Paired t-test and Lowess normalization were performed with Genespring software and gene expression changes defined as significant if $p<0.05$. The expression of 672 genes in B6 ob and 477 genes in C3H ob was altered in response to the shear stress. 515 genes were affected only in B6 ob. Preliminary grouping (according to gene functions or pathways) of known mouse genes that were affected only in B6 ob revealed that (consistent with an anabolic response) genes involved in proliferation and energy metabolism were upregulated. Several genes of the IGF-I (IGFBP-5, IGF-IR, MKK3, Big MAPK1, c-Fos, c-Jun) and ER (ERα, NCOA1) pathways were upregulated only in B6 ob. Moreover, several genes of the BMP/TGFβ pathways (BMP-4, TGFβ1, TGFβ2, BMP2/4 receptor, Mef2, Dlx-1, Necdin) and the Wnt pathway (Wnt-5a, Lef-1, β-catenin) were also upregulated in B6 but not C3H ob. Regarding the Wnt pathway, the upregulation of gene expression of Wnt-5a, Lef-1, LRP-5, and β-catenin in B6 but not C3H ob was confirmed by real-time PCR and western blots. Importantly, endostatin (a potent inhibitor of wnt pathway) abolished the upregulation of β-catenin gene expression and blocked the shear stress-induced proliferation in B6 ob. In summary, the robust mitogenic response to steady shear stress in B6 but not C3H ob was associated with significant increased gene expression in the IGF, ER, BMP/TGFβ, and Wnt pathways. The differential regulation in these anabolic pathways could contribute to the good and poor response, respectively, in the B6 and C3H mice to fluid shear stress.

Mechanical loading induced gene expression and BMD changes are different in two inbred mouse strains

Chandrasekhar Kesavan[1], Subburaman Mohan[1, 2], Susanna Oberholtzer[1], Jon E. Wergedal[1, 2] and David J. Baylink[1, 2]

[1]Musculoskeletal Disease Center, VA Loma Linda Healthcare System, Loma Linda, CA

[2]Department of Medicine, Loma Linda University, Loma Linda, CA

Running Title: Skeletal response to mechanical loading.

Corresponding Author: Subburaman Mohan, Ph.D.

Research Professor of Medicine and Biochemistry

Loma Linda University

Musculoskeletal Disease Center (151)

Jerry L. Pettis Memorial VA Medical Center

11201 Benton Street

Loma Linda, CA 92357

Phone:909-825-7084, ext. 2932

FAX: 909-796-1680

E-Mail: Subburaman.Mohan@med.va.gov

Abstract

Our goal is to use QTL analysis to identify the genetic traits that contribute to variation in bone adaptive response to mechanical loading. Loads of varying magnitudes (6- 9N) were applied at 2Hz, 36cycles for 12 days on tibia of 10-week female B6 & C3H mice. 9N load on varying age groups. Changes in the bone parameters were measured using pQCT and gene expression by Real time PCR. Total vBMD was increased by 5% and 15%, respectively, at the 8 and 9N loads in the B6 mice, but not in the C3 mice. Periosteal circumference increased by 20% and 12%, respectively, which is reflected by a dramatic 44% and 26% increase in total area in the B6 and C3 mice. Bone response to bending showed no difference in the three age groups of the B6 and C3 mice. At day 2, mechanical loading caused significant down regulation in the expression of bone resorption (BR) marker genes with no change in the expression of bone formation (BF) marker genes. Four and eight days of loading caused 2-3 fold increases in the expression of BF genes (ColA1, ALP, OC, BSP) and 2-5 fold decreases in the expression of BR marker genes (MMP-9, TRAP). While expression of BF marker genes were up-regulated by 4-8 fold at 12 days of training, the expression levels of BR marker genes were up regulated by 7-9 fold. 4.point bending caused significantly greater changes in the expression levels of both BF and BR marker genes in the bones of the B6 mice compared to the C3 mice. Based on these data, we conclude that mechanical loading induced molecular pathways are activated to greater extent in B6 mice compared to C3 mice, ultimately resulting in a higher anabolic response in B6 mice

Key Words:

Mechanical Loading; bone density; mice; bone size; gene expression

Introduction

It is well established that maintenance of bone mass and the development of skeletal architecture are dependent on mechanical stimulation. A number of studies have shown that mechanical loading promoted bone formation in the modeling skeleton and that removal of this stimulus resulted in a reduction in bone mass (1, 9, 13, 28, 29). In addition, recent studies have also shown that the increase in bone mass was variable in different subjects given the same amount of mechanical stress, with some exhibiting a robust osteogenic response and others responding more modestly (8, 24, 26). We and others have found evidence that this variation in response to mechanical loading is, in large part, genetically determined (12, 13, 19). Accordingly, we have identified two inbred mouse strains that differ in peak bone density and exhibit considerable differences in their bone response to immobilization and mechanical loading. In our studies, we found that the C57Bl/6J mouse strain showed a greater loss of bone in response to hind limb immobilization by sciatic neurectomy compared to the C3H/HeJ strain. Furthermore, studies by Umemura et al. and Kodama et al. (13, 28) as well as four-point bending studies by Akhter et al. (1) have revealed that an identical amount of mechanical force applied to both mouse models produced a greater increase in the bone formation [periosteal and endosteal formation] parameters in the C57Bl/6J mice compared to the C3H/HeJ mice.

A number of *in vitro* studies have employed mechanical stimulation using various models in mouse and human cells, and have found that several signaling pathways, including mitogen activated protein kinase (16, 17, 31), focal adhesive kinase (4, 18, 30) and nitric oxide (3, 11, 15, 32) mediate the effects of mechanical loading in bone. However, the genetic mechanisms that contribute to any variations in anabolic response to loading remain unclear. One approach often used to identify the genetic factors or genes that contribute to differences in phenotypic variation

is the QTL (Quantitative Trait Loci) technique. In the QTL approach, two inbred mouse strains exhibiting a phenotypic difference of interest are crossed and any genetic loci that co-segregate with the phenotype are identified. A successful QTL approach requires the following components: a) an optimized *in vivo* loading model; b) valid endpoints to measure the difference in bone anabolic response; and c) an optimal age that shows a greatest difference in the phenotype in response to mechanical loading. In this study, we proposed the hypothesis that the magnitude of skeletal anabolic response in the B6 and C3H mouse strains is dependent on the age of the mice and the amount of load applied, which is reflected by changes in expression levels of bone formation and /or bone resorption marker genes. To test the above hypothesis, our initial objectives for the present study were to: 1) evaluate bone's response to different loads applied by four-point bending; 2) determine if any differences in the bone response to mechanical strain between the B6 and C3H mice can be accurately quantitated using peripheral quantitative computed tomography (pQCT) and/or the expression levels of bone formation marker genes; and 3) evaluate if the bone response induced by four-point bending varies in different age groups in the B6 and/or C3H mouse strains.

Materials and Methods

Animals

Different age groups (10wk, 16wk & 36wk) of female C57BL/6J (B6) and C3H/HeJ (C3H) inbred mice were purchased from the Jackson Laboratory (Bar Harbor, ME) and housed at the Animal Research facility, Jerry L. Pettis Memorial VA Medical Center (Loma Linda, CA) under appropriate conditions. Animal procedures performed in this study were approved by the Animal Studies Subcommittee of the Jerry L. Pettis Medical Center. The bodyweight (gm) in the 10-

week (wk) female B6 mice were 18.8 ± 0.1, in 16-week 20.7 ± 0.3 and in 36-week 26.2 ± 0.5. The bodyweight (gm) in 10-week female C3H mice were 19.1 ± 0.1, in 16-week 20.7 ± 0.5 and in 36-week 27.8 ± 0.4.

***In-vivo* loading model/ regimen**

We used the four-point bending method developed by Akther et al. (1) as our *in vivo* loading regimen. In brief, the four-point bending device [Instron, Canton, MA] consists of two upper vertically movable points covered with rubber pads, which are 4mm (millimeter) apart, and two 12mm lower non-movable points covered with rubber pads. During bending, the two upper pads touch the lateral surface of the tibia through overlaying muscle and soft tissue, while the lower pads touch the medial surface of the proximal and distal parts of the tibia. The loading protocol consists of a 6-9 N (Newton) load at a frequency of 2Hz (frequency) for 36 cycles and the training is performed once per day. The right tibia is used for the loading test while the left tibia is used as an internal control. After anesthetizing the mice, the ankle of the tibia was positioned on the second lower immobile points of instron such that the region of tibia loaded did not vary in different mice. To anesthetize the mice we used halothane [95% Oxygen and 5% Halothane] for 2-3 minutes and performed mechanical loading while the mice were anesthetized. The mice were trained for 6 days/week with 1 day of rest for 2-weeks. On the 15th day, after 48 hrs following the last loading regimen, mice were sacrificed, the tibias collected and stored at 4°C until pQCT is performed.

pQCT densitometry

To determine if there was a significant change in the geometrical properties of loaded and unloaded tibias, we used the pQCT system from Stratec XCT Research [Stratec Medizintechnik, Berlin, Germany]. This instrument was specifically modified for the use of small bone specimens to measure the bone mineral content, periosteal and endosteal circumferences, total area, and total content. Routine calibration was performed daily with a defined standard containing hydroxyapatite crystals embedded in Lucite. Scanning was performed using the manufacturer supplied software program, designed to analyze the data and generate the values for the change in bone parameters. Furthermore, the X-ray attenuation data were analyzed based upon the software-defined threshold. We set up two thresholds for our analysis. A 180-730 mg/cm^3 threshold was used to measure total area, total mineral content (TC), periosteal circumference (PC), and endosteal circumference (EC) in the loaded vs. unloaded bones and a 730-730-mg/cm^3 threshold was used to measure cortical thickness (CT), total volumetric density (vBMD), and material bone mineral density (mBMD).

In order to minimize the measurement errors caused by positioning of tibia for pQCT, we used the tibia-fibular junction as the reference line. We selected four-slices that start 3 mm proximal from tibia-fibular junction for pQCT measurement. This region corresponds to the loading zone. Each slice is at a 1mm interval and the values presented in the results are an average of these four slices.

Strain measurement

The differences in the amount of mechanical strain (με) on the loaded region produced by different loads were measured in the B6 and C3H mice using the strain gauge-technique (2, 7,

25). We used only the loaded region of the tibia to measure the strain because that was the area most affected by 4mm vertical movable points according to our pQCT analysis. Briefly, a P-3500 portable strain indicator and strain gauge of a specific range (EP-XX-015DJ-120) were used to measure the amount of mechanical strain produced by different loads. Initially, the ends of the strain-gauge circuits were soldered to copper wire and glued on the medial side of the tibia, 2.09 mm away from the tibia-fibular junction to provide a consistent position on the 4mm loading zone. These copper wires were connected to the indicator and the amounts of strain produced by the loads on the loading zone were recorded. The strain-gauge data from four individual mice were averaged for each load.

Micro-crack detection using en block staining

We performed four-point bending for 12 days at 9N load in 10-week old B6 and C3H mice and 2 days after last loading tibias were collected and stored at 10% formalin. One thick section was made on the loaded and unloaded bones, and both sides were measured for micro-cracks (Bone area mm^2). The data mentioned in the results are mean ± SE of six animals in each strain of mouse. We used the fuchsin staining method to detect microcracks (5).

RNA Extraction

A Qiagen lipid extraction kit [Qiagen, Valencia, CA] was used to extract RNA from bones with the following modification. After euthanization, tissues were removed from test mice and immediately transferred into liquid nitrogen and stored at –80°C until RNA extraction. Bones were ground into fine powder using mortar and pestle with liquid nitrogen. Approximately 1ml of Trizol was added to each sample and ground until it became a fine powder. This fine bone

powder was transferred to fresh 1.5ml (milliliter) RNase free tubes. Chloroform (200µl) was added to each sample, and each sample was vortexed for 15 seconds (sec) and incubated at room temperature for 3 minutes. The samples were then centrifuged at 12,000g for 15 minutes and an aqueous layer was removed to a fresh tube after centrifugation. Approximately 700µl (microliter) of ethanol was added to the fresh samples and vortexed for 15 sec. The samples were then transferred to a spin column and the RNA was purified according to the manufacturer's instructions. Quality and quantity of RNA were analyzed using Bio-analyzer and Nano-drop instrumentation [Agilent, California, USA].

Reverse Transcriptase - Real time PCR

Quantitation of messenger Ribonucleic acid (mRNA) expression was carried out according to the manufacturer's instructions (ABIPRISM, Foster City, CA.) using the SYBR Green method on 7900 Sequence Detection systems from Applied Biosystems. Briefly, purified total RNA [200µg/µl] was used to synthesize the first strand cDNA by reverse transcription using random hexamers and Superscript II reverse transcriptase according to the manufacturer's instructions [Invitrogen, Carlsbad, CA]. One µl of this first strand cDNA reaction was subjected to real time PCR amplification using gene specific primers. The primers were designed according to the ABI primer express instructions using Vector NTI software and were purchased from IDT-DNA. Approximately 25µl of reaction volume was used for the real time PCR assay that consisted of 1X [12.5µl] Universal SYBR green PCR master mix [Master mix consists of SYBR Green dye, reaction buffers, dNTPs mix, and Hot Start Taq polymerase] [Applied Biosystems, Foster City, CA], 50nM of primers, 24µl of water, and 1ul of template. The thermal conditions consisted of an initial denaturation at 95°C for 10 minutes followed by 40 cycles of denaturation at 95°C for

15 seconds (sec), annealing and extension at 60°C for 1 minute, and a final step melting curve of 95°C for 15 sec, 60°C for 15 sec, and 95°C for 15 sec. All reactions were carried out in duplicate to reduce variation. The data were analyzed using SDS software, version 2.0, and the results were exported to Microsoft Excel for further analysis. Data normalization was accomplished using the endogenous control [β-actin] and the normalized values were subjected to a $2^{-\Delta\Delta}Ct$ formula to calculate the fold change between the control and experiment groups. The formula and its derivations were obtained from the ABI Prism 7900 Sequence Detection System user guide.

Statistical analysis

Data are presented as Mean ± Standard Error (SE). Regression analysis, ANOVA (Bonferroni-Post Hoc Test) and standard T-test were used to compare differences from loading between the strains using the percentage obtained from loaded vs. unloaded bones. We used STATISTICA software for our analysis and the results were considered significantly different at $p<0.05$.

Results:

Bone anabolic response to varying magnitude of loading

Total bone mineral content: Four-point bending caused an increase in total bone mineral content in both the B6 and C3H mouse strains. The magnitude of increase varied depending on the amount of load between the B6 and C3H (Table-1). At 9N, the percentage increase in total bone mineral content in response to four-point bending was significantly greater in the B6 (48%) mice than in the C3H (19%) mice (Fig.1a).

Area: Total area increased in response to four-point bending in both the B6 and C3H strains of mice. A dramatic increase of 44% and 26% in total area was seen after 12 days of four-point bending in the B6 and C3H mice, respectively (Table-1). The B6 mice ($p<0.05$) showed a greater increase in total area than in the C3H mice at a 9N load in contrast to other loads (Table-1 & Fig.1a).

Periosteal circumference: The periosteal circumference increased by 20% and 12% in the B6 and C3H mice, respectively, in response to four-point bending (Table-1). The B6 mice showed a greater increase in periosteal circumference than the C3H ($p<0.05$) mice at 9N compared to other loads (Table-1 & Fig.1a).

Total volumetric density: Four-point bending caused a dose-dependent increase in the total bone density seen in the B6 mice (regression analysis $p<0.01$), but not in the C3H mice (Table-1). The B6 mice showed 5% and 15% greater density at loads of 8 and 9N, respectively, after 12 days of loading, while the C3H mice exhibited no change (Table-1, Figs.1a & 1b).

Cortical density: Cortical density increased by 4% in the B6 mice, but not in the C3H mice, at a load of 9N after 12 days of four-point bending (Fig.1a).

Cortical thickness: Four-point bending increased cortical thickness in both the B6 and C3H mouse strains after two-weeks of mechanical loading at a load of 9N. The magnitude of increase was much greater in the B6 mice (27%) compared to that seen in the C3H mice (7%) (Fig.1a).

Endosteal circumference: Endosteal circumference in response to four-point bending increased by 23% and 18% in both the B6 and C3H mouse strains, respectively (Table-1). The C3H mice showed a greater increase in the endosteal circumference compared to the B6 mice at a load of 8N ($p<0.05$).

Strain measurement

Since the B6 and C3H mouse strains differ in their bone geometrical properties, we next evaluated if the difference in bone anabolic response to different loads in the two strains of mice could be explained on the basis of a difference in the amount of mechanical strain produced by the loads. Therefore, we measured the amount of mechanical strain produced by varying load magnitudes applied by four-point bending on the tibia of 10-week old B6 and C3H mice using the strain-gauge technique. The results from our study (Table-2) revealed an increase in mechanical strain with an increase in mechanical load in both the B6 and C3H mice. The C3H mice showed slightly higher mechanical strains compared to the B6 mice in all the loads and the differences were statistically significant ($p<0.01$, ANOVA) (Table-2).

Micro-crack detection

In order to rule out the possibility that the changes on bone parameters induced by a load of 9N are due to micro-crack induced healing, we measured micro-cracks by histological analysis. The micro-cracks area (mm^2) was not significantly different between the loaded vs unloaded bones for either B6 (0.82 ± 0.05 vs. 0.60 ± 0.04) or C3H (0.87 ± 0.07 vs 0.95 ± 0.02) mice. Furthermore, the micro-crack area was not significantly different between the two strains in either the loaded or unloaded bone.

Mechanical loading in response to varying age groups of B6 and C3H strains of mice

We carried out four-point bending with a similar loading regimen as above in varying age groups [10-week, 16-week, and retired breeders] of the B6 and C3H mice to study the response of bone to a load of 9N as a function of age. The results from our experiment indicated that four-point bending caused significant increases in the bone parameters in the 10, 16, and 36-week age groups of both strains of mice when measured by pQCT. As shown in Table 3, 4 & Figure 2a & b, the B6 mice showed greater changes than the C3H mice in the total mineral content, total area, periosteal circumference, and total volumetric density and cortical density in all 3 age groups studied. Using the Bonferroni Post hoc test, we found no statistical difference in the bone responses between the age groups of the B6 and C3H mice.

Gene expression changes in response to four-point bending

In order to evaluate the involvement of osteoblast and osteoclast cell function in producing the an optimal response to a given skeletal load, we measured gene expression changes using real time PCR after 2, 4, 8, and 12 days of mechanical loading in 10-week old female B6 mice. As shown in Table-5, 2 days of four-point bending performed on the B6 mice caused significant decreases in the expression of bone resorption genes, but had no significant effect on the expression levels of bone formation genes in loaded tibia compared to unloaded tibia. In addition, 4 days of loading induced expression of both type-I collagen (Cola1) and bone sialoprotein (BSP) by 2-fold and downregulated MMP-9 and TRAP by 3- and 4- fold, respectively. No change was found in the expression of osteocalcin and alkaline phosphatase (Table-5). Eight days of loading caused an increase in the expression of type-I collagen, bone

sialoprotein, alkaline phosphatase (ALP), and osteocalcin (OC) by 3-fold, and down regulation of TRAP by 3-fold. No change in expression was found between loaded and unloaded bones for MMP-9 after 8 days of loading (Table-5). Prolongation of loading of up to 12 days showed significant changes in expression for both bone formation (type-I collagen, bone sialoprotein, alkaline phosphatase and osteocalcin with 4.1-, 7.8-, 6-, and, 4-fold) and resorption marker genes (MMP-9, TRAP with 7.5-, and 12.2-fold, respectively) (Table-5). The expression level of RANKL was increased by 5-fold after 12 days of training in the loaded bone compared to unloaded bone.

Difference in expression of genes between B6 and C3H mice

Although there was increase in expression levels of both BF and BR marker genes in both strains, B6 mice showed a significantly greater increase in the expression levels compared to C3H mice. Bone sialoprotein showed the most significant difference in the expression levels between the two mouse strains (Table-6).

Discussion

The salient features of the present study are as follows: a) Four-point bending increased vBMD and mBMD significantly in the B6 mouse strain but not in the C3H mice; b) Age (10 week to 36-week-old mice) had no effect on bone response to four-point bending; c) Four-point bending caused acute changes in both bone resorption and formation genes expression; and d) Four-point bending-induced expression changes were greater in the bones of B6 mice than in C3H mice.

One of the major findings of this study is that 12 days of mechanical loading using the four-point bending technique caused a striking 15% increase in total vBMD in the tibia of the B6 mouse strain at a load of 9N. The vBMD was increased by 4.5% at a load of 8N in the B6 mice. In contrast to the response observed in the B6 mice, none of the four loading regimens applied (i.e. 6, 7, 8, and 9N) produced any significant increase in total vBMD in the tibia of the C3H mice. Interestingly, this lack of significant change in vBMD cannot be explained by inadequate mechanical strain, since a load of 9N produced 3865 με in the tibia of the C3H mice, which is above the physiological range (300-3000με) and, notably, is higher than the mechanical strain produced in the tibia of the B6 mice. Furthermore, a mechanical load of 9N caused a significant increase in both total area and periosteal circumference in the C3H mice, suggesting that the observed increase in vBMD response in the tibia of this strain is not caused by a lack of mechanosensitivity.

In terms of the rapid increase in total vBMD observed in the B6 mice in response to four-point bending, we found that cortical thickness was increased by 27%. Consistent with this increase in cortical thickness, bone area increased significantly as well in the B6 strain's response to mechanical loads of 9N. The increase in bone area and cortical thickness can be explained by the observed increase of nearly 20% in periosteal circumference, which results in a near 50% increase in total area in the loaded tibia compared to unloaded tibia after 12 days of four-point bending. In contrast to the increases observed in the B6 mice, the magnitude of increase in periosteal circumference, total area, and cortical thickness were substantially less in the C3H mice. Consistent with these data, Akhter et al. (1) have found a greater increase in the periosteal bone formation response in B6 mice compared to C3H mice after four-point bending. Similarly, we found a significantly greater increase in the expression of bone formation marker genes in the

loaded tibia of tested B6 mice compared to C3H mice (Table-6). Based on these data, we have concluded that a greater increase in periosteal bone response in the B6 mouse contributes, in part, to the observed increase in total vBMD in the tibia of loaded bones of this strain.

Our findings demonstrate for the first time that mechanical loading results in a significant increase in material BMD, which also contributes to an increase in total vBMD. In this regard, we consider the increase in cortical density to represent changes in mBMD since the vascular canal volume as determined by histological analysis was too low in the loaded bones to account for the increase in cortical BMD. Therefore, we believe that a mechanical load of 9N caused a maximum mineralization and increase in bone maturation (age) in the tibia of the B6 mice. Consistent with this interpretation, we found that four-point bending caused an acute down regulation of expression of bone resorption marker genes at 2 and 4 days of four-point bending. Thus, the loading-induced decrease in remodeling could contribute to an increase in the rate of mineralization, and thereby contribute to the observed increase in mBMD and total vBMD in the tibia of the B6 mice.

Our dose response studies with different mechanical loads revealed that a significant bone anabolic response to loading was only observed at loads of 8 and 9N, which produced mechanical strains slightly above the physiological range (500-3000 με). Earlier studies (6) have demonstrated that mechanical strain produced by loads above the physiological range may lead to an accumulation of micro-cracks in the loaded bone. In order to determine if the bone anabolic response observed after the 8 and 9N loads was due to micro-cracks, we performed histological analysis on the cross section loaded-region of the tibia of the B6 and C3H mice after 12 days loading to identify potential micro-cracks. However, we did not observe any micro-cracks in either the B6 or C3H mice at the highest loads of 9N. These findings imply that differences in

bone anabolic response between the C3 and B6 strains cannot be ascribed to a difference in the amount of micro-cracks as evaluated by the method used in this study.

In order to include the newly formed bone, which may not have been fully mineralized, we used a threshold of 180-730 mg/cm3 for evaluation of loading-induced changes in total area, total mineral content, as well as periosteal and endosteal circumference. Thus, it is possible that the dramatic changes in mineral content and bone size after 2 weeks of loading may represent woven bone in addition to mature lamellar bone. Further studies are needed to evaluate the relative contribution of woven and lamellar bone to loading-induced increases in bone size and total mineral content.

Surprisingly, we found that mechanical strain-induced bone response showed no difference regardless of age in three age groups tested [10, 16, and 36 weeks] in either the B6 or the C3H mouse strains. In contrast to our report, other studies on rats, turkeys, and humans (10, 14, 20, 27) have shown that bone response induced by mechanical stimuli declines with age. There are a number of potential explanations for the discrepancy between our data and the observations of previous studies, which include: 1) age-related impairment in bone anabolic response may be seen in mice older than 36-weeks of age; 2) aging may have a greater effect on bone's response to loading in some inbred strains of mice more than in others; and 3) bone's response to mechanical loading may vary with age at lower loads, but not at higher loads.

Another interesting finding from our study was that mechanical load caused an acute inhibition of bone resorption, as evidenced by down regulation of MMP-9 and TRAP. This finding is consistent with the previous *in vitro* study in which mechanical stress reduced the expression of RANKL, inhibiting both osteoclast formation and activation (21, 22, 23). However, 12 days of prolonged loading induced expression of bone resorption marker genes, as shown in table-5. The

increased bone resorption that occurs at 12 days after loading may be a consequence of remodeling in response to increased bone formation. Accordingly, endosteal circumference is increased after 12 days of loading. Furthermore, expression of RANKL, a key regulator of bone resorption, was increased by 5-fold after 12 days of loading, suggesting that any loading-induced increase in bone resorption at the endosteum may be mediated via an increase in the production of RANKL.

In this study, we compared gene expression changes between B6 and C3H mice to test the hypothesis that the difference in the bone response between these strains in pQCT can be observed in the expression levels of BF and/or BR marker genes. As anticipated, we found B6 and C3H mice showed increased expression of both bone formation and resorption markers genes after 12 days loading. However, the magnitude of increases in the expression phenotypes was significantly greater in B6 compared to C3H mice (Table-6). This is consistent with our pQCT data that showed greater increase in the bone parameters in B6 compared to C3H mice after 12 days of 9N load. Thus, we have convincingly shown using BMD changes and gene expression changes as end points that the skeletal response to mechanical loading is in part genetically determined. Our ongoing QTL studies will examine the genetic traits that contribute to variation in bone anabolic response using BMD and gene expression changes as end points.

Acknowledgements

This work was supported by Assistance Award No. DAMD17-01-1-0074. The U.S. Army Medical Research Acquisition Activity, 820 Chandler Street, Fort Detrick 21702-5014, is the awarding and administering acquisition office. The information contained in this publication does not necessarily reflect the position or the policy of the government, and no official endorsement should be inferred. All work was performed in facilities provided by the Department of Veterans Affairs. We would like to thank James Dekeyser for his valuable technical support in setting up the four-point bending device and strain gauge measurement.

References

1. **Akhter MP, Cullen DM, Pedersen EA, Kimmel DB, and Recker RR.** Bone response to in vivo mechanical loading in two breeds of mice. *Calcif Tissue Int* 63: 442-449, 1998.

2. **Akhter MP, Raab DM, Turner CH, Kimmel DB, and Recker RR.** Characterization of in vivo strain in the rat tibia during external application of a four-point bending load. *J Biomech* 25: 1241-1246, 1992.

3. **Bacabac RG, Smit TH, Mullender MG, Dijcks SJ, Van Loon JJ, and Klein-Nulend J.** Nitric oxide production by bone cells is fluid shear stress rate dependent. *Biochem Biophys Res Commun* 315: 823-829, 2004.

4. **Boutahar N, Guignandon A, Vico L, and Lafage-Proust MH.** Mechanical strain on osteoblasts activates autophosphorylation of focal adhesion kinase and proline-rich tyrosine kinase 2 tyrosine sites involved in ERK activation. *J Biol Chem* 279: 30588-30599, 2004.

5. **Burr DB and Hooser M.** Alterations to the en bloc basic fuchsin staining protocol for the demonstration of microdamage produced in vivo. *Bone* 17: 431-433, 1995.

6. **http://www.realscience.breckschool.org/upper/research/research97-99pub/mechtrans/intereasearch**

7. **Cochran GV.** Implantation of strain gages on bone in vivo. *J Biomech* 5: 119-123, 1972.

8. **Dalsky GP, Stocke KS, Ehsani AA, Slatopolsky E, Lee WC, and Birge SJ, Jr.** Weight-bearing exercise training and lumbar bone mineral content in postmenopausal women. *Ann Intern Med* 108: 824-828, 1988.

9. **Iwamoto J, Takeda T, and Sato Y.** Effect of treadmill exercise on bone mass in female rats. *Exp Anim* 54: 1-6, 2005.

10. **Jarvinen TL, Pajamaki I, Sievanen H, Vuohelainen T, Tuukkanen J, Jarvinen M, and Kannus P.** Femoral neck response to exercise and subsequent deconditioning in young and adult rats. *J Bone Miner Res* 18: 1292-1299, 2003.

11. **Klein-Nulend J, Helfrich MH, Sterck JG, MacPherson H, Joldersma M, Ralston SH, Semeins CM, and Burger EH.** Nitric oxide response to shear stress by human bone cell cultures is endothelial nitric oxide synthase dependent. *Biochem Biophys Res Commun* 250: 108-114, 1998.

12. **Kodama Y, Dimai HP, Wergedal J, Sheng M, Malpe R, Kutilek S, Beamer W, Donahue LR, Rosen C, and Baylink DJ.** Cortical tibial bone volume in two strains of mice: effects of sciatic neurectomy and genetic regulation of bone response to mechanical loading. *Bone* 25(2):183-90. 1999.

13. **Kodama Y, Umemura Y, Nagasawa S, Beamer WG, Donahue LR, Rosen CR, Baylink DJ, and Farley JR.** Exercise and mechanical loading increase periosteal bone formation and whole bone strength in C57BL/6J mice but not in C3H/Hej mice. *Calcif Tissue Int* 66: 298-306., 2000.

14. **Kohrt WM.** Aging and the osteogenic response to mechanical loading. *Int J Sport Nutr Exerc Metab* 11 Suppl: S137-142, 2001.

15. **Kunnel JG, Igarashi K, Gilbert JL, and Stern PH.** Bone anabolic responses to mechanical load in vitro involve COX-2 and constitutive NOS. *Connect Tissue Res* 45: 40-49, 2004.

16. **Matsuda N, Morita N, Matsuda K, and Watanabe M.** Proliferation and differentiation of human osteoblastic cells associated with differential activation of MAP kinases in response to

epidermal growth factor, hypoxia, and mechanical stress in vitro. *Biochem Biophys Res Commun* 249: 350-354, 1998.

17. **Peverali FA, Basdra EK, and Papavassiliou AG.** Stretch-mediated activation of selective MAPK subtypes and potentiation of AP-1 binding in human osteoblastic cells. *Mol Med* 7: 68-78, 2001.

18. **Rezzonico R, Cayatte C, Bourget-Ponzio I, Romey G, Belhacene N, Loubat A, Rocchi S, Van Obberghen E, Girault JA, Rossi B, and Schmid-Antomarchi H.** Focal adhesion kinase pp125FAK interacts with the large conductance calcium-activated hSlo potassium channel in human osteoblasts: potential role in mechanotransduction. *J Bone Miner Res* 18: 1863-1871, 2003.

19. **Robling AG and Turner CH.** Mechanotransduction in bone: genetic effects on mechanosensitivity in mice. *Bone* 31: 562-569, 2002.

20. **Rubin CT, Bain SD, and McLeod KJ.** Suppression of the osteogenic response in the aging skeleton. *Calcif Tissue Int* 50: 306-313, 1992.

21. **Rubin J, Fan X, Biskobing DM, Taylor WR, and Rubin CT.** Osteoclastogenesis is repressed by mechanical strain in an in vitro model. *J Orthop Res* 17: 639-645, 1999.

22. **Rubin J, Murphy T, Nanes MS, and Fan X.** Mechanical strain inhibits expression of osteoclast differentiation factor by murine stromal cells. *Am J Physiol Cell Physiol* 278: C1126-1132, 2000.

23. **Rubin J, Murphy TC, Fan X, Goldschmidt M, and Taylor WR.** Activation of extracellular signal-regulated kinase is involved in mechanical strain inhibition of RANKL expression in bone stromal cells. *J Bone Miner Res* 17: 1452-1460, 2002.

24. **Snow-Harter C, Bouxsein ML, Lewis BT, Carter DR, and Marcus R.** Effects of resistance and endurance exercise on bone mineral status of young women: a randomized exercise intervention trial. *J Bone Miner Res* 7: 761-769, 1992.

25. **Stephen C. Cowin.** Bone Mechanics Handbook, Second Editions, 2001, CRC Press, Washington.

26. **Tajima O, Ashizawa N, Ishii T, Amagai H, Mashimo T, Liu LJ, Saitoh S, Tokuyama K, and Suzuki M.** Interaction of the effects between vitamin D receptor polymorphism and exercise training on bone metabolism. *J Appl Physiol* 88: 1271-1276, 2000.

27. **Turner CH, Takano Y, and Owan I.** Aging changes mechanical loading thresholds for bone formation in rats. *J Bone Miner Res* 10: 1544-1549, 1995.

28. **Umemura Y, Baylink DJ, Wergedal JE, Mohan S, and Srivastava AK.** A time course of bone response to jump exercise in C57BL/6J mice. *J Bone Miner Metab* 20: 209-215, 2002.

29. **Umemura Y, Ishiko T, Yamauchi T, Kurono M, and Mashiko S.** Five jumps per day increase bone mass and breaking force in rats. *J Bone Miner Res* 12: 1480-1485, 1997.

30. **Wozniak M, Fausto A, Carron CP, Meyer DM, and Hruska KA.** Mechanically strained cells of the osteoblast lineage organize their extracellular matrix through unique sites of alphavbeta3-integrin expression. *J Bone Miner Res* 15: 1731-1745, 2000.

31. **You J, Reilly GC, Zhen X, Yellowley CE, Chen Q, Donahue HJ, and Jacobs CR.** Osteopontin gene regulation by oscillatory fluid flow via intracellular calcium mobilization and activation of mitogen-activated protein kinase in MC3T3-E1 osteoblasts. *J Biol Chem* 276: 13365-13371, 2001.

32. **Zaman G, Pitsillides AA, Rawlinson SC, Suswillo RF, Mosley JR, Cheng MZ, Platts LA, Hukkanen M, Polak JM, and Lanyon LE.** Mechanical strain stimulates nitric oxide

production by rapid activation of endothelial nitric oxide synthase in osteocytes. *J Bone Miner Res* 14: 1123-1131, 1999.

Table-1 Changes in the bone parameters in response to varying magnitude of loads applied by four-point bending in 10-week old female B6 and C3H inbred strains of mice.

Bone parameters	C57BL/6J							
	6N		7N		8N		9N	
	Unloaded	Loaded	Unloaded	Loaded	Unloaded	Loaded	Unloaded	Loaded
Total area, mm^2	1.42±0.02	1.52±0.02[a]	1.40±0.02	1.60±0.04[b]	1.47±0.01	1.74±0.01[c]	1.50±0.04	2.13±0.04[d]
Total mineral content, mg/mm	0.89±0.01	0.96±0.02[a]	0.83±0.02	0.96±0.02[a]	0.89±0.01	1.08±0.008[c]	0.87±0.008	1.29±0.02[d]
Periosteal circumference, mm	4.21±0.03	4.36±0.03[a]	4.18±0.04	4.47±0.05[b]	4.30±0.02	4.67±0.02[c]	4.33±0.05	5.17±0.04[d]
Endosteal circumference, mm	3.12±0.04	3.21±0.02	3.15±0.01	3.35±0.04[b]	3.25±0.02	3.46±0.02[c]	3.29±0.06	4.02±0.05[d]
Total density, mg/ccm	678±12.94	680±7.63	637±12.2	655±11.4	646±9.83	675±6.31[a]	626±17.00	721±11.9[c]
Cortical density mg/ccm	1110.0±6.96	1114.8±6.14	1090±8.60	1095±7.37	1095±5.73	1110±2.71[a]	1078±17.8	1115±14.3[b]

Bone parameters	C3H/HeJ							
	6N		7N		8N		9N	
	Unloaded	Loaded	Unloaded	Loaded	Unloaded	Loaded	Unloaded	Loaded
Total area, mm^2	1.15±0.01	1.2±0.02	1.16±0.01	1.30±0.04[b]	1.15±0.01	1.41±0.03[b]	1.13±0.03	1.42±0.02[d]
Total mineral content, mg/mm	1.03±0.01	1.07±0.01[a]	1.04±0.01	1.16±0.02[b]	1.04±0.02	1.24±0.02[b]	1.04±0.02	1.24±0.01[c]
Periosteal circumference, mm	3.79.02	3.88±0.04	3.81±0.02	4.04±0.0.6[b]	3.79±0.02	4.20±0.04[b]	3.76±0.04	4.22±0.03[d]
Endosteal circumference, mm	2.31±0.01	2.38±0.06	2.32±0.01	2.49±0.04[b]	2.30±0.02	2.62±0.06[b]	2.26±0.04	2.70±0.06[c]
Total density, mg/ccm	1001±4.79	1017±10.5	1013±6.8	1019±10.1	1021±4.95	1029±4.87	1047±3.9	1042±8.07
Cortical density mg/ccm	1267±3.56	1264±6.96	1272±5.7	1258±3.27	1267±5.32	1256±1.5	1269±14.7	1250±13.93

The values shown are Mean ± SE of loaded zone from compared to controlateral-unloaded bones from the same mice.

[a] $p<0.05$, [b]$p<0.01$, [c]$p<0.001$, [d]$p<0.0001$ vs. corresponding unloaded bones

N=6 for each load in both strains

Table-2- Mechanical strain produced by varying magnitude of load applied by four-point bending in tibia of 10-week old B6 and C3H mice measured by strain gauge.

Load	με (Mean ± SE)	
	B6	C3H
6N	2610 ± 109.5	2763 ± 32
7N	3020 ± 86.5	3188 ± 58
8N	3371 ± 71.5	3545 ± 78.5
9N	3682 ± 90.5	3865 ± 91

N=4 in each load

$p<0.01$ is significant difference between the B6 and C3H (two-way ANOVA)

Table-3: Changes in the bone (Tibia) geometrical parameters in response to 12 days four-point bending at 9N load in different age groups of B6 mice.

Bone parameters	10-week old B6		16-week old B6		36-week old B6	
	Unloaded	Loaded	Unloaded	Loaded	Unloaded	Loaded
Total area, mm^2	1.50±0.04	2.13±0.04 [d]	1.38±0.02	2.0±0.06[d]	1.47±0.04	1.91±0.06 [c]
Total mineral content, mg/mm	0.87±0.008	1.29±0.02 [d]	0.95±0.01	1.36±0.02[d]	0.84±0.02	1.14±0.01 [d]
Periosteal circumference, mm	4.33±0.05	5.17±0.04 [d]	4.15±0.03	4.99±0.1[d]	4.30±0.06	4.90±0.07 [d]
Endosteal circumference, mm	3.29±0.06	4.0±0.05 [d]	2.99±0.02	3.68±0.1[c]	3.40±0.06	3.80±0.10[b]
Total density, mg/ccm	626±17.00	721±11.9 [c]	756±8.3	825±12.6[c]	649±23.3	678±16.6
Cortical density, mg/ccm	1078±17.8	1115±14.3 [b]	1158±5.33	1177±5[a]	1086±8.00	1131±13.3[a]

The values shown here are Mean ± SE of loaded zone from compared to controlateral unloaded bones from the same mice in each strain.

10-week age, N=6; 16-week age, N=9; 36-week age, N=9

[a] $p<0.05$, [b] $p<0.01$, [c] $p<0.001$, [d] $p<0.0001$ vs. corresponding un loaded bones.

Table-4: Changes in the bone (Tibia) geometrical parameters in response to 12 days four-point bending at 9N load in different age groups of C3H mice.

Bone parameters	10-week old C3H		16-week old C3H		36-week old C3H	
	Unloaded	Loaded	Unloaded	Loaded	Unloaded	Loaded
Total area, mm^2	1.13±0.03	1.42±0.02[d]	1.15±0.03	1.51±0.02[d]	1.38±0.02	1.60±0.02[d]
Total mineral content, mg/mm	1.0±0.02	1.24±0.01[c]	1.13±0.02	1.43±0.03[d]	1.29±0.02	1.53±0.01[d]
Periosteal circumference, mm	3.76±0.04	4.22±0.03[d]	3.80±0.05	4.34±0.04[d]	4.15±0.03	4.47±0.03[d]
Endosteal circumference, mm	2.26±0.04	2.70±0.06[c]	2.25±0.03	2.62±0.05[d]	2.57±0.04	2.70±0.05[d]
Total density, mg/ccm	1047±3.9	1042±8.07	1140±8.33	1144±12.6	1054±17.3	1088±13
Cortical density, mg/ccm	1269±14.7	1250±13.93	1343±5.66	1311±8.33	1344±10	1345±7.6

The values shown here are Mean ± SE of loaded zone from compared to controlateral unloaded bones from the same mice in each strain.

10-week age, N=6; 16-week age, N=9; 36-week age, N=9

[a] $p<0.05$, [b] $p<0.01$, [c] $p<0.001$, [d] $p<0.0001$ vs. corresponding un loaded bones

Table-5. Fold change in the mRNA expression of bone formation and resorption genes in response to 2, 4, 8, and 12 days of four-point bending in 10-week old female B6 mice.

(a) Bone Formation genes

Duration of loading	Genes	$2^{-\Delta\Delta}Ct$	Fold Change	P-value
2-days	Type-I collagen	-0.27 ± 0.19	1.21	0.45
	Bone sialoprotein	-0.05 ± 0.48	1.03	0.29
	Alkaline phosphatase	-0.41 ± 0.37	1.3	0.66
	Osteocalcin	-1.20 ± 0.16	-2.3	0.08
4-days	Type-I collagen	-1.02 ± 0.13	2.04	0.03
	Bone sialoprotein	-1.03 ± 0.16	2.04	0.006
	Alkaline phosphatase	-0.53 ± 0.17	1.45	0.18
	Osteocalcin	-0.12 ± 0.45	1.0	0.73
8-days	Type-I collagen	-1.93 ± 0.11	3.84	0.001
	Bone sialoprotein	-1.89 ± 0.51	3.71	0.003
	Alkaline phosphatase	-1.53 ± 0.32	2.88	0.001
	Osteocalcin	-1.45 ± 0.43	2.72	0.01
12-days	Type-I collagen	-2.06 ± 0.09	4.18	0.001
	Bone sialoprotein	-3.01 ± 0.07	7.82	0.002
	Alkaline phosphatase	-2.55 ± 0.16	5.86	0.005
	Osteocalcin	-2.01 ± 0.12	4.03	0.005

(b) Bone Resorption genes

Duration of loading	Genes	$2^{-\Delta\Delta}Ct$	Fold Change	P-value
2-days	TRAP	-1.88 ± 0.35	-3.70	0.005
	MMP-9	-1.61 ± 0.39	-3.06	0.002
4-days	TRAP	-1.68 ± 0.34	-3.20	0.004
	MMP-9	-1.98 ± 0.23	-3.95	0.002
8-days	TRAP	-1.61 ± 0.44	-3.06	0.007
	MMP-9	-0.28 ± 0.21	1.21	0.2
12-days	TRAP	-3.61 ± 0.20	12.24	0.003
	MMP-9	-2.91 ± 0.13	7.54	0.008
	RANKL	-2.65 ± 0.14	5.17	0.001

N=5 at 2-, 4- and 8 days
N=7 at 12 days

Table-6 Fold change in the mRNA expression of bone formation and resorption markers genes in response to 12 days four-point bending in 10-week old female B6 and C3H mice.

Genes	B6*	C3H	p-value
	Mean ± SE	Mean ± SE	
Type-I collagen	4.23 ± 0.28	3.19 ± 0.29	0.02
Bone sialoprotein	7.88 ± 0.39	2.90 ± 0.20	0.0000
Alkaline phosphatase	6.08 ± 1.75	3.83 ± 0.42	0.01
Osteocalcin	4.13 ± 0.37	2.93 ± 0.29	0.02
TRAP	13.02 ± 1.91	7.66 ± 0.87	0.02
MMP-9	7.75 ± 0.76	4.20 ± 0.47	0.001
RANKL	5.38 ± 0.63	3.36 ± 0.53	0.04

N=7 in both B6 and C3H mice

*B6 is significant over C3H in the expression of bone markers genes.

Figure Legend

Figure 1a: Changes in the bone geometrical parameters after 12 days of four-point bending at 9N load in 10-week old B6 and C3H inbred strains of mice *in vitro.* The data shows percentage change in Total content-TC, Total area-TA, Periosteal circumference-PC, Cortical thickness-CT, Endosteal circumference-EC, Total density-TD and Cortical density-CD. The values shown are as Mean ± standard error of loaded zone from compared to corresponding unloaded controlateral bones. The y-axis represents the percentage change and x-axis represents various bone phenotypes as measured by pQCT. N=6, $^{a}p<0.05$ and $^{c}p<0.001$ between the strains of mice

Figure 1b: Changes in the total vBMD in response to varying magnitude of loads applied by four-point bending in 10-week old female B6 and C3H inbred strains of mice *in vitro*.The values shown are Mean ± standard error of loaded zone from compared to controlateral-unloaded bones from the same mice. The y-axis represents the percentage increase and x-axis represents varying magnitude of load. N=6 for each load in both strains, $^{a}p<0.05$, $^{c}p<0.001$ vs corresponding unloaded bones

Figure 2: Changes in the total area (a) and vBMD (b) in response to 12 days four-point bending in different age groups of female B6 and C3H mice *in vitro*. The values shown here are Mean ± standard error of loaded zone from compared to unloaded bone from the same mice in each strain. The y-axis represents percentage increase and x-axis represents varying ages. $^{a}p<0.05$ vs unloaded control bones and $^{b}p<0.05$ vs C3H mice. N=6; 10-week, N=9; 16-week and 36-week in both inbred strains of mice

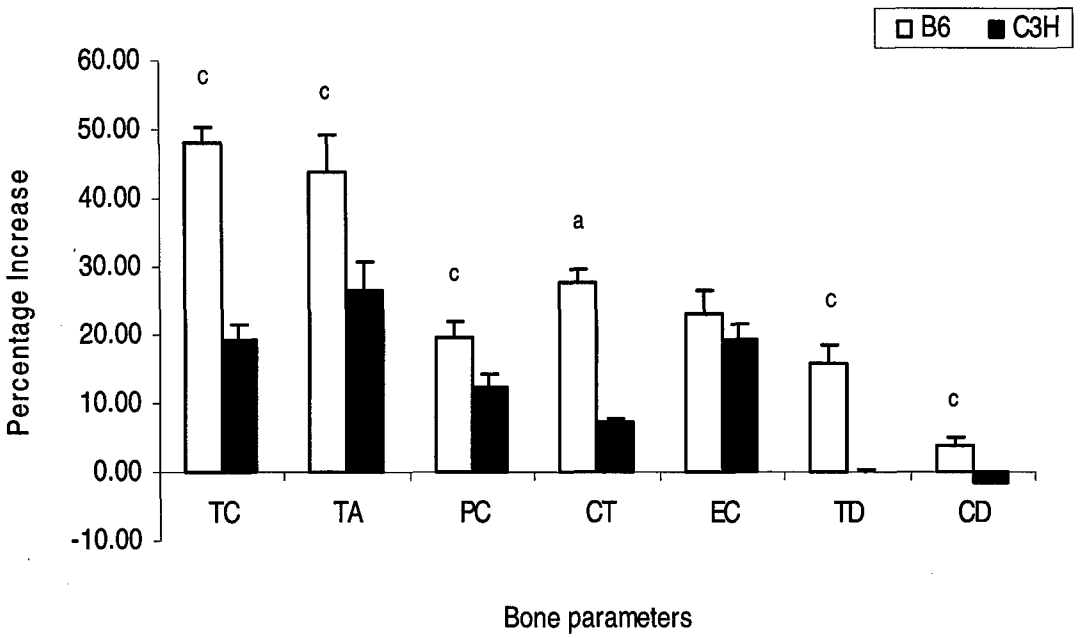
B6
C3H
60.00
50.00
40.00
30.00
20.00
10.00
0.00
-10.00
Percentage Increase
c
c
c
a
c
c
TC
TA
PC
CT
EC
TD
CD
Bone parameters

Figure 1a

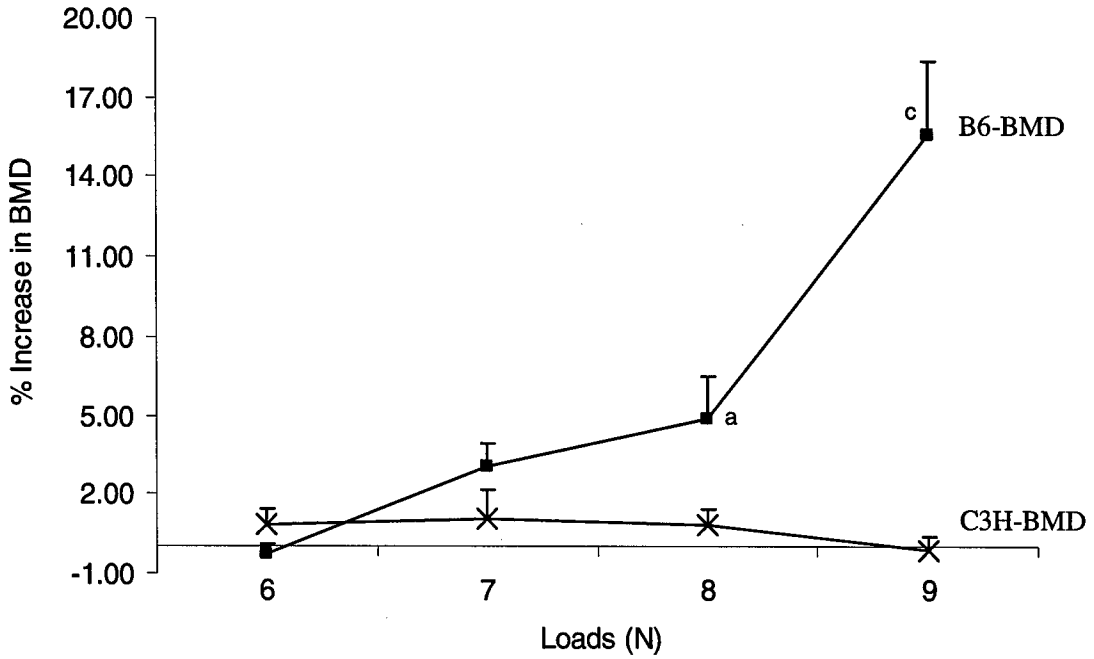
20.00
17.00
14.00
11.00
8.00
5.00
2.00
-1.00
% Increase in BMD
6
7
8
9
Loads (N)
c
a
B6-BMD
C3H-BMD

Figure 1b

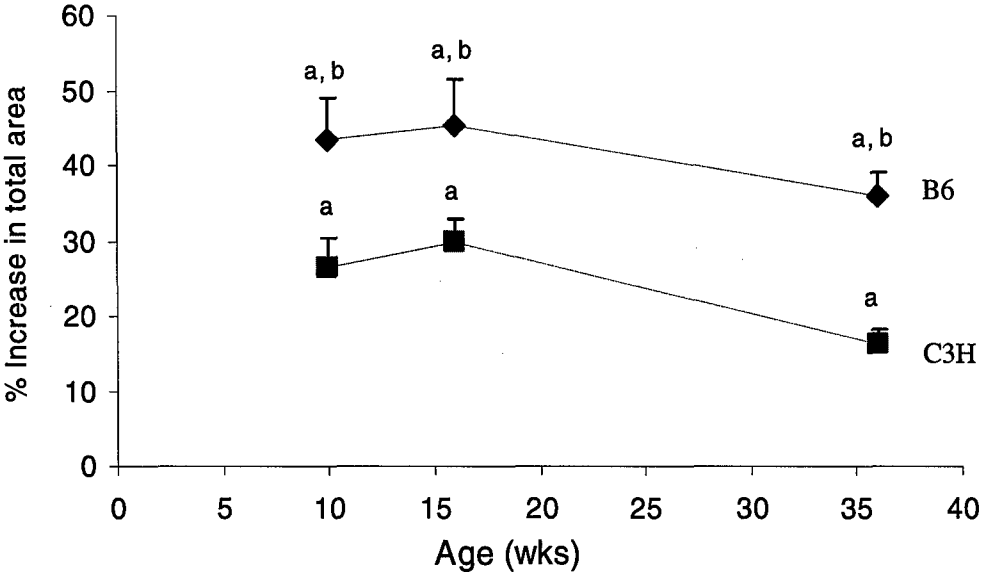
60
50
40
30
20
10
0
% Increase in total area
a, b
a, b
a, b
B6
a
a
a
C3H
0
5
10
15
20
25
30
35
40
Age (wks)

(a)

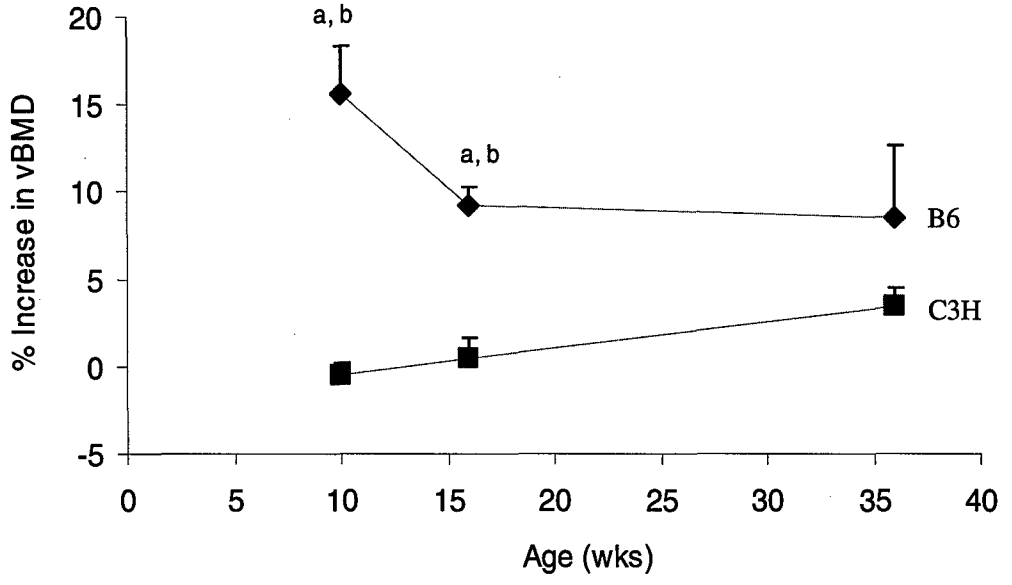
20
15
10
5
0
-5
% Increase in vBMD
a, b
a, b
B6
C3H
0
5
10
15
20
25
30
35
40
Age (wks)

(b)

Figure 2

THE JOURNAL OF BIOLOGICAL CHEMISTRY Vol. 280, No. 20, Issue of May 20, pp. 20163–20170, 2005
Printed in U.S.A.

Fluid Shear Stress Synergizes with Insulin-like Growth Factor-I (IGF-I) on Osteoblast Proliferation through Integrin-dependent Activation of IGF-I Mitogenic Signaling Pathway*

Received for publication, February 8, 2005, and in revised form, March 14, 2005
Published, JBC Papers in Press, March 18, 2005, DOI 10.1074/jbc.M501460200

Sonia Kapur‡§, Subburaman Mohan‡§, David J. Baylink‡§, and K.-H. William Lau‡§¶

From the ‡Musculoskeletal Disease Center, Jerry L. Pettis Memorial Veterans Affairs Medical Center, and §Departments of Medicine and Biochemistry, Loma Linda University, Loma Linda, California 92357

This study tested the hypothesis that shear stress interacts with the insulin-like growth factor-I (IGF-I) pathway to stimulate osteoblast proliferation. Human TE85 osteosarcoma cells were subjected to a steady shear stress of 20 dynes/cm^2 for 30 min followed by 24-h incubation with IGF-I (0–50 ng/ml). IGF-I increased proliferation dose-dependently (1.5–2.5-fold). Shear stress alone increased proliferation by 70%. The combination of shear stress and IGF-I stimulated proliferation (3.5- to 5.5-fold) much greater than the additive effects of each treatment alone, indicating a synergistic interaction. IGF-I dose-dependently increased the phosphorylation level of Erk1/2 by 1.2–5.3-fold and that of IGF-I receptor (IGF-IR) by 2–4-fold. Shear stress alone increased Erk1/2 and IGF-IR phosphorylation by 2-fold each. The combination treatment also resulted in synergistic enhancements in both Erk1/2 and IGF-IR phosphorylation (up to 12- and 8-fold, respectively). Shear stress altered IGF-IR binding only slightly, suggesting that the synergy occurred primarily at the post-ligand binding level. Recent studies have implicated a role for integrin in the regulation of IGF-IR phosphorylation and IGF-I signaling. To test whether the synergy involves integrin-dependent mechanisms, the effect of echistatin (a disintegrin) on proliferation in response to shear stress ± IGF-I was measured. Echistatin reduced basal proliferation by ~60% and the shear stress-induced mitogenic response by ~20%. It completely abolished the mitogenic effect of IGF-I and that of the combination treatment. Shear stress also significantly reduced the amounts of co-immunoprecipitated SHP-2 and -1 with IGF-IR, suggesting that the synergy between shear stress and IGF-I in osteoblast proliferation involves integrin-dependent recruitment of SHP-2 and -1 away from IGF-IR.

Mechanical loading is essential for the maintenance of skeletal architectural integrity. Loading increased bone formation and inhibited bone resorption, leading to an increase in bone mass, whereas unloading decreased bone mass through an increase in resorption and a decrease in formation (1). Although the phenomenon of increased bone formation through an increase in osteoblast proliferation and activity in response to skeletal loading has been well described, the underlying mechanism(s) remains largely undefined. Loading produces strains in the bone that generate interstitial fluid flow through the lacunar-canalicular spaces (2). It is believed that this fluid flow exerts a shear stress at surfaces of bone cells lining the lacunar-canalicular spaces and that the shear stress generates biochemical signals in bone cells to stimulate osteoblast proliferation and activity. Shear stress stimulates bone cell proliferation and activity through multiple interacting signaling pathways (3).

Bone growth factors function as autocrine and paracrine mediators of bone formation (4, 5). The mechanism whereby mechanical loading stimulates osteoblast proliferation and activity could involve bone growth factors and corresponding signaling pathways. IGF-I[1] is one of the most abundant growth factors in bone (4), produced by bone cells (4–7), and an important stimulator of bone formation (4–7). Loading increases bone cell production of IGF-I *in vivo* (8) and *in vitro* (9). The signaling pathway of IGF-I involves Erk1/2 activation, which is essential for mechanical stimulation of bone cell proliferation (10). It has been reported that the bone cell mitogenic response to mechanical strain is mediated by the IGF-IR (11). In addition, recent studies suggested that loading might have a permissive role in the IGF-I mitogenic action in bone, as skeletal unloading induces resistance to IGF-I with respect to bone formation. Accordingly, unloading blocked the ability of IGF-I to stimulate bone formation in the rat (12). IGF-I administration stimulates bone formation in the loaded bone, but not in unloaded bone *in vivo* (12) and *in vitro* (12, 13). There is evidence that unloading-related resistance to IGF-I is mediated by inhibiting the activation of IGF-I pathway through down-regulation of integrin expression (13). Because unloading blocked the osteogenic action of IGF-I, we postulated that increased loading enhances the osteogenic action of IGF-I. Accordingly, it has been suggested that loading enhances the anabolic effects of IGF-I on articular cartilage formation (14) and also in nasopremaxillary growth (15).

Recent studies in smooth muscle cells (16–22) revealed that the ability of IGF-I to initiate its intracellular signals is regulated not only by its binding to its own transmembrane receptor (IGF-IR) but also by other transmembrane proteins, such as SHPS-1 and $\alpha v\beta 3$ integrin, to recruit essential signaling pro-

* This work was supported in part by a special appropriation to the Musculoskeletal Disease Center, Jerry L. Pettis Memorial Veterans Administration Medical Center, and by a merit review provided by the Office of Research and Development, Medical Research Service, Department of Veteran Affairs and also in part by Assistance Award DAMD17-01-1-0744.

¶ To whom correspondence should be addressed: Musculoskeletal Disease Ctr. (151), Jerry L. Pettis Memorial Veterans Affairs Medical Ctr., 11201 Benton St., Loma Linda, CA 92357. Tel.: 909-825-7084 (ext. 2836); Fax: 909-796-1680; E-mail: William.Lau@med.va.gov.

[1] The abbreviations used are: IGF-I, insulin-like growth factor-I; IGF-IR, insulin-like growth factor-I receptor; pIGF-IR, phosphorylated IGF-IR; FGF-2, basic fibroblast growth factor; Erk1/2, extracellular regulated kinase 1/2; pErk1/2, phosphorylated Erk1/2; SHP-1, Src-homology 2 domain-containing protein-tyrosine phosphatase 1; SHP-2, Src-homology 2 domain-containing protein-tyrosine phosphatase 2; SHPS-1, SHP substrate 1; ANOVA, analysis of variance.

teins, such as SHP-2 and Shc. The integrin recruitment of SHP-2 is essential for regulation of the overall IGF-IR phosphorylation level (18) and the propagation of downstream signaling events (19). Accordingly, ligand occupancy of $\alpha v\beta 3$ integrin results in phosphorylation of the $\beta 3$ integrin subunit, which leads to Downstream of tyrosine kinase I (DOKI)-mediated recruitment of SHP-2 (20). Blocking ligand occupancy of $\alpha v\beta 3$ integrin inhibited IGF-I-dependent downstream signaling events, membrane recruitment of SHP-2, and cell migration and proliferation (21, 22). Expression of a dominant negative mutant of the $\beta 3$ integrin subunit in smooth muscle cells completely abolished the mitogenic activity of IGF-I (16). Thus, integrin activation may have a permissive action in the IGF-IR signaling pathway.

Integrins, which consist of a large family of heterodimers of α- and β-subunits, function as cell surface adhesion receptors for extracellular matrices (23) and link extracellular matrix components with various intracellular signaling mechanisms (24). It is believed that mechanical strains and shear stresses are distributed to cells through extracellular matrix scaffolds that hold the cells together and that mechanical signals that propagate from the extracellular matrix converge on integrins (25). The interaction between specific bone matrix ligands and corresponding integrin receptors has been suggested to be involved in the signal transduction process linking the extracellular mechanical signals to changes in gene expression, cytoskeletal reorganization, and DNA synthesis in osteoblasts and/or osteocytes (26). Specific antibodies for several integrins blocked mechanical strain-induced cellular responses (27). The integrin-β-catenin signal pathway has also been suggested to be involved in the cellular responses of human articular chondrocytes to mechanical stimulation (28). Thus, integrin activation has an important role in the transduction of mechanical signals. Consequently, we postulate that the integrin-dependent regulation of the IGF-I mitogenic signaling pathway could, in part, be involved in the mechanical stimulation of bone formation.

This study investigated the potential relationship between the signaling mechanism of mechanical stimulation of osteoblast proliferation and that of IGF-I-induced osteoblast proliferation by testing two hypotheses: 1) increased mechanical strain in the form of fluid shear stress could synergistically enhance the osteogenic action of IGF-I, and 2) the synergy between IGF-I and fluid shear stress involves the integrin-dependent up-regulation of IGF-IR phosphorylation through an inhibition of SHP-mediated IGF-IR dephosphorylation.

EXPERIMENTAL PROCEDURES

Materials—Tissue culture plasticware was obtained from Falcon (Oxnard, CA). Dulbecco's modified Eagle's medium was from Mediatech (Herndon, VA). Bovine calf serum was purchased from HyClone (Logan, UT). Trypsin and EDTA were products of Irvine Scientific (Santa Ana, CA). Bovine serum albumin was from United States Biochemical Corp. (Cleveland, OH). [^{3}H]Thymidine (48 Ci/mmol) and [^{125}I]NaI (2,215 Ci/mmol) were from ICN Biochemicals (Irvine, CA). Recombinant human IGF-I and FGF-2 were purchased from R & D Systems (Minneapolis, MN). Anti-actin, anti-IGF-IR, and anti-pErk1/2 antibodies were purchased from Santa Cruz Biotechnology (Santa Cruz, CA). Anti-pIGF-IR and anti-pan Erk antibodies were products of BIOSOURCE International (Camarillo, CA) and Transduction Labs (San Diego, CA), respectively. Other chemicals were from Fisher or Sigma.

Fluid Shear Stress Experiments—Human TE85 osteosarcoma cells were plated on glass slides (75 × 38 mm) at 5×10^4 cells/slide in Dulbecco's modified Eagle's medium supplemented with 10% bovine calf serum. When the cells reached ~80% confluency, the cells were serum-deprived for 24 h and subjected to a steady fluid shear stress of 20 dynes/cm^2 for 30 min in Cytodyne flow chambers as previously described (3). The static controls were performed on cells grown in identical conditions in Cytodyne chambers but without exposing to the shear stress.

Cell Proliferation Assays—Cell proliferation was assessed by [^{3}H]thymidine incorporation into cell DNA as described previously (29). Briefly, after 30 min of the shear stress, the treated and corresponding static control cells were incubated with the indicated dosages of IGF-I (or FGF-2) for 24 h, and [^{3}H]thymidine (1.5 μCi/ml) was added during the final 6 h of the incubation. Effects of a 2-h pretreatment with U0126 (10 μM) or a 24-h pretreatment with a disintegrin, echistatin (100 nM), on shear stress and/or IGF-I-induced cell proliferation were also tested.

Western Immunoblot Analyses and Immunoprecipitation—Immediately following the 30-min shear stress and 10-min IGF-I treatments, the treated cells and corresponding controls were washed with phosphate-buffered saline and lysed in radioimmune precipitation assay buffer as described previously (3). The protein concentration of each extract was assayed with the bicinchoninic acid method. Ten μg of extract protein from each extract was loaded onto 10% SDS-polyacrylamide gels and transblotted to polyvinylidene difluoride membrane for Western immunoblot analysis. Erk1/2 activation was assessed by pErk1/2 level using the anti-pErk1/2 antibody normalized against the total Erk1/2 level. The pIGF-IR level was determined with an antibody against pIGF-IR, normalized against the level of total IGF-IR.

The relative level of IGF-IR-bound SHP-1 and -2 was each measured by co-immunoprecipitation followed by Western immunoblot analyses. Briefly, 1 mg of cell extract protein each from treated cells and corresponding controls was incubated with 2 μg of anti-IGF-IR or anti-integrin $\beta 3$ antibodies for 2 h at 4 °C. A predetermined amount of anti-rabbit IgG beads (eBiosciences, San Diego, CA) was added for an additional 1 h at 4 °C. The bead-bound complex was washed three times with ice-cold lysis buffer (50 mM Tris-HCl, pH 8.0, 150 mM NaCl, 1% Nonidet P-40, 10 mg/ml phenylmethylsulfonyl fluoride, 10 μg/ml aprotinin, and 1 mM sodium orthovanadate). The washed complex was then resuspended in 40 μl of 2× SDS sample buffer and boiled for 5 min. The relative amounts of co-immunoprecipitated SHP-1 or SHP-2 were analyzed by Western analysis using anti-SHP-1 or anti-SHP-2 antibodies, respectively.

IGF-IR Binding Assays—Specific IGF-I binding to IGF-IR was measured by receptor-bound [^{125}I]IGF-I in the presence of 100-fold "cold" IGF-I. Radio-iodination of IGF-I was performed by a modified chloramine T method (30). Aliquots were immediately stored at −70 °C until assay. Assays were performed within 1 week of iodination. For the IGF-IR binding assay, TE85 cells were plated on glass slides and subjected to fluid shear stress as described above. Immediately after the shear stress, the treated and corresponding static control cells were rinsed with Dulbecco's modified Eagle's medium containing 20 mM HEPES, pH 7.4, and 1 mg/ml bovine serum albumin (binding medium). Fresh binding medium was then added, and the cells were incubated with 5×10^4 to 2×10^5 counts/min of [^{125}I]labeled IGF-I in the absence or presence of 25–100 ng (*i.e.* 100-fold) of unlabeled IGF-I for total and specific binding, respectively. The cells were incubated at room temperature for 3 h, and the radioactive medium was removed and the slides rinsed five times with ice-cold binding medium. The cells were then lysed in the lysis buffer (10 mM Tris-HCl, pH 7.4, 5 mM EDTA, and 0.2% SDS). The amount of bound ^{125}I-labeled IGF-I was then quantified by γ counting.

Statistical Analyses—Results are shown as mean ± S.D. with at least six replicates. The statistical significance of the differences between independent groups was determined with the two-tailed Student's *t* test. The dose-dependent effects were assessed with one-way ANOVA, followed by Tukey post-hoc test. Interactions between two treatments (*e.g.* shear stress and IGF-I) were evaluated by two-way ANOVA. The difference was considered significant when $p < 0.05$.

RESULTS

Effects of Fluid Shear Stress on the Bone Cell Mitogenic Action of IGF-I in TE85 Cells—IGF-I at 10–50 ng/ml concentrations significantly and dose-dependently ($p < 0.01$, one-way ANOVA) increased the proliferation (*i.e.* [^{3}H]thymidine incorporation) of TE85 cells by ~1.5–2.5-fold (Fig. 1*A*). The 30-min steady shear stress of 20 dynes/cm^2 also significantly ($p < 0.05$) increased [^{3}H]thymidine incorporation in TE85 cells by 70% compared with the corresponding static control cells. The combination of the 30-min shear stress and IGF-I treatment produced much greater than additive stimulations (3.5–5.5-fold) of each treatment alone (Fig. 1*A*). Two-way ANOVA indicates a highly significant ($p < 0.01$) interaction between the two treatments, suggesting a synergistic interaction between shear

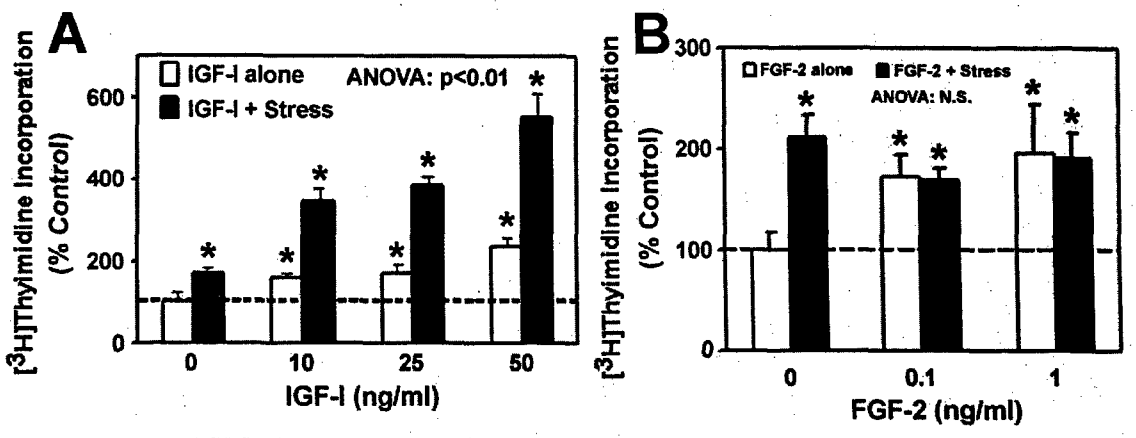

FIG. 1. **Interaction between IGF-I (*A*) or FGF-2 (*B*) and fluid shear stress on the proliferation of TE85 osteosarcoma cells.** The effect of IGF-I or FGF-2 at the indicated concentrations with (*filled bars*) or without (*open bars*) a 30-min steady shear stress of 20 dynes/cm^2 on TE85 cell proliferation, which was assessed by measuring [^{3}H]thymidine incorporation 24 h later. Results are shown as mean ± S.D. ($n = 6$). *, $p < 0.01$ (compared with the static control). ANOVA indicates a significant ($p < 0.01$) interaction between IGF-I and shear stress (*A*) but not between FGF-2 and shear stress (*B*) on [^{3}H]thymidine incorporation. *N.S.*, not significant ($p > 0.05$).

stress and IGF-I on bone cell proliferation.

To test whether the synergistic interaction between shear stress and IGF-I on human bone cell proliferation is a general feature between bone cell growth factors and shear stress, we evaluated whether shear stress would also synergistically enhance the mitogenic activity of FGF-2 (another potent bone cell growth factor) in TE85 cells. Fig. 1*B* shows that FGF-2 alone significantly and dose-dependently ($p < 0.01$) stimulated the TE85 cell proliferation (by ~1.5–2.0-fold). The combined treatment of the shear stress and FGF-2 yielded no further enhancement (not significant, two-way ANOVA) than FGF-2 alone, indicating that the synergistic interaction between shear stress and IGF-I is not universal to all bone growth factors.

Effects of Fluid Shear Stress on the IGF-I-mediated Activation of the Erk1/2 Mitogenic Signaling Pathway in Human TE85 Cells—Because the mitogenic action of IGF-I is mediated through Erk1/2 activation and fluid shear stress also activates Erk1/2 in osteoblasts (3, 10), we investigated the effect of shear stress and/or IGF-I (or FGF-2) on Erk1/2 phosphorylation (an index of Erk1/2 activation). Fig. 2*A* confirms that IGF-I alone, at the test doses, significantly and dose-dependently ($p < 0.01$, one-way ANOVA) increased the pErk1/2 level (by ~1.2–5-fold) in TE85 cells. The 30-min steady shear stress alone also significantly ($p < 0.01$) increased the pErk1/2 level (by ~2.5-fold). The combination of shear stress and IGF-I treatment produced a synergistic ($p < 0.01$, two-way ANOVA) enhancement (up to 12-fold) in Erk1/2 phosphorylation. Fig. 2*B* indicates that the mitogenic doses of FGF-2 (0.1 and 1 ng/ml) alone also markedly and significantly increased the pErk1/2 levels in TE85 cells ($p < 0.01$, one-way ANOVA). In contrast to IGF-I, the combination treatment of shear stress and FGF-2 did not result in a further increase in the pErk1/2 level compared with the FGF-2 treatment alone (not significant, two-way ANOVA). These findings further support the conclusions that the synergistic interaction between shear stress and IGF-I on bone cell proliferation is mediated through synergistic enhancement of IGF-I-dependent activation of the Erk1/2 mitogenic signaling pathway and that the synergy between shear stress and IGF-I on human bone cell proliferation is not shared by FGF-2.

To further evaluate whether activation of the Erk1/2 mitogenic signaling pathway is essential for the synergy, we tested the effect of U0126 (a specific inhibitor of mitogen-activated protein kinase/extracellular signal-regulated kinase kinase 1) on the stimulation of cell proliferation and Erk1/2 phosphorylation induced by IGF-I with or without the shear stress. Fig. 3*A* shows that pretreatment with U0126 at 10 μM completely blocked the IGF-I-mediated as well as the shear stress-induced TE85 cell proliferation. It also completely abolished the synergistic enhancement of IGF-I and shear stress. Fig. 3*B* reveals that the U0126 pretreatment also completely eliminated the synergistic enhancement on Erk1/2 activation by shear stress and IGF-I. Thus, these results are consistent with the conclusion that the synergistic activation of Erk1/2 by IGF-I and shear stress is associated with the synergistic enhancement on osteoblast proliferation. These findings indicate that the synergy between shear stress and IGF-I leading to activation of bone cell proliferation occurs upstream to the Erk1/2 activation. Consistent with previous findings (3, 10), U0216 had no inhibitory effect on either basal proliferation or basal Erk1/2 activation, indicating that basal TE85 cell proliferation is mediated primarily through Erk1/2-independent pathways.

Effect of Shear Stress on the IGF-I-mediated Phosphorylation of IGF-IR in TE85 Cells—We next tested whether the synergy between IGF-I and shear stress occurs prior to or after the phosphorylation of IGF-IR receptor. As expected, IGF-I at the test mitogenic doses significantly increased the IGF-IR phosphorylation level in a dose-dependent manner by 2–3.5-fold (Fig. 4). The 30-min steady shear stress alone also significantly ($p < 0.01$) increased the IGF-IR phosphorylation by 2.5-fold. The combination treatment of shear stress and IGF-I yielded a highly significant synergistic ($p < 0.01$, two-way ANOVA) enhancement in IGF-IR phosphorylation level (up to 8-fold).

Effects of Fluid Shear Stress on the Specific Binding of IGF-I to IGF-IR in TE85 Cells—Because shear stress synergistically enhanced IGF-IR phosphorylation, which is initiated by the binding of IGF-I to IGF-IR, we next assessed whether the synergistic enhancement between IGF-I and shear stress was because of an increase in IGF-I binding to IGF-IR. Fig. 5 shows that the application of a 30-min fluid shear stress at 20 dyne/cm^2 led to a relatively small, but statistically significant ($p < 0.05$, one-way ANOVA) enhancement in the specific binding of IGF-I to IGF-IR in TE85 cells. However, this increase appeared to be of additive nature, as the two binding curves (*i.e.* with or without shear stress) were parallel to each other.

Effects of Echistatin on the IGF-I- and/or Shear Stress-induced Proliferation of TE85 Cells—Because shear stress involves integrin activation in bone cells (3, 26, 27), we evaluated whether integrin activation is involved in the synergy between IGF-I and shear stress in TE85 cells by determining the effect of the disintegrin echistatin (a competitive integrin receptor antagonist) on IGF-I- and/or shear stress-mediated cell proliferation and IGF-IR phosphorylation. Fig. 6*A* shows that echistatin, not only reduced the basal (by ~60%) and shear stress-induced TE85 cell proliferation (by ~20%), but also com-

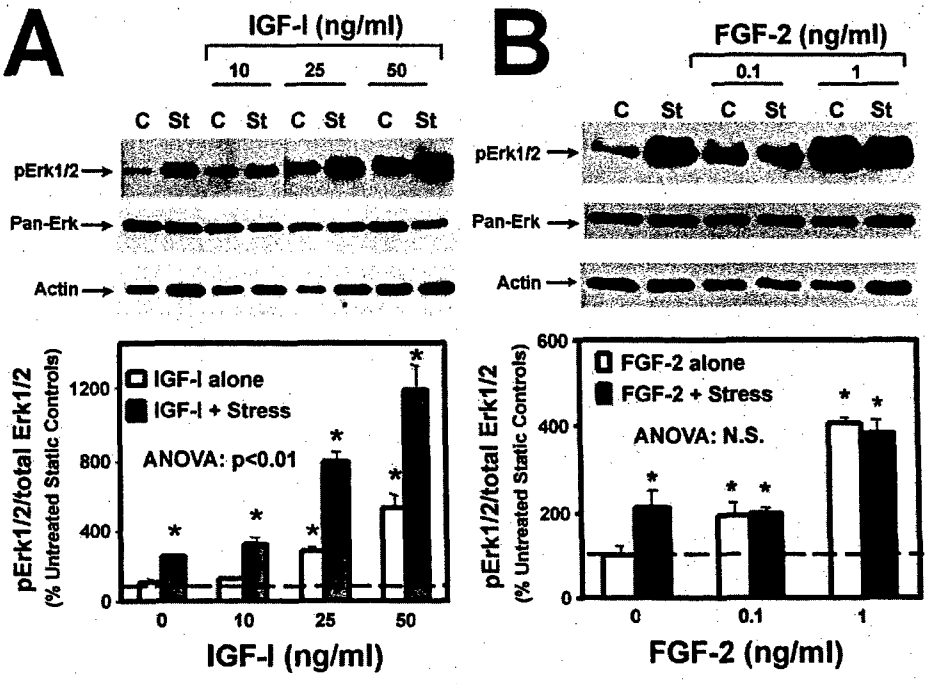

FIG. 2. **Interaction between IGF-I (*A*) or FGF-2 (*B*) and fluid shear stress on Erk1/2 phosphorylation in TE85 cells.** *Top panels* show representative Western blots of phosphorylated Erk1/2 (pErk1/2). Each blot was stripped and reblotted against anti-pan-Erk and anti-actin antibodies for loading controls. *Bottom panels* summarize the results of three separate repeat experiments. Results are shown as mean ± S.D. *, $p < 0.01$ (compared with no addition control). Two-way ANOVA indicates a significant ($p < 0.01$) interaction between IGF-I and shear stress but not between FGF-2 and shear stress on [^{3}H]thymidine incorporation. *C*, control; *St*, stressed; *Pan-Erk*, the anti-pan Erk antibody recognized all forms of Erks.

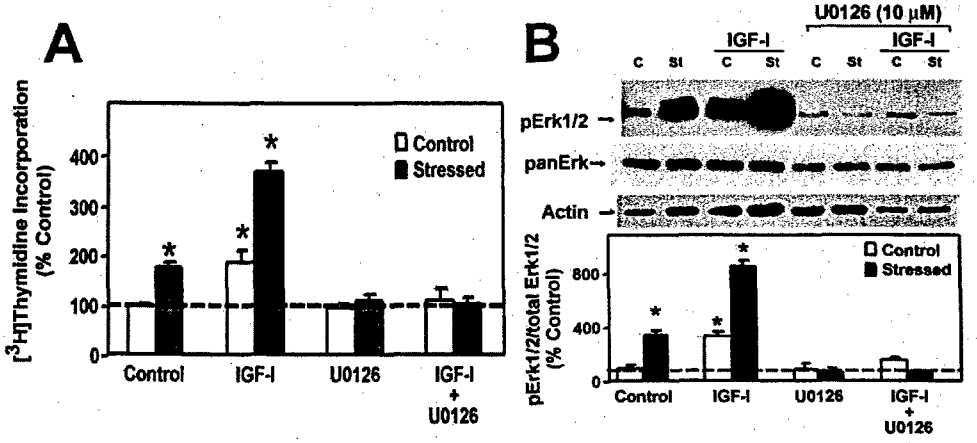

FIG. 3. **Effects of U0126 (a specific inhibitor of the Erk signaling pathway) on the stimulation of cell proliferation (*A*) and Erk1/2 protein-tyrosine phosphorylation (*B*) mediated by IGF-I and/or shear stress in TE85 cells.** TE85 cells were pretreated with 10 μM U0126 overnight before subjecting to the shear stress and/or IGF-I treatments. *A* shows the effects of U0126 on [^{3}H]thymidine incorporation in response to the 30-min steady shear stress of 20 dynes/cm^2 and/or 10 ng/ml IGF-I. *Top panel* of *B* shows a representative Western blot of pErk1/2. Each blot was stripped and reblotted against anti-pan-Erk and anti-actin antibodies for loading controls. *Bottom panel* of *B* summarizes the results of three separate repeat experiments. Results are shown as mean ± S.D. *, $p < 0.01$ (compared with no addition control). *C*, control; *St*, stressed; *Pan-Erk*, the anti-pan Erk antibody recognized all forms of Erks.

pletely abolished the increase in cell proliferation induced by IGF-I alone as well as that by the combination treatment. Similarly, echistatin also completely abolished the basal, shear-stress, or IGF-I-induced IGF-IR phosphorylation (Fig. 6*B*). These findings suggest that the synergy between IGF-I and shear-stress on the proliferation and that on IGF-IR phosphorylation level may involve integrin activation.

Effects of Fluid Shear Stress on the Association of SHP-1 or -2 with IGF-IR in TE85 Cells—To test whether integrin-dependent recruitment of SHP-2 could be involved in the synergy between IGF-I and shear stress, we determined the effect of IGF-I and/or fluid shear stress on the relative amounts of SHP-2 associated with integrin β3 or with IGF-IR, determined by co-immunoprecipitation (Fig. 7, *IP*) followed by immunoblotting (*IB*). This study focused on integrin β3, because this integrin subunit is one of the major subunits in osteoblasts (31) and also because integrin αvβ3 has been implicated to be the essential integrin subunit in regulating the IGF-I-dependent cellular responses in smooth muscle cells (16–22). The results of Fig. 7 suggest that fluid shear stress, IGF-I, and the combination treatment each significantly enhanced the recruitment of SHP-2 to integrin β3 and away from the IGF-IR. We also determined whether the synergistic interaction could also involve integrin-dependent recruitment of the related SHP-1 away from the IGF-IR. Fig. 8 shows that fluid shear stress, IGF-I, and the combination treatment each also significantly enhanced the recruitment of SHP-1 to integrin β3 and away from the IGF-IR. However, the effects of fluid shear stress on the recruitment of SHP-2 away from the IGF-IR appeared to be more pronounced than those on the SHP-1 recruitment. On the other hand, treatment of IGF-I alone, although it markedly reduced the amounts of IGF-IR-bound SHP-2, did not significantly affect the amounts of SHP-2 bound to integrin β3.

DISCUSSION

Mechanical loading is essential and required for normal bone physiology. Defective cellular responses to mechanical loading has been implicated as the etiology and progression of a number of musculoskeletal diseases, including disuse osteoporosis, senile osteoporosis, and osteoarthritis (32, 33). Appropriate

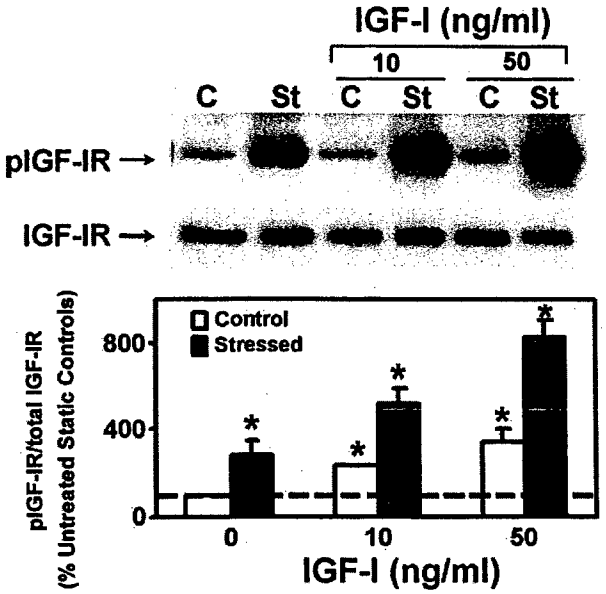

FIG. 4. **Interaction between IGF-I and fluid shear stress on IGF-IR phosphorylation in TE85 cells.** *Top panel* shows a representative Western blot of phosphorylated IGF-IR (*pIGF-IR*). The blot was stripped and reblotted against an anti-IGF-IR antibody for loading controls. *Bottom panels* summarize the results of three separate repeat experiments. Results are shown as mean ± S.D. *, $p < 0.01$ (compared with no addition control). Two-way ANOVA indicates a significant ($p < 0.01$) interaction between IGF-I and shear stress. *C*, control; *St*, stressed.

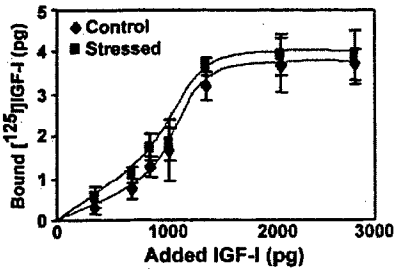

FIG. 5. **Effects of fluid shear stress on specific binding of IGF-I to IGF-IR in TE85 cells.** The binding of IGF-I to surface IGF-IR of TE85 cells was performed by measuring the receptor-bound [^{125}I]IGF-I. Total and nonspecific IGF-I binding was determined in the absence and presence of 100× non-radioactive cold IGF-I, respectively. Specific binding of IGF-I to IGF-IR was calculated by subtracting the nonspecific binding from the total binding. Only specific binding is shown in this figure. The *filled squares* were cells receiving the shear stress, whereas the *filled diamonds* were the corresponding static controls.

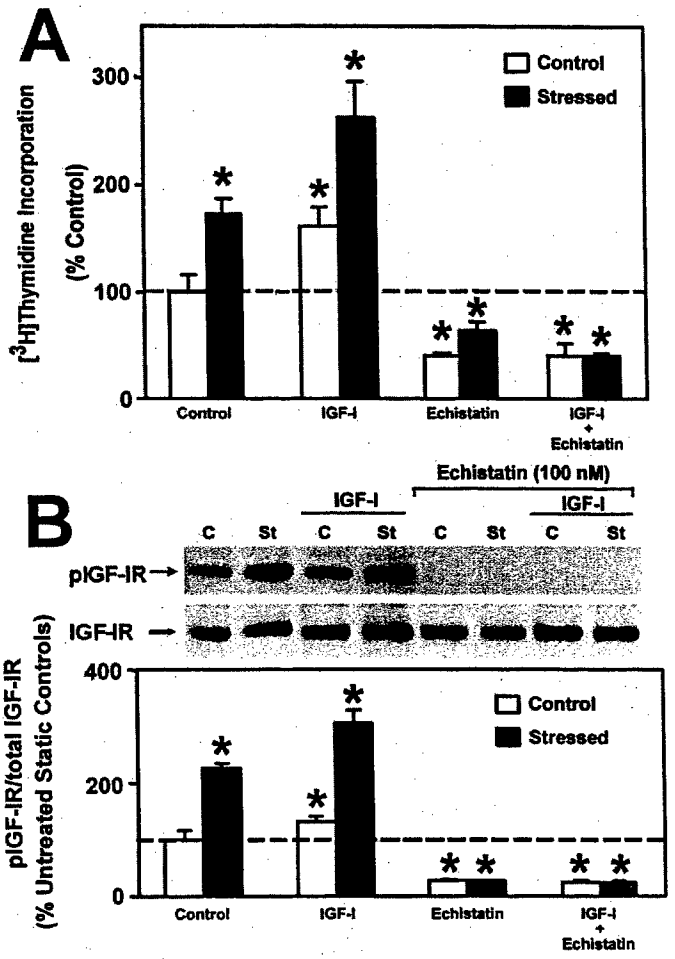

FIG. 6. **Effect of echistatin on the synergy between IGF-I and shear stress with respect to cell proliferation (*A*) and IGF-IR phosphorylation (*B*).** TE85 cells were pretreated with 100 nM echistatin overnight prior to the 30-min shear stress and/or the IGF-I treatment. In *A*, cell proliferation was measured by [^{3}H]thymidine incorporation as described under "Experimental Procedures." The shear stress stimulated TE85 cell proliferation by 73 and 58% in the absence or presence of the echistatin pretreatment, respectively. Thus, the echistatin pretreatment reduced the shear stress-induced proliferation by ~20%. In *B*, the IGF-IR phosphorylation level was determined by Western analysis as described under "Experimental Procedures." The *top panel* shows a representative Western blot of pIGF-IR. The blot was stripped and reblotted against an anti-IGF-IR antibody. *Bottom panels* summarize the results of three separate repeat experiments. Results are shown as mean ± S.D. *, $p < 0.01$ (compared with no addition control). *C*, control; *St*, stressed.

mechanical loading is also required for fracture healing (34). Thus, it is not surprising that the molecular mechanism of this important physiological process to regulate bone formation is complex and involves multiple interacting signal transduction pathways (3, 35). Information about the nature and molecular mechanism of the interaction among these various pathways should provide, not only a better understanding of the mechanical regulation of bone formation, but also important insights into the etiology of various musculoskeletal diseases. In this regard, this investigation addresses the potential mechanism of a cross-talk between the IGF-I and integrin signaling pathways in the stimulation of bone cell proliferation in response to a steady shear stress.

In this study, we demonstrated for the first time that a 30-min steady fluid shear stress of 20 dynes/cm^2 in human TE85 osteosarcoma cells enhanced synergistically the mitogenic action of IGF-I through an up-regulation of the Erk1/2-mediated IGF-I mitogenic signaling pathway. Our findings that the disintegrin echistatin completely abolished the synergy on IGF-IR and bone cell proliferation raise the strong possibility that the synergy between shear stress and IGF-I on bone cell proliferation involves integrin activation. Bikle and co-workers (12, 13) have recently reported that skeletal unloading by hind limb suspension induced a resistance to IGF-I with respect to bone formation in the rat. They also concluded that unloading-induced resistance to IGF-I was caused by inhibition of the IGF-I signaling pathway through down-regulation of the integrin pathway. This conclusion was based on the findings that 1) skeletal unloading down-regulated integrin expression and blocked the ability of IGF-I to stimulate cell proliferation in osteoblasts and 2) echistatin also blocked the IGF-I-mediated stimulation of bone cell proliferation *in vitro* (13). Consistent with the results of Bikle and co-workers, our findings demonstrated that shear stress interacts synergistically with the IGF-I signaling pathway to promote bone cell proliferation and that this interaction involves integrin β3 signaling. Consequently, it appears that mechanical loading not only plays a permissive role in the osteogenic actions of IGF-I, but also

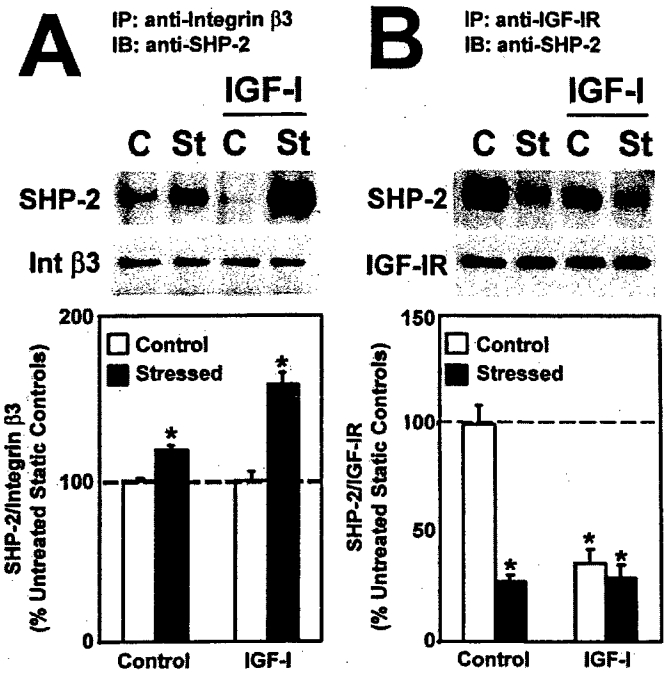

FIG. 7. **Effect of IGF-I or shear stress on recruitment of SHP-2 to integrin β3 or to IGF-IR.** The recruitment of SHP-2 to integrin β3 and away from IGF-IR was assessed by measuring the relative amounts of SHP-2 co-immunoprecipitated (*IP*) with integrin β3 (*A*) or with IGF-IR (*B*) as described under "Experimental Procedures." The amounts of immunoprecipitated SHP-2 were normalized against the corresponding levels of immunoprecipitated integrin β3 and IGF-IR, respectively. *Top panels* show representative Western immunoblots (*IB*) against SHP-2 or integrin β3 and IGF-IR, respectively. *Bottom panels* summarize the results as percentage of respective untreated control (mean ± S.D.) of four replicate experiments. *, $p < 0.01$; *C*, control; *St*, stressed; *Int*, integrin.

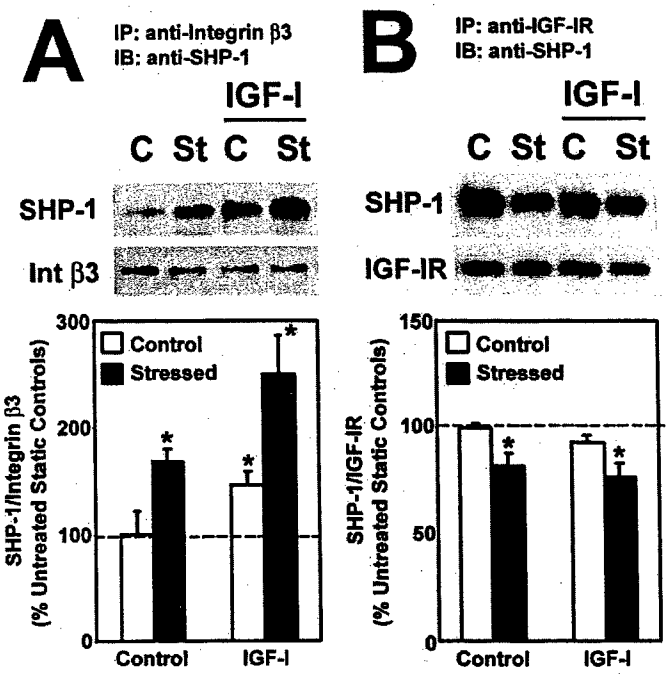

FIG. 8. **Effect of IGF-I or shear stress on recruitment of SHP-1 to integrin β3 or to IGF-IR.** The recruitment of SHP-1 to integrin β3 and away from IGF-IR was assessed by measuring the relative amounts of SHP-1 co-immunoprecipitated with integrin β3 (*A*) or with IGF-IR (*B*) as described under "Experimental Procedures." The amounts of immunoprecipitated (*IP*) SHP-1 were normalized against the corresponding levels of immunoprecipitated integrin β3 and IGF-IR, respectively. *Top panels* show representative Western immunoblots (*IB*) against SHP-1 or integrin β3 and IGF-IR, respectively. *Bottom panels* summarize the results as percentage of respective untreated control (mean ± S.D.) of four replicate experiments. *, $p < 0.01$; *C*, control; *St*, stressed; *Int*, integrin.

interacts synergistically with the IGF-I signaling pathway to promote bone formation.

The conclusion that the loading-mediated activation of integrin signaling pathways may not only allow the IGF-I signaling pathway to function (16–22) but also cross-talks with the IGF-I signaling pathway to synergistically enhance the mitogenic effects of IGF-I in bone cells is consistent with the findings of several previous studies in fibroblasts (36–39) and smooth muscle cells (16–22), showing that integrin activation has an essential regulatory role in the mediation of the signal transduction pathways and cellular responses of a number of growth factors, including platelet-derived growth factor, epidermal growth factor, FGF-2, and IGF-I. Consistent with an important role for integrin signaling pathways in mediating mechanical stimulation of bone cell proliferation and activity (23–28, 40), we found synergy between the shear stress and IGF-I on bone cell proliferation and the IGF-IR-Erk1/2 signaling pathway. In contrast to fibroblasts, which show an enhancing interaction between FGF-2 and integrin activation (36, 39), our study did not find a synergistic enhancement of shear stress on the bone cell mitogenic activity of FGF-2 and FGF-2-mediated stimulation of Erk1/2 activation in TE85 cells. This would suggest that the synergistic interaction between IGF-I and shear stress is not shared by FGF-2 in osteoblastic cells. Future work is needed to confirm whether similar synergy occurs between shear stress and platelet-derived growth factor or epidermal growth factor in bone cells to determine whether the synergy is unique to IGF-I in bone cells.

Bikle and co-workers (13) have also reported that mechanical unloading markedly diminished the ability of IGF-I to activate several members of its mitogenic signaling pathway (*i.e.* IGF-IR, Ras, Erk1/2) in osteoblasts. Accordingly, we found that shear stress potentiates the IGF-I-mediated Erk1/2 activation. To gain insights into the molecular mechanism whereby shear stress interacts with the IGF-I signaling pathway to promote osteoblast proliferation, we examined whether synergy between shear stress and IGF-I also occurred at Erk1/2 activation and IGF-IR phosphorylation, two important steps of the IGF-I mitogenic signaling pathway. We reasoned that if the point of interaction (*i.e.* cross-talk) occurs prior to a given step in a pathway, a synergy would be evident at and after that particular step of the pathway. Conversely, if the point of interaction happens after a given step, no synergy would be expected at or prior to that given step. Accordingly, our findings that shear stress also synergized with IGF-I on Erk1/2 activation and IGF-IR phosphorylation strongly suggest that the synergy between shear stress and IGF-I to promote bone cell proliferation occurs prior to or at the step of IGF-IR phosphorylation.

Although Bikle and co-workers (13) report that skeletal unloading or the blocking of integrin activation by echistatin has no effect on the binding of IGF-I to IGF-IR in osteoblasts, our study showed that the shear stress slightly but significantly enhanced the IGF-I binding to IGF-IR. However, the increase in ligand binding was too small to explain the large synergic enhancement of shear stress in the stimulatory action of IGF-I on IGF-IR phosphorylation (8-fold), Erk1/2 activation (12-fold), and cell proliferation (5-fold). In addition, we noted that the ligand binding curves in the absence or presence of the shear stress were parallel to each other. This would argue against a synergy between shear stress and IGF-I on IGF-IR ligand binding.

The relatively low amounts of receptor-bound IGF-I (*i.e.* <2%) compared with the total amounts of added IGF-I, presumably because of the fact that bone cells (including TE85

cells) release a large amount of IGF binding proteins (41) that compete with IGF-IR for IGF-I binding, has precluded an accurate determination of receptor number and/or binding affinity by Scatchard analysis. Thus, it is not known whether the small increase in IGF-I binding in response to shear stress was because of an increase in the number of IGF-IR or to an increase in ligand binding affinity. However, the parallel binding curves in the absence or presence of shear stress suggest that the increase in IGF-I binding could be due to a small increase in IGF-IR number. The reason for shear stress to increase the IGF-IR number is not clear, but the main point of the concept of our work is that the synergy between shear stress and IGF-I in the stimulation of bone cell proliferation occurs after the ligand binding, but prior to or at the step of IGF-IR phosphorylation, and that activation of the integrin signaling is essential for the synergy.

Recent studies from Clemmons and co-workers (16–22) in smooth muscle cells have disclosed important information about the nature of the cross-talk between the integrin signaling pathway and the IGF-I signaling pathway. Specifically, they found that activated integrin $\beta 3$ serves to recruit SHP-2 from the cytosol and subsequently to transfer SHP-2 to SHPS-1 and IGF-IR for activating and terminating, respectively, the IGF-I signaling pathway. These findings have provided the basis that integrin activation is potentially relevant to the molecular mechanism whereby shear stress interacts with IGF-I to enhance the IGF-I signaling mechanism in bone cells. The IGF-I signaling pathway is initiated, not only by IGF-IR autophosphorylation induced by ligand binding, but also by the recruitment of activated SHP-2 to SHPS-1 from activated integrins. The transfer of activated SHP-2 to IGF-IR is responsible for the dephosphorylation of IGF-IR and the termination of the IGF-I signaling pathway (16–22). Accordingly, we postulate that mechanical strains or shear stresses, which activate the integrin signaling pathways in bone cells, enhance SHP-2 recruitment to activated integrins and also to SHPS-1. At the same time, the integrin activation in response to shear stresses inhibits the transfer of activated SHP-2 to IGF-IR, resulting in a reduction in the dephosphorylation of IGF-IR and an overall increase in IGF-IR phosphorylation level. This model would explain the synergy between shear stress and IGF-I on the IGF-IR phosphorylation level, Erk1/2 activation, and bone cell proliferation.

Our findings that shear stress, IGF-I, and the combination treatment each increased the relative amount of SHP-2 that was associated with integrin $\beta 3$ and that each also reduced the relative amount of SHP-2 co-immunoprecipitated with IGF-IR in TE85 cells are consistent with our hypothesis that the shear stress-mediated recruitment of SHP-2 to activated integrins and away from IGF-IR may be responsible for the synergy between shear stress and IGF-IR to promote bone cell proliferation. It should be noted that the IGF-I-mediated and shear stress-induced recruitment of SHP-2 to integrin $\beta 3$ was relatively small (*i.e.* <2-fold). However, human osteoblasts, including TE85 cells, synthesize multiple members of the integrin family (42). There is evidence that mechanical loading also up-regulated and activated other members of integrins (such as integrin $\beta 1$) in bone cells, including TE85 cells (26). Therefore, it is highly possible that shear stress and/or IGF-I also increased SHP-2 recruitment to other members of the integrin family, including $\beta 1$, and that this may explain why the enhancement in SHP-2 recruitment to integrin $\beta 3$ induced by IGF-I and/or shear stress was relatively low. More importantly, we found that shear stress, IGF-I, and the combination treatment each also increased the relative amount of the integrin $\beta 3$-associated SHP-1 and reduced the relative amount of IGF-IR-associated SHP-1. This suggests that SHP-2 and the related SHP-1 are both involved in the IGF-I signaling mechanism as well as in the synergy between shear stress and IGF-I in enhancing the overall IGF-IR phosphorylation level.

The effect of unloading on recruitment of SHP-2 (or SHP-1) to integrins has not been assessed previously (13). Thus, it is unclear at this time whether or not the unloading-induced resistance to IGF-I may also involve a reduction of SHP-2 (and/or SHP-1) recruitment to integrins. However, because unloading down-regulated integrin expression in osteoblasts (13) and because SHP-2 recruitment to integrins is essential for IGF-I signaling (16–22), it is likely that the reduced integrin recruitment of SHP-2 and/or SHP-1 in response to unloading-mediated down-regulation of the integrin pathway could also play a pivotal role in the permissive effect of mechanical loading on the IGF-I anabolic action in bone (12, 13).

In conclusion, this study provides the first evidence for a synergistic interaction between shear stress and IGF-I in the stimulation of osteoblastic proliferation. This study also provides strong circumstantial evidence that the synergy involves an integrin-dependent up-regulation of IGF-IR phosphorylation level through an inhibition of the recruitment of SHP-1 and/or SHP-2 to IGF-IR as well as an inhibition of the SHP-1 and/or SHP-2-mediated IGF-IR dephosphorylation. These findings not only confirm that the integrin activation is essential for the IGF-I mitogenic pathway, but also provide mechanistic insights into the cross-talk between the integrin and IGF-I signaling pathways in the underlying molecular mechanisms of enhanced bone formation in response to mechanical loading.

REFERENCES

1. Hillam, R. A., and Skerry, T. M. (1995) *J. Bone Miner. Res.* **10,** 683–689
2. Hillsley, M. V., and Frangos, J. A. (1994) *Biotechnol. Bioeng.* **43,** 573–581
3. Kapur, S., Baylink, D. J., and Lau, K.-H. W. (2003) *Bone* **32,** 241–251
4. Mohan, S., and Baylink, D. J. (1991) *Clin. Orthop. Relat. Res.* **263,** 30–48
5. Canalis, E., MaCarthy, T., and Centrella, M. (1988) *J. Clin. Investig.* **81,** 277–281
6. Wergedal, J. E., Mohan, S., Lundy, M., and Baylink, D. J. (1990) *J. Bone Miner. Res.* **5,** 179–186
7. Hock, J. M., Centrella, M., and Canalis, E. (1988) *Endocrinology* **122,** 254–260
8. Lean, J. M., Jagger, C. J., Chambers, T. J., and Chow, J. W. (1995) *Am. J. Physiol.* **268,** E318–E327
9. Mikuni-Takagaki, Y., Suzuki, Y., Kawase, T., and Saito, S. (1996) *Endocrinology* **137,** 2028–2035
10. Kapur, S., Chen, S.-T., Baylink, D. J., and Lau, K.-H. W. (2004) *Bone* **35,** 525–534
11. Cheng, M. Z., Rawlinson, S. C., Pitsillides, A. A., Zaman, G., Mohan, S., Baylink, D. J., and Lanyon, L. E. (2002) *J. Bone Miner. Res.* **17,** 593–602
12. Sakata, T., Halloran, B. P., Elalieh, H. Z., Munson, S. J., Rudner, L., Venton, L., Ginzinger, D., Rosen, C. J., and Bikle, D. D. (2003) *Bone* **32,** 669–680
13. Sakata, T., Wang, Y., Halloran, B. P., Elalieh, H. Z., and Bikle, D. D. (2004) *J. Bone Miner. Res.* **19,** 436–446
14. Mauck, R. L., Nicoll, S. B., Seyhan, S. L., Ateshian, G. A., and Hung, C. T. (2003) *Tissue Eng.* **9,** 597–611
15. Tokimasa, C., Kawata, T., Fujita, T., Kaku, M., Kawasoko, S., Kohno, S., and Tanne, K. (2000) *Arch. Oral Biol.* **45,** 871–878
16. Ling, Y., Maile, L. A., and Clemmons, D. R. (2003) *Mol. Endocrinol.* **17,** 1824–1833
17. Clemmons, D. R., and Maile, L. A. (2005) *Mol. Endocrinol.* **19,** 1–11
18. Maile, L. A., and Clemmons, D. R. (2002) J. *Biol. Chem.* **277,** 8955–8960
19. Maile, L. A., Badley-Clarke, J., and Clemmons, D. (2003) *Mol. Biol. Cell* **14,** 3519–3528
20. Ling, Y., Maile, L. A., Badley-Clarke, J., and Clemmons, D. R. (2005) *J. Biol. Chem.* **280,** 3151–3158
21. Zheng, B., and Clemmons, D. R. (1998) Proc. *Natl. Acad. Sci. U. S. A.* **95,** 11217–11222
22. Maile, L. A., and Clemmons, D. R. (2002) *Endocrinology* **143,** 4259–4264
23. Burridge, K., and Chrzanowska-Wodnicka, M. (1996) *Annu. Rev. Cell Dev. Biol.* **12,** 463–519
24. Hynes, R. O. (1999) *Trends Cell Biol.* **9,** 33–37
25. Alenghat, F. J., and Ingber, D. E. (2002) *Science's STKE* http://stke.sciencemag.org/cgi/content/full/OC_sigtrans;2002/119/pe6
26. Carvalho, R. S., Scott, J. E., and Yen, E. H. (1995) *Arch. Oral Biol.* **40,** 257–264
27. Salter, D. M., Robb, J. E., and Wright, M. O. (1997) *J. Bone Miner. Res.* **12,** 1133–1141
28. Lee, H. S., Millward-Sadler, S. J., Wright, M. O., Nuki, G., and Salter, D. M. (2000) *J. Bone Miner. Res.* **15,** 1501–1509
29. Lau, K.-H. W., Lee, M. Y., Linkhart, T. A., Mohan, S., Vermeiden, J., Liu, C. C., and Baylink, D. J. (1985) *Biochim. Biophys. Acta* **840,** 56–68
30. Greenwood, F. C., Hunter, W. M., and Glover, J. S. (1963) *Biochem. J.* **89,**

114–123
31. Gronthos, S., Stewart, K., Graves, S. E., Hay, S., and Simmons, P. J. (1997) *J. Bone Miner. Res.* **12,** 1189–1197
32. Mosley, J. R. (2000) *J. Rehabil. Res. Dev.* **37,** 189–199
33. Carter, D. R., Beaupre, G. S., Wong, M., Smith, R. L., Andriacchi, T. P., Schurman, D. J., and Smith, R. L. (2004) *Clin. Orthop. Relat. Res.* **427,** (suppl.) S69–S77
34. Carter, D. R., Beaupre, G. S., Giori, N. J., and Helms, J. A. (1998) *Clin. Orthop. Relat. Res.* **355,** (suppl.) S41–S55
35. Lau, K.-H. W., Kapur, S., and Baylink, D. J. *J. Bone Miner. Res.* **19,** Suppl. 1, S79 (Abstr. F264)
36. Miyamoto, S., Teramoto, H., Gutkind, S., and Yamada, K. M. (1996) *J. Cell Biol.* **135,** 1633–1642
37. Lin, T. H., Chen, Q., Howe, A., and Juliano, R. L. (1997) *J. Biol. Chem.* **272,** 8849–8852
38. Sundberg, C., and Rubin, K. (1996) *J. Cell Biol.* **132,** 741–752
39. Howe, A., Aplin, A. E., Alahari, S. K., and Juliano, R. L. (1998) *Curr. Opin. Cell Biol.* **10,** 220–231
40. Schwartz, M. A., and Ingber, D. E. (1994) *Mol. Biol. Cell* **5,** 389–393
41. Lau, K.-H. W., Goodwin, C., Arias, M., Mohan, S., and Baylink, D. J. (2002) *Bone* **30,** 705–711
42. Clover, J., and Gowen, M. (1994) *Bone* **15,** 585–591

Fluid Shear Stress Synergizes with IGF-I on Osteoblast Proliferation Through Integrin-Dependent Activation of IGF-I Receptor

K. H. W. Lau, S. Kapur, D. J. Baylink. Musculoskeletal Disease Center, Jerry L. Pettis Mem VAMC, Loma Linda, CA, USA.

Presentation Number: SA263

Mechanical strain increases osteoblast proliferation. Recent studies suggested that mechanical strain has a permissive role in the IGF-I mitogenic action in osteoblasts. The present study tested the hypothesis that mechanical strain interacts with the IGF-I pathway in the stimulation of osteoblast proliferation ([^{3}H]Thymidine incorporation, TdR). Human TE85 osteosarcoma cells were subjected to steady shear stress of 20 dynes/cm^2 for 30 min followed by 24-hr incubation with IGF-I (0 to 50 ng/ml). IGF-I increased TdR (1.5- to 2.5-fold, $p<0.01$) in a dose-dependent manner. Shear stress alone increased TdR by 70% ($p<0.01$). The combination of shear stress and IGF-I stimulated TdR (3.5- to 5.5-fold) much greater than the additive effects of each treatment alone (ANOVA), suggesting a synergistic interaction. IGF-I dose-dependently increased the phosphorylation level of Erk1/2 (1.2- to 5.3-fold) and IGF-I receptor (IGF-IR) (2- to 4-fold). Shear stress alone also increased the phosphorylation Erk1/2 and IGF-IR (2-fold each). The combination treatment resulted in synergistic enhancements in both Erk1/2 and IGF-IR phosphorylation (up to 12-fold for Erk1/2 and 8-fold for IGF-IR). Shear stress did not alter the binding affinity or number of IGF-IR, indicating that the synergy occurred at the post-ligand binding level. Recent studies have implicated a role for integrin in the regulation of IGF-IR phosphorylation and activation of IGF-I signaling mechanism (i.e., integrin activation recruits away SHP-2 from the IGF-IR, allowing sustained IGF-IR phosphorylation and activation). To test the hypothesis that the synergy between IGF-I and shear stress involve integrin-dependent mechanisms, we measured the effect of echistatin (an inhibitor of integrin) on TdR in response to shear stress ± IGF-I. Echistatin reduced basal TdR by 60%, and slightly but not significantly reduced the mitogenic response to the shear stress (173±16% vs. 157±20% of control). However, echistatin completely abolished the mitogenic effect of IGF-I and that of the combination treatment, indicating that the IGF-I action and the synergy between shear stress and IGF-I involves integrin activation. Shear stress also significantly ($p<0.05$ for each) reduced the amounts of SHP-1 and SHP-2 co-immunoprecipitated with IGF-IR, supporting that the synergy involves the integrin-dependent recruitment of SHP-1 or -2 away from IGF-IR. In conclusion, shear stress interacts synergistically with the IGF-I signaling pathway in osteoblast proliferation and this interaction involves integrin-dependent upregulation of IGF-IR phosphorylation and activation

FLUID SHEAR STRESS SYNERGIZES WITH IGF-I ON OSTEOBLAST PROLIFERATION THROUGH INTEGRIN-DEPENDENT UPREGULATION OF IGF-I RECEPTOR PHOSPHORYLATION LEVELS

*Lau, K.-H.W., *Kapur, S., *Mohan, S., and *Baylink, D.J.
*Musculoskeletal Disease Center, J.L. Pettis Memorial VAMC and Loma Linda, CA
laub@lom.med.va.gov

INTRODUCTION: Mechanical loading is important for the maintenance of skeletal architectural integrity. Increased loading increased bone formation and bone mass. Loading produces strains in the bone that generates interstitial fluid flow through the lacunar-canalicular spaces. It is believed that this fluid flow exerts a shear stress at surfaces of bone cells lining the lacunar-canalicular spaces and that the shear stress then generates biochemical signals that transduce to the nucleus of bone cells to stimulate osteoblast proliferation and activity. Knowledge of the molecular mechanisms whereby shear stress induces bone formation would not only yield information about the mechanical loading-dependent regulation of bone formation but may also provide insights into the pathophysiology of osteoporosis and other bone-wasting diseases. It is known clear that the molecular mechanism whereby shear stress enhances bone cell proliferation and activity is complex and involves multiple signaling molecules and pathways (1).

Recent studies suggest that mechanical loading has a permissive role in the IGF-I mitogenic action in osteoblasts in that skeletal unloading induces resistance to IGF-I with respect to bone formation. Accordingly, IGF-I administration stimulates bone formation in the loaded bone, but not in unloaded bone in vivo and in vitro (2,3). The unloading-related resistance to IGF-I is mediated by inhibiting the activation of IGF-I signaling pathways (3). Therefore, we reason that increased mechanical loading could enhance the osteogenic action of IGF-I. Accordingly, the present study tested whether fluid shear stress would enhance the mitogenic action of IGF-I on osteoblast proliferation; and determined the mechanism(s) involved in the enhancement.

METHODS: Human TE85 osteoblasts were plated on glass slides and were serum deprived for 24-hrs before subjection to fluid shear stress. Shear stress experiments were performed in flow chambers using the flow loop apparatus designed by Frangos et al (4). All cells were subjected to steady shear stress of 20 dynes/cm^2 for 30 min. The static controls were performed on cells grown in identical conditions but without the shear stress. After the shear stress, the treated or static control cells were treated with IGF-I (or FGF-2) for 24 hrs (for [^{3}H]thymidine incorporation) or for 10 min (for western analyses or immunoprecipitation). Effects of Erk1/2 inhibitor (U0126, 10 μM) or integrin inhibitor (echistatin, 100 nM) were also tested.

Cell proliferation was assessed by [^{3}H]thymidine incorporation into cell DNA. Erk1/2 activation was reflected by Erk1/2 phosphorylation level, which was determined with western blots using an antibody against phosphorylated Erk1/2, normalized against the total Erk1/2 levels. IGF-I receptor (IGF-IR) phosphorylation level was also determined with western blots using an antibody against phosphorylated IGF-IR, normalized against the level of total IGF-IR. IGF-I binding to IGF-IR was measured by receptor-bound [^{125}I]IGF-I in the presence of 100X "cold" IGF-I. The relative level of IGF-IR-bound SHP-1 and SHP-2 was measured by co-immunoprecipitation with anti-IGF-IR followed by western blot analysis with anti-SHP-1 or anti-SHP-2, respectively.

RESULTS: The 30-min steady shear stress of 20 dynes/cm^2 significantly increased [^{3}H]thymidine incorporation in TE85 cells by 70% ($p<0.05$). IGF-I at doses of 10-50 ng/ml also increased proliferation by 1.5- to 2.5-fold, $p<0.01$, ANOVA). Combination treatment produced much greater stimulation (3.5- to 5.5-fold) than additive effects of each treatment alone. Two-way ANOVA indicates a significant ($p<0.001$) synergistic interaction. No such synergy occurred between shear stress and FGF-2 suggesting that the synergistic interaction between shear stress and IGF-I may be unique to IGF-I.

The mitogenic action of IGF-I is mediated through Erk1/2 activation, and shear stress activates Erk1/2 in osteoblasts (1). Thus, we next investigated the effect of shear stress and/or IGF-I on Erk1/2 phosphorylation (an index of Erk1/2 activation). As expected, IGF-I at the test doses increased Erk1/2 phosphorylation (1.2- to 5-fold, $p<0.01$), and shear stress alone increased Erk1/2 phosphorylation by 2.5-fold ($p<0.01$). The combination treatment resulted in synergistic enhancement in Erk1/2 phosphorylation (12-fold, $p<0.01$). Consistent with the contention that the synergy on Erk1/2 activation is associated with the synergistic enhancement on osteoblast proliferation, U0126 completely abolished the synergistic enhancement on cell proliferation and Erk1/2 by shear stress and IGF-I. While FGF-2 treatment increased Erk1/2 phosphorylation, combination treatment with FGF-2 and shear stress did not lead to further enhancement in Erk1/2 phosphorylation, supporting the premise that the synergy between shear stress and IGF-I on osteoblast proliferation may be unique to IGF-I.

The mitogenic action of IGF-I is initiated with IGF-IR phosphorylation induced by binding of IGF-I to IGF-IR. To test if the synergy involves an enhancement of IGF-IR, the effect of IGF-I and/or shear stress on IGF-IR was determined. IGF-I increased IGF-IR phosphorylation ins a dose-dependent manner (2- to 3.5-fold, $p<0.01$). Shear stress alone also increased IGF-IR phosphorylation by 2.5-fold, $p<0.01$). Combination of shear stress and IGF-I again yielded a highly significant synergistic enhancement in IGF-IR (up to 8-fold, $p<0.01$). To assess whether the synergistic enhancement was due to an increase in IGF-IR number and affinity, the effect of shear stress on specific binding of [^{125}I] IGF-I to IGF-IR was measured. The shear stress had no significant effect on IGF-I binding to IGF-IR, a finding that does not support the concept that the synergistic enhancement in IGF-IR phosphorylation was due to increased IGF-IR number or affinity.

Recent studies revealed that IGF-I signaling pathway is regulated by integrin-dependent inhibition of IGF-IR dephosphorylation (5). Accordingly, IGF-IR phosphorylation and activation in response to IGF-I binding led to recruitment of SHP2 to the IGF-IR. SHP2 would then dephosphorylate IGF-IR, terminating the activation of IGF-I signaling pathway. However, activation and phosphorylation of the integerin pathway results in recruitment of SHP2 away from the IGF-IR complex, leading to the sustained IGF-IR phosphorylation and activation of IGF-I pathway. Because shear stress is known to activate the integrin pathway (1), we next tested whether the synergy between IGF-I and shear stress would involve integrin activation and the integrin-dependent recruitment of SHP2 and the related SHP1 away from the IGF-IR complex. Echistatin (a potent inhibitor of integrin pathway) not only reduced ~60% of basal and stress-induced proliferation and Erk1/2 activation, but also completely abolished the IGF-I- and the combination-induced cell proliferation and Erk1/2 activation. Similarly, echistatin completely abolished basal, shear-stress-, or IGF-I-induced IGF-IR phosphorylation. Co-immunoprecipitation studies revealed that shear stress markedly reduced the amounts of both IGF-IR associated SHP2 and SHP1.

DISCUSSION: This study provides the first evidence for a synergistic interaction between shear stress and IGF-I in stimulation of osteoblastic proliferation. There is strong evidence that the synergy involves the integrin-dependent upregulation of IGF-IR phosphorylation through an inhibition of SHP-mediated IGF-IR dephosphorylation. These findings not only confirm that the integrin activation is essential for the IGF-I mitogenic pathway, but also provide mechanistic insights into the functional roles of integrin and IGF-I signaling pathways in the molecular mechanisms whereby loading enhances bone formation.

REFERENCES:

1. Kapur S t al. (2003) Bone 32:241-251.
2. Sakata T et al. (2003) Bone 32:669-680.
3. Sakata T et al. (2004) J Bone Miner Res 19:436-446.
4. Frangos JA et al. (1988) Biotech Bioeng 32:1053-1060.
5. Ling Y et al. (2003) Mol Endocrinol 17:1824-1833.

This work is supported in parts by funding from the VA and US Army.